Characterization of Temporal Claudin Expression and Analysis of Sequence Variants in Early Kidney Development

Maria Paula Laverde

Department of Human Genetics
McGill University, Montreal, Quebec, Canada
April, 2018

A thesis submitted to the Faculty of Graduate and Postdoctoral Studies in partial fulfillment of the requirements of the degree of Master of Science

Abstract

Congenital Anomalies in the Kidney and Urinary Tract (CAKUT) refer to a range of phenotypes in the kidney and the urinary tract. CAKUT is present in 1 to 6 of every 1,000 live births, and is a major cause of kidney failure in children. To better understand how congenital kidney malformations arise in children, it is important to define the molecular and cellular events of two important processes in kidney development: nephric duct elongation and branching morphogenesis. The nephric duct elongates caudally and gives rise to the ureteric bud, which will undergo branching morphogenesis, thereby forming the collecting duct system of the kidney. Defects in either of these processes can lead to congenital renal malformations. Several genes have been associated with renal malformations in mice and in humans from sequencing cohorts with CAKUT. However, the variants discovered so far only account for a small subset of patients with CAKUT. Thus, it is necessary to sequence more patients for genes outside of the ones already implicated in kidney development.

Previous studies by our group showed that members of the claudin family of tight junction proteins are required for nephric duct elongation and branching morphogenesis during kidney development. I hypothesize that claudin sequence variants in patients with kidney malformations will result in defects in nephric duct elongation and/or ureteric bud branching. To test this hypothesis, I first analyzed the expression patterns of claudins during nephric duct elongation in mouse and chick. *Claudin-1*, *-3* and *-4* were expressed in the chick nephric duct from HH12 (Hamburger Hamilton stage), when the nephric duct starts to form, and they continued to be expressed once the entire nephric duct was epithelialized. In the mouse embryo, *Claudin-4* was expressed in the nephric duct at E10.5, as well as in the ureteric bud and trunk, and the ureter at E13.5 and E16.5. Next, I analyzed the claudin coding sequences of 96 patients with congenital renal malformations from the NIH-sponsored CKiD cohort (Chronic Kidney Disease). I identified 17 rare and novel heterozygous variants, 11 of which are predicted to be pathogenic. A rare variant in *CLDN8*, and a novel variant in *CLDN14* were subjected to functional analysis. Retroviral overexpression of these variants in the chick embryo resulted in impaired elongation of the nephric duct, when assessing the embryos by *in situ* hybridization using a marker of the duct.

Résumé

Les anomalies congénitales du rein et des voies urinaires (Congenital Anomalies in the Kidney and Urinary Tract, CAKUT) font référence à un spectre de malformations du rein et des voies urinaires. Les CAKUT touchent 1 à 6 nouveau-nés sur 1000 naissances, et sont une cause majeure d'insuffisance rénale chez les enfants. Pour mieux comprendre comment les malformations congénitales du rein surviennent chez les enfants, il est important de définir les événements moléculaires et cellulaires de deux processus importants dans le développement du rein: l'allongement du canal de Wolff et la morphogenèse de ramification. Le canal de Wolff s'allonge caudalement et donne naissance au bourgeon urétéral, qui va se ramifier, formant ainsi le système du canal collecteur rénal. Une anomalie dans l'un ou l'autre de ces processus peuvent entraîner des malformations congénitales du rein. Plusieurs gènes ont été associés à des malformations rénales chez la souris et chez l'homme en séquençant des cohortes atteintes de CAKUT. Cependant, les variantes génétiques découvertes jusqu'à présent ne représentent qu'un petit sous-groupe de patients avec des CAKUT. Ainsi, il est nécessaire de séquencer plus de patients pour des gènes en dehors de ceux déjà impliqués dans le développement du rein.

Notre groupe de recherche a démontré dans des études antérieures que les claudines, une famille de protéines situées dans les jonctions serrées, sont nécessaires pour l'élongation du canal de Wolff et dans la morphogenèse de ramification au cours du développement du rein. Je fais l'hypothèse que les variantes dans la séquence des claudines chez les patients atteints de malformations rénales entraîneront des anomalies dans l'allongement du canal de Wolff et/ou de la ramification du bourgeon urétéral. Pour tester cette hypothèse, j'ai d'abord analysé les profils d'expression des claudines au cours de l'allongement du canal de Wolff chez la souris et le poussin. Les *Claudin-1, -3* et *-4* sont exprimées dans le canal de Wolff du poulet au stade HH12 (stade Hamburger Hamilton), lorsque le canal de Wolff commence à se former, et ils continuent à être exprimés suite à l'épithélialisation complète du canal de Wolff. Chez la souris, au stade E10.5 (jour 10.5 du développement embryonnaire), la *Claudin-4* est exprimée dans le canal de Wolff. Elle est aussi exprimée dans le bourgeon et le tronc urétéral, et l'uretère à E13.5 et E16.5. Ensuite, j'ai analysé les séquences codantes des claudines de 96 patients atteints de malformations congénitales du rein de la cohorte CKiD parrainée par le NIH (Chronic Kidney Disease). J'ai identifié 17 rares et nouvelles variantes hétérozygotes dont 11 étaient pathogènes.

Une variante rare dans CLDN8 et une nouvelle variante dans CLDN14 ont été soumises à une analyse fonctionnelle. La surexpression rétrovirale de ces variantes dans l'embryon de poulet a entraîné une altération de l'allongement du canal de Wolff observée lors de l'évaluation des embryons par hybridation *in situ* en utilisant un marqueur du canal de Wolff.

Table of Contents

List of Figures

List of Tables

List of Abbreviations

°C: Degrees Celsius
µg: Microgram
µl: Microlitre
µm: Micrometre
BMP: Bone morphogenetic protein
BSA: Bovine serum albumin
Ca^{2+}: Calcium ion
CAKUT: Congenital anomalies of the kidney and the urinary tract
C-CPE: C-terminus of *Clostridium perfringens* enterotoxin
cDNA: Complementary deoxyribonucleic acid
Cl^-: Chloride ion
CLDN: Claudin
CPE: *Clostridium perfringens* enterotoxin
DF-1: Chicken embryonic fibroblast cell line
DNA: Deoxyribonucleic acid
E: Embryonic day
ECL: Extracellular loop
EphA2: Ephrin type-A receptor 2
ExAC: Exome Aggregation Consortium
EYA1: Eyes absent homolog 1
FHHNC: Familial Hypomagnesemia with Hypercalciuria and Nephrocalcinosis
Gata: GATA binding protein
GDNF: Glial-cell-line-derived neurotrophic factor
GFP: Green fluorescent protein
GFRα1: GDNF family receptor alpha 1
Ghrl2: Grainyhead-like2
GST: Glutathione-S-transferase
HH: Hamilton and Hamburger stage in chick
HNF1β: Hepatocyte nuclear factor 1β
JAM: Junctional adhesion molecule
kDa: kiloDalton
LB: Luria broth
Lim1: LIM homeobox protein 1
MAF: Minor allele frequency
MDCK: Madin-Darby canine kidney
MET: Mesenchymal-to-epithelial transition
mIMCD3: Mouse inner medullary collecting duct cell
ml: Millilitre
mm: Millimetre
mM: Millimolar
mRNA: Messenger ribonucleic acid
MUPP1: Multi-PDZ domain protein 1
Na^2HPO^4: Sodium phosphate dibasic
NaCl: Sodium chloride

ng: nanogram
OCT: Optimum cutting temperature
Pax2: Paired-box gene 2
PBS: Phosphate buffered saline
PBT: Phosphate buffered saline plus 0.1% Tween-20
PDZ: Post-synaptic density 95 *Drosophila* disc large zonula occludens-1
PFA: Paraformaldehyde
pH: Potential of hydrogen
PKC: Protein kinase C
PP2A: Protein phosphatase 2
RCAS: Replication-competent avian retrovirus
Ret: Ret proto-oncogene
RNA: Ribonucleic acid
RPM: Revolution per minute
SDS: Sodium dodecyl sulfate
SiRNA: Small interfering RNA
SIX2: Homeobox protein SIX2
SSC: Saline sodium citrate buffer
TAL: Thick ascending limb of loop of Henle
TER: Transepithelial resistance
tRNA: Transfer ribonucleic acid
WT1: Wilm's tumor 1
ZO: Zonula Occludens

Acknowledgments

I would first like to thank my supervisors, Aimee Ryan and Indra Gupta. Aimee always encouraged me to be a better scientist, and more than that, a better writer. She pushed my critical thinking and showed me that with determination and dedication anything can be accomplished. Indra was always enthusiastic about my work, she constantly questioned it but with the intentioned of intriguing me into researching more and to take it a step further. Without them my years as a master´s student would have not been the same. I really appreciate their efforts, constant commitment, and availability to me and my research. This was an experience that made me grow as a person and as a scientist.

I would also like to thank Dr. Loydie Majewska and the members of her lab, who contributed with their opinions and comments on how to troubleshoot my experiments. Even though it was not always fun to answer the hard questions, I appreciated the scientific discussions. I want to thank Dr. Pierre Lepage at the Genome Center for his contributions on how to better analyze the raw CLDN sequences of the CAKUT patients. I would also like to acknowledge Clémence Guiraut for making the illustrations for our lab for kidney branching morphogenesis and nephrogenesis and the CAKUT phenotypes.

I think my experience at the lab would have not been such an enjoyable ride without my lab partners. A lot of my knowledge and technical expertise at the bench I owe to Amanda Baumholtz. Thank you for supervising my work and for being there to support my successes and give me advice to overcome my failures. To Enrique, thank you for the good and bad jokes in times of serious work, and for never letting the lab get to quiet. Thank you for the little extra scientific advices. Simon, thank you for enjoying my sarcasm. Jasmine, I am glad you are as forgetful as me sometimes, and thank you for always having time to answer all of my questions. Last, but not least, Fatima, you were the one who kept me going the last few months when it got really hard, thank you for all the cheerful texts and for the conversations in the side room.

I want to dedicate my thesis to my family for their non-stop support and for always believing I can do anything. Gianni, this is also for you because none of this would have been possible without you by my side. You withstood all the bad days and celebrated with me all the good ones. Thank you for your unconditional friendship and love.

Preface

This master´s thesis was written according to the guidelines and format stated by Graduate and Postdoctoral Studies, McGill University. The candidate prepared, and performed all the experiments presented here. The candidate together with her two supervisors, Aimee Ryan and Indra Gupta, analysed the data and edited all the content in this thesis.

CHAPTER I: Introduction

1.1 Kidney Development

Kidney development requires the formation and elongation of tubular structures through the epithelialization of mesenchymal cells. Cells shape changes and molecular signalling control the tissue movements that contribute to the formation of the kidneys. Two of the key processes necessary for kidney development are nephric duct elongation and ureteric bud branching. All vertebrates go through the same morphological changes and embryological tissue movements leading to the formation of the kidneys, differing only in the temporal occurrence of these events.

1.1.1 Nephric Duct Development

The Wolffian duct or nephric duct is the first tubular epithelial structure that forms in the urogenital system (reproductive and urinary system have common origin, the intermediate mesoderm). It is the structure that will give rise to the kidneys and the male reproductive tract. Mesenchymal cells, with migratory properties and lack of cell polarity, are found in the intermediate mesoderm, adjacent to the lateral plate of the embryo. These cells become specified through signals from the lateral plate and start to aggregate (James and Schultheiss, 2003; Attia et al., 2012; Obara-Ishihara et al., 1999).

Aggregated mesenchymal cells transition into fully-differentiated epithelial cells, surrounding a continuous lumen. This tubular structure is known as the nephric duct, which elongates in a rostral to caudal direction. Once the nephric duct is epithelialized, it inserts into the cloaca at the posterior end of the embryo (Joseph et al., 2009). The elongation of the nephric duct is due to the migration and aggregation of mesenchymal-like cells at the posterior end of the embryo as shown in Figure 1. A study in 2015 shows that at the anterior end of the duct, cells are static with a polygonal shape and epithelial. At the posterior end, cells are less differentiated, more motile and mesenchymal-like, extending and retracting in the direction of the elongation. The study suggested that neither cell proliferation nor cell death are implicated in nephric duct elongation (Atsuta and Takahashi, 2015).

As the nephric duct elongates, a series of transient tubules that serve as a filtering system for water, nutrients and waste during different embryological stages develops adjacent to it

(Hiruma and Nakamura, 2003). The first set of tubules is called the pronephros, which is non-functional in most species. Once the pronephros degenerates, the mesonephric tubules start to develop. The mesonephros serves an excretory purpose during early embryogenesis in most vertebrates, and as the mature kidney in fish and amphibians. Once the nephric duct reaches the level of the hindlimb of the embryo, the final metanephric kidney develops through a process known as ureteric bud branching (Attia et al., 2012). Table 1 shows the different stages at which these processes occur in human, mouse and chick.

As mentioned above, the nephric duct will also form the reproductive system in males. During sex determination, the presence of the SRY gene on the Y chromosome specifies the gonads to develop into the testes, which produce testosterone. Secretion of testosterone will promote the development of the nephric duct into the epididymis, vas deferens, seminal vesicle, and efferent ducts. In the female, the absence of SRY leads to a lack of testosterone, which in turn, results in the regression of the nephric duct and the elongation of a second tubular epithelial structure, known as the Müllerian duct (or paramesonephric duct). The Müllerian duct will then give rise to the Fallopian tubes, the uterus, the uterine cervix, and part of the vagina (Renfree et al., 2009; Atsuta and Takahashi, 2016).

When the nephric duct extends, the length of the tube as well as the cell epithelialization that maintains the internal lumen are synchronized both, temporally and spatially. The transcription factors and molecular signalling pathways involved in the regulation and coordination of the mesenchymal and epithelial lineages in the nephric duct have been well described. However, few studies have investigated the cell shape changes and tissue movements mediated by the cytoskeleton that control lengthening of the duct. Cell junctions acquired during epithelialization are essential for these cell shape changes to occur (Atsuta and Takahashi, 2015). In my thesis project I will examine a family of proteins essential for formation of cell junctions and their support for nephric duct elongation.

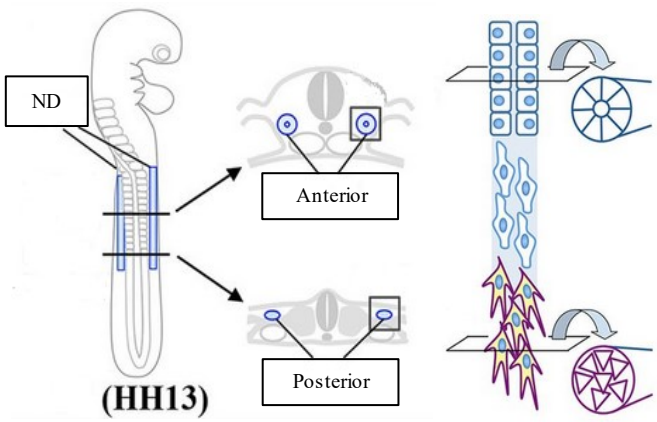

Figure 1. Nephric Duct Elongation in HH13 Chick embryo

On the left is a schematic of a HH13 chick embryo. The elongating nephric duct is illustrated in blue. The middle panel shows schematic transverse sections at a more anterior and a more posterior region of the duct. In the anterior section the nephric duct (blue) is a fully-differentiated tubular structure. In the more posterior section, there is no lumen formed and only undifferentiated mesenchymal cells aggregated. The far-right panel illustrates epithelialization of cells as the nephric duct elongates (Atsuta and Takahashi, 2015).

1.1.2 Ureteric Bud Branching

Ureteric bud branching starts when an outgrowth from the nephric duct, known as the ureteric bud, invades the adjacent metanephric mesenchyme, which is a population of mesenchymal cells derived from the intermediate mesoderm. Reciprocal signalling between the ureteric bud and the metanephric mesenchyme will induce the ureteric bud to elongate and bifurcate in a process called branching morphogenesis (Figure 2). Repetitive branching of the ureteric bud gives rise to the collecting duct system and induces the formation of nephrons, which are the filtering system of the kidney, in a process known as nephrogenesis. Nephrons are formed through signalling from the ureteric bud that induces the mesenchymal cells in the metanephric mesenchyme to condense around the ureteric bud tips. These mesenchymal cells polarize into renal vesicles, which become comma-shaped bodies, and then S-shape bodies. The S-shape body will form the glomerulus, where waste products are first filtered from the blood (Dressler, 2006; Blake and Rosenblum, 2014). The ureteric bud will undergo a number of repeated divisions (approximately 15 times in humans) that will give rise to 900,000 to 1 million nephrons per kidney (Bertram et al., 2011).

There are several key molecules that control both the elongation of the nephric duct and the branching of the ureteric bud, mentioned bellow (Section 1.1.4). It is important to examine the genes that contribute to kidney development and their mouse model studies to better understand the renal system. I am interested on how cell rearrangements can induce the structural changes necessary for tubular formation of the early structures in this system. These cell transitions occur during mesenchymal to epithelial transition (MET), which induces the cell polarization and cell adhesion properties that promote cell epithelialization. How cell shape changes and rearrangements occur can help better understand how groups of cells are regulated to give rise to the kidney.

	Human (gestation day)	Mouse (embryonic day)	Chick (Hamburger Hamilton stages)
Nephric Duct	Day 15	E7	12h (HH13)
Pronephros	Day 18-22	E8 - 8.5	Day 2.5 (HH17)
Mesonephros	Day 24	E9.5	Day 3 (HH20)
Ureteric bud	Day 35-37	E10.5-11	Day 5 (HH25)

Table 1. Timing of Kidney Development in Human, Mouse and Chick.

The morphological processes that occur during nephric duct elongation and ureteric bud branching during kidney development are highly conserved between vertebrates. In humans, the first 9 to 10 branching generations occur by the 15th week of gestation, while in mice it occurs by E15.5. In all three species, branching ceases postnatally but the kidney continues to develop (Takasato and Little, 2015; Davidson, 2009; Uhlenhaut and Treier, 2008; Hamburger and Hamilton, 1992).

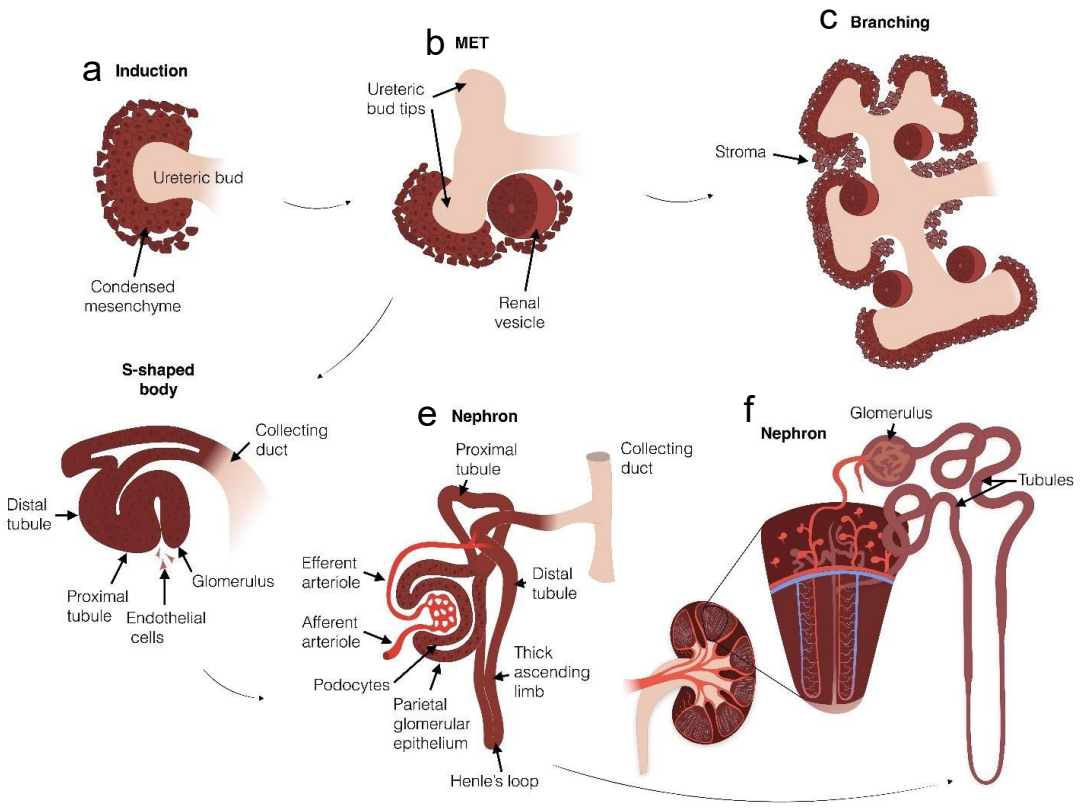

Figure 2. Kidney Branching Morphogenesis and Nephrogenesis

(a) Ureteric bud tip surrounded by condensed mesenchymal cells. (b) Reciprocal signalling between the ureteric bud tip and the surrounding mesenchymal cells will initiate MET of the mesenchymal cells to form renal vesicles. (c) Elongation and bifurcation of the ureteric buds lead to ranching morphogenesis. (d) Renal vesicles will give rise to the nephron by differentiating first into comma- and then into S-shaped bodies that give rise to the distal and proximal tubules, and the glomerulus. The ureteric buds give rise to the collecting duct system of the kidneys (e) Final nephron with vascularization and renal collecting duct system. (f) Ureteric bud branching and MET of mesenchymal cells form the cortex of the kidney, while ureteric bud trunks elongate into the inner kidney forming the medulla.

1.1.3 Cell Shape Changes During Kidney Development

During nephric duct elongation and ureteric bud branching there are several cell shape changes and transitions, such as apical constriction, that induce the organization of epithelial cells into complex structures. Communication of outside-in signals through membrane proteins to the actin cytoskeleton is necessary for cells to move and transition during morphogenesis. Cell junctions, such as the adherens junction and the tight junction, are essential to anchor the cytoskeleton. Cell junctions are necessary for acquisition of apical-basal polarity and cell-to-cell contact (Tepass and Hartenstein, 1994), which is important for cell shape changes during epithelialization.

The purse-string hypothesis has been invoked to explain the cellular changes that occur during branching morphogenesis. This hypothesis is based on apical constriction, a process that occurs as the apical actin microfilaments of epithelial cells contract to decrease the surface area on the apical side of the cell (Baker and Schroeder, 1967) causing cells to change from a columnar to a wedged shape. As the epithelial cell monolayer of the ureteric bud protrudes into the extracellular matrix, the cells start to change shape inducing the formation of an outpouch as shown in Figure 3. Cells involved in the 'outpouches' maintain cell to cell contact and the basement membrane of the epithelial layer remains intact as the lumen extends (Meyer et al., 2004). Apical constriction of cells is necessary for branching of the ureteric bud.

In the ureteric bud, wedge-shaped cells are located at the tip, while columnar cells form the stalk. The equilibrium in the distribution of proliferating and apoptotic cells between the ureteric bud tip and the stalk helps drive the outpouch during branching morphogenesis. At the site of the outpouch, more cell undergo proliferation, compared to the stalk. In contrast, in the stalk there are more apoptotic cells (Meyer et al., 2004).

Some of the signaling molecules, transmembrane proteins, transcription factors, cell junction proteins, growth factors, and others proteins that have been shown to be important for kidney development through mouse studies and sequencing of human patients are highlighted below.

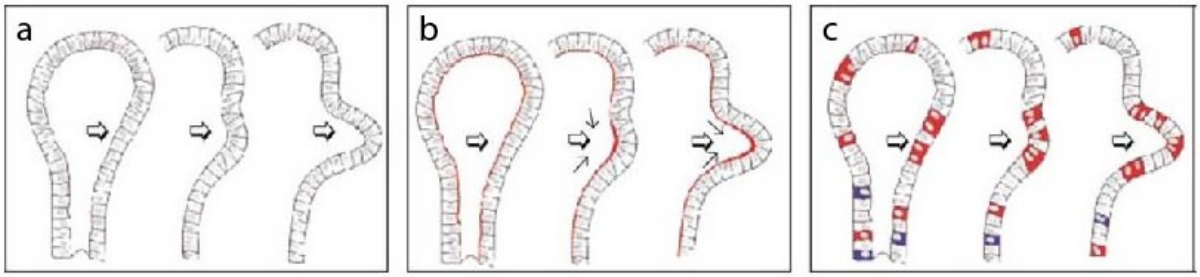

Figure 3. Purse-string Hypothesis in Branchpoint Formation

(a) Branching morphogenesis occurs through the formation of outpouches (open arrows). The epithelial monolayer invades the extracellular matrix by maintaining the basement membrane (red lining) of cells. (b) Cells at the outpouch (arrows) contract into wedge-shape by decreasing the apical surface area through a process called apical constriction. (c) Cells at the outpouch are predominantly proliferating (red), compared to the stalks, where more apoptotic cells (blue) are found (Meyer et al., 2004).

1.1.4 Signalling Molecules and Genes Involved in Kidney Development

There are several proteins involved in the molecular signaling pathways required for nephric duct elongation and ureteric bud branching. In the following section, I will discuss the function of some these proteins, including transcription factors that have been found to regulate signaling molecules. Roles for transcription factors in kidney development have been identified through knock-out, null and conditional mouse model studies (Nagalakshmi and Yu, 2015). Patients with urogenital diseases were found to have mutations in most of these genes, reiterating their importance in kidney development.

1.1.4.1 WT1

WT1, Wilms tumor 1, is a transcription factor that is essential for the development of the urogenital system. WT1 is expressed in the metanephric mesenchyme, in the progenitors of the nephron and in Sertoli cells in the testis (Hammes et al., 2001; Jiang et al., 2017). WT1 has a role in cell differentiation, cell growth, and apoptosis, and it has been shown to be necessary for ureteric bud invasion into the adjacent metanephric mesenchyme (Kreidberg, 2010).

Targeted mutations in *Wt1* in mice lead to bilateral renal agenesis, where both kidneys are absent. This phenotype is caused by apoptosis of the cells in the metanephric mesenchyme as well as the inability of the ureteric bud to invade the metanephric mesenchyme (Kreidberg et al., 1993; Davies et al., 1999).

Mutations in humans reflect the importance of *Wt1* in the development of the urogenital system. Several syndromes including Denys-Drash syndrome (DDS), and Frasier syndrome (FS) are associated with mutations in *WT1*. Both syndromes are autosomal dominant and affect the development of the urogenital system, often resulting in tumors in the genitalia and in the kidney. DDS is caused by point mutations in *WT1* and can result in nephrotic syndrome. Affected patients exhibit diffuse mesangial sclerosis (glomerular damage) that progresses to renal failure. FS is caused by an intronic mutation, has overlapping features with DDS and also affects the kidney and genitalia (Hammes et al., 2001).

1.1.4.2 GDNF and RET

GDNF, glial-cell-line derived neurotrophic factor, signals through a receptor tyrosine kinase RET and its co-receptor GRFα1. Both receptors are expressed in the nephric duct and ureteric bud epithelium (Costantini and Kopan, 2010). GDNF is only expressed in the metanephric mesenchyme and induces ureteric bud outgrowth from the nephric duct (Nagalakshmi and Yu, 2015). Once the ureteric bud develops, Ret expression becomes restricted to the distal bud tips and decreases in the ureteric bud trunk and the nephric duct. Similarly, GDNF becomes restricted to the undifferentiated mesenchyme around the ureteric bud tips. In the absence of Ret, GDNF signals through GRFα1, which has a slightly broader expression in the ureteric bud compared to Ret (Costantini and Shakya, 2006).

In mice, null mutants for *Ret* or *Gdnf* do not form the ureteric bud, which results in renal agenesis (Nigam and Shah, 2009). However, in the absence of these genes there are some mice that develop rudimentary kidneys. Heterozygous mutant mice also develop blind ending ureters and dysplastic kidneys, suggesting that GDNF is important to induce the outgrowth of the ureteric bud and branching morphogenesis (Schuchardt et al., 1996).

A small percentage of patients with renal agenesis have mutations in both *RET* and *GDNF* (Davis et al., 2014). Even though GDNF and Ret play an important role in regulating the outgrowth of the ureteric bud, the formation of rudimentary kidneys in mutant mice suggests that there are other molecular factors that regulate outgrowth. Upstream of GDNF there are other transcription factors that regulate kidney development, such as Pax2, Eya1, and Six.

1.1.4.3 PAX2

Pax2 is a transcription factor and member of the paired box family. It is expressed in the developing kidney, the ureter, the mesenchymal cells adjacent to the nephric duct, the nephric duct, the pronephros, the mesonephros and the metanephros (Dressler et al., 1990; Brophy et al., 2001). Studies have shown that Pax2 is a target of WT1 in the metanephric mesenchyme (Hartwig et al., 2010).

In the mouse, *Pax2* homozygous mutants lack kidneys, ureters and genital tracts, demonstrating the role of *Pax2* in development of the urogenital system (Torres et al., 1995).

PAX2 mutations have been found in many patients with kidney and urinary tract defects. In 2006, the ESCAPE (European multicenter effect of strict blood pressure control and ACE inhibition on CRF progression in pediatric patients) study published the discovery of four heterozygous *PAX2* mutations in seven different patients with renal hypoplasia and/or dysplasia (Weber et al., 2006). A more recent study published in 2016, which sequenced 453 patients with kidney hypodysplasia, reported only three patients with *PAX2* mutations (Nicolaou et al., 2016). In a published study on the CKiD (Chronic Kidney Disease) cohort, 73 children with renal hypodysplasia and aplasia were sequenced for *PAX2* and *HNF1B* mutations. They found three different mutations in *PAX2*, including a splice site, a frameshift and a missense mutation, and a frameshift and missense mutation in *HNF1B* (Thomas et al., 2011). Thus, only a subset of cases with kidney disease can be explained by mutations in *PAX2*. However, due to the fact that homozygous *Pax2* mutations have a severe phenotype in mice leading to a lethal outcome, CAKUT patients may have a reduced frequency of these mutations.

1.1.4.4 EYA1 and SIX2

Eya1, eyes absent homolog 1 transcription factor, is expressed in the mesonephros, and in the progenitor cells of the metanephric kidney. Eya1 is necessary for the initial elongation and bifurcation of the ureteric bud and it continues to be expressed in the renal tubules throughout mouse development (Xu et al., 1999). In the mouse, deletion of *Eya1* leads to premature differentiation of nephron progenitor cells.

Six2, encodes a homeobox protein expressed in the mouse kidney throughout development. It is necessary to maintain undifferentiated nephron progenitor cells in the metanephric mesenchyme. Knock-out mouse models of *Six2* have severe renal dysplasia (Xu et al., 2014; Weber et al., 2008), and loss of Six2 leads to premature epithelization of the nephron progenitors. Eya1 requires Six2 to localize to the nucleus, and Eya1 regulates phosphorylation of Myc, a transcription factor involved in cell cycle progression. Myc has been shown to play a role in cell proliferation of the metanephric mesenchymal cell progenitors (Xu et al., 2014; Kobayashi et al., 2007).

In humans, mutations in *EYA1* and *SIX1* cause branchio-otorenal (BOR) syndrome which results in renal abnormalities, the most common being kidney hypoplasia (Li et al., 2010; Ruf et

al., 2004). There are also mutations in *EYA1* in patients with otic defects (Li et al., 2010). Human mutations in *SIX2* are associated with defects in the formation of mesonephric tubules and renal hypodysplasia (Kobayashi et al., 2007).

1.1.4.5 LIM1

Lim1, a member of the LIM-class of homeodomain transcription factor expressed in the intermediate mesoderm, the nephric duct, the mesonephros and the metanephros. It is also observed in the comma-shaped body, the S-shaped body, and the glomerulus in the mouse (Shawlot and Behringer, 1995; Kobayashi et al., 2005).

In the mouse, *Lim1* homozygous mutants do not develop kidneys or gonads. Mutant mice start to form a nephric duct, but after the mesonephros has formed, the posterior end of the duct starts to degenerate and it fails to give rise to the ureteric bud (Shawlot and Behringer 1995; Tsang et al., 2000). Another study showed that in *Lim1* mutant mice, differentiation of lateral plate and intermediate mesoderm was affected, resulting in disorganized tissues and decreased expression of *Pax2* (Tsang et al., 2000). The presence of *Pax2* expression in the mesonephros of *Wt1* and *Lim1* mouse mutants suggests that *Pax2* acts upstream of *Lim1* and *Wt1* (Bouchard et al., 2002).

1.1.4.6 HNF1β

The transcription factor HNF1β, hepatocyte nuclear factor 1β, is highly expressed in the kidney, liver, and pancreas. During mouse kidney development it is required for invasion of the ureteric bud into the metanephric mesenchyme and for the mesenchymal to epithelial transition required for nephron formation (Lokmane et al., 2010).

Conditional knock-out models for *HNF1β* show a range of phenotypes that depend on the developmental time point of inactivation. When *HNF1β* is inactivated in the germline, it is embryonic lethal. However, in *HNF1β* homozygous mutant mouse embryos the expression patterns of *Lim1*, *Pax2*, *Gdnf* and *Ret* expression are affected suggesting that *HNF1β* is important during nephric duct differentiation, and ureteric bud branching through the control of *Gdnf* and *Ret* signaling (Lokmane et al., 2010). Other studies have shown that inactivation of *HNF1β* in the metanephric mesenchyme leads to the absence of proximal and distal tubules, and deformed S-

shaped bodies in early nephron precursors (Massa et al., 2013). In humans, mutations in *HNF1β* are associated with maturity-onset diabetes of the young (Edghill et al., 2013), and with kidney malformations. Four mutations in *HNF1β* were previously identified in 73 children with congenital kidney malformations (Thomas et al., 2011).

1.1.4.7 GRHL2

Grainyhead-like 2 (Grhl2) is a transcription factor important for epithelialization. Grhl2 is involved in epithelial barrier formation, neural tube closure and tumor suppression (Narasimha et al., 2008; Pifer et al., 2016). It also has a role in epidermis assembly, neural crest formation, and wound healing. Furthermore, Grhl2 acts as a tumor suppressor by being involved in the deregulation of epithelial to mesenchymal transition (Cieply et al., 2013). *Grhl2* is expressed in the nephric duct, the ureteric bud, and the collecting ducts in the kidney (Werth et al., 2010). Homozygous mutant mice for *Grhl2* have craniofacial and neural tube closure defects and die during embryogenesis (Pyrgaki et al., 2011).

Aue and colleagues (2015) found that in *Grhl2* deficient mice, the lumen of the nephric duct at E10 fails to expand and in some mice it collapses (Aue et al., 2015). Functional analysis using TER (transepithelial electrical resistance) in murine inner medullary collecting duct cells (IMCD-3) showed that Grlh2 has a function in epithelial barrier formation and lumen expansion. Grhl-2 acts as a transcriptional activator, activating *Rab25* expression, a GTPase involved in epithelial morphogenesis, *Claudin-4*, a tight junction protein, and *Ovol2* (ovo-like 2 zinc finger transcription factor), which are necessary for epithelial development and differentiation (Aue et al., 2015).

The transcription factors, receptors, and signalling molecules described above are all important for kidney development at different embryonic stages. The coordination of stage and tissue-specific expression of these genes model and direct tissue movements that are critical for kidney development. However, as previously mentioned, mutations in any of these particular genes can result in developmental defects in the kidney, which are known, together with urinary tract defects, as CAKUT (Congenital anomalies of the kidney and the urinary tract).

1.2 CAKUT

1.2.1 What is CAKUT?

Congenital anomalies of the kidney and the urinary tract (CAKUT) are developmental defects that affect the kidneys, the ureter and/or the urethra. CAKUT comprises a range of heterogeneous phenotypes that result from different genetic and environmental factors. In children, CAKUT is responsible for most cases of end-stage renal disease and it has an incidence rate of around 1-6 per 1,000 live births (Harambat et al., 2012; Hildebrandt, 2010).

Although ultrasound imaging during pregnancy has facilitated the diagnosis of CAKUT, there are cases that can remain undiagnosed (Capone et al., 2017). For instance, some forms of CAKUT are clinically silent, in which the patient has no critical consequences during their whole life and might never find out of the defect. The fact that some cases are not diagnosed might suggest a higher incidence of CAKUT than what has been reported in the past. Knowledge of mutations in specific genes can help the screening process in families with a history of the disease. However, the variability and the incomplete penetrance of the CAKUT phenotypes has made the screening process difficult. So far, there are no available targeted treatments other than dialysis or a kidney transplant. Among the renal phenotypes seen in patients are hypoplasia, dysplasia, agenesis, hydronephrosis, multicystic kidney, and horseshoe kidney (Nicolaou et al., 2015). For the purpose of this thesis, we have focused on renal agenesis, hypoplasia, and dysplasia (Figure 4).

1.2.2 Genetic Background

Renal agenesis is the absence of one (unilateral) or both (bilateral) kidneys. It is as rare as 1 in every 10,000 live births and when it occurs unilaterally it can be clinically silent. When it occurs bilaterally it results in severe deficiency of amniotic fluid during pregnancy, which can result in further malformations and lead to a lethal outcome (Hwang et al., 2014). Renal hypoplasia is defined as a smaller kidney with a reduced number of nephrons. By ultrasound imaging, renal hypoplasia might look the same as dysplasia, a renal malformation in which nephrons are not fully developed resulting in a smaller kidney composed of malformed or undifferentiated tissue. Only a renal biopsy or a nephrectomy can establish if the tissue is

hypoplastic or dysplastic (Sanna-Cherchi et al., 2007). All three of these phenotypes are represented in Figure 4.

When finding the cause of CAKUT it is also important to consider that familial CAKUT presents itself with a range of different phenotypes within a single family. Several families with renal hypoplasia and dysplasia have been identified with autosomal dominant inheritance and low penetrance (Bulum et al., 2013). However, not all family members are sequenced or diagnosed. Here is when sequencing cohorts of patients becomes important for the discovery of new mutations and in the diagnostic process.

1.2.2.1 Genetic Studies Approaches

1.2.2.1.1 Candidate Gene Studies

Mouse model studies have demonstrated the importance of several genes for kidney development (Nicolaou et al., 2015). Screening of CAKUT patients for single genes that were previously identified in mouse studies, has led to the identification of disease-causing mutations. Mutations that caused similar phenotypes in patients as those seen in mouse models led to the conclusion that CAKUT was a monogenic disease. Hence, it was previously thought that only a handful of genes were responsible for renal and urinary tract malformations. Several studies with candidate gene approaches showed a number of mutations in single genes in different patients and in familial cases with renal and/or urinary tract phenotypes. Amongst these genes were *BMP*, *SIX2*, *EYA1*, *HNF1B*, *PAX2*, *GATA*, and *RET* (Weber et al., 2006; Ruf et al., 2004; Nicolaou et al., 2016; Thomas et al., 2011; Saisawat et al., 2012; Hwang et al., 2014).

Candidate gene approaches in familial cases led to the discovery of disease causing mutations in single genes in different syndromes. An example of this is the mutational analysis done in a family with optic nerve colobomas, renal hypoplasia, mild proteinuria, and vesicoureteral reflux (Sanyanusin et al., 1995). The phenotype was the consequence of a single nucleotide deletion in exon 5 in *PAX2*, causing the renal coloboma syndrome. Another example is a pedigree study of a Norwegian family with mild diabetes, renal disease, and genital malformations in which *HNFIβ* mutations segregated with the phenotype (Lindner et al., 1999).

To date, mutations in single genes have been identified in less than 12% of sequenced CAKUT patients (Nicolaou et al., 2016). A study in 2013 suggests that familial cases only account for a small percentage (10-20%) of all CAKUT, yet there is a high number of undiagnosed relatives in families with CAKUT (Bulum et al., 2013). This suggests that approximately 80% of cases will be due de novo or rare genetic mutations, environmental factors only, or a combination of both environmental and genetic factors that are yet to be identified. In order to start identifying all the genes contributing to CAKUT more efforts are put every year into next-generation sequencing.

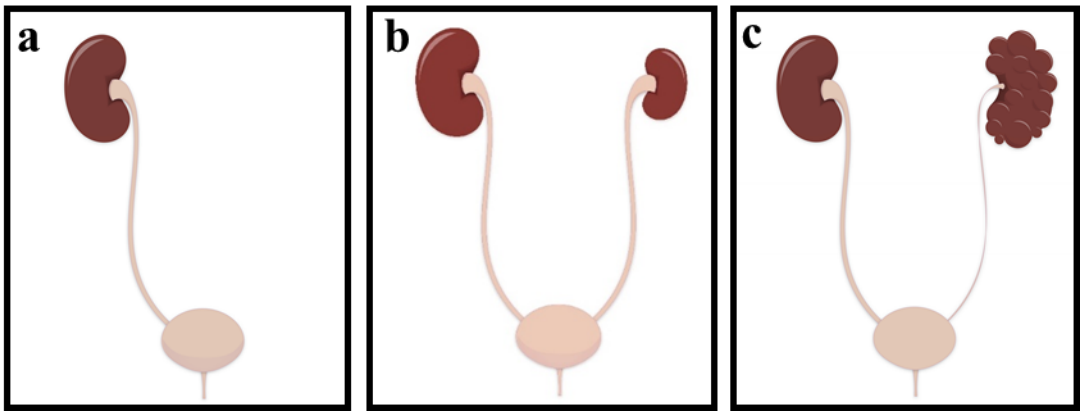

Figure 4. CAKUT Phenotypes: Renal Agenesis, Hypoplasia and Dysplasia

Schematic of three different kidney malformation classified under CAKUT. (a) Renal agenesis, when one or both kidney are absent, due to potential developmental defects in nephric duct elongation, ureteric bud branching or MET. (b) Kidney hypoplasia, underdevelopment of the kidney which makes it smaller with fewer nephrons than a normal adult kidney. (c) Kidney dysplasia, similar in ultrasound to hypoplasia, is abnormal kidney tissue that can potentially lead to formation of cysts.

1.2.2.1.1 Next-generation Sequencing

Defining the cause of CAKUT has been challenging because of its phenotypic and genetic variability. Within a single family there is sometimes incomplete penetrance causing the range and the expression of phenotypes to differ vastly between families and individuals (Nicolaou, et al., 2015). Next-generation sequencing permits the rapid sequencing of genomes at lower costs every year. With the increasing use of NGS technologies more patients and their families are sequenced in the hope of finding disease-causing mutations. Although there is still uncertainty with respect to the genetic causes of CAKUT, the effort on sequencing more patients worldwide each year is increasing the number of variants discovered.

For instance, a study with targeted exome sequencing of 330 genes that included 55 candidate genes and 275 genes with no previous links to CAKUT, revealed 24 highly penetrant pathogenic mutations in seven genes (Heidet et al., 2017). However, other studies suggest that the number of sequenced variants is low in the CAKUT population and sequencing cohort studies tend to have a small number of patients. In 2006, Weber *et al.* sequenced 99 unrelated children with renal failure from renal hypoplasia or dysplasia for mutations in *HNF1β*, *PAX2*, *EYA1*, *SIX1*, and *SALL1*. Only 15% of the patients harboured a mutation in one of these genes. Mutations in *SIX1, SALL1,* and *EYA1*, were less frequently observed as compared to mutations in *HNF1B* and *PAX2* (Weber et al., 2006). Another study in a Japanese cohort, screened patients for *HNF1β* mutations. The results showed that only 5 out of 50 patients with CAKUT had genetic alterations in *HNF1β*, including deletions, and truncating mutations. Showing that 10% of cases are explained by mutations in *HNF1β* or *PAX2* (Nakayama et al., 2010).

In a similar study, a group at the University Medical Center Utrecht in The Netherlands sequenced 208 candidate genes that were previously linked to CAKUT. They identified ~12,000 variants in 453 patients, the largest sequenced CAKUT cohort yet. After variant filtering based on amino acid change and predicted sequence variance, 180 variants were confirmation by Sanger sequencing. Only five variants in four different genes, *PAX2*, *SIX5*, *HNF1β*, and *UMOD* (uromodulin) were considered fully penetrant and causal mutations of CAKUT (Nicolaou, et al., 2016).

Gene mutations may either account for some or all renal malformations, have an additive effect to the already known mutations, or act as risk factors in combination with environmental causes. There are few studies that look at the environmental factors affecting CAKUT patients, but here are some of the most relevant.

1.2.3 Environmental Factors

Environmental factors can contribute to kidney malformations. Familial cases can arise from heritable or common shared environmental factors, such as poverty or maternal nutrition. For instance, in a case-control study in Colorado, prenatal environmental risk factors such as pre-gestational maternal diabetes mellitus and maternal age were associated with renal agenesis (Parikh et al. 2002). The risk for renal agenesis is known to be increased if the mother is less than 18 years old or over 35 years old. Other environmental risk factors for CAKUT include maternal obesity and excessive maternal alcohol consumption (Woroniecki, et al., 2012). Another study in Canada looked at the difference between pre-gestational and gestational exposure to diabetes mellitus as a risk factor for developing CAKUT. The conclusion was that exposure to diabetes in the first 20 weeks of pregnancy is associated with CAKUT (Dart et al., 2015).

Even though there have been mouse models, candidate approach studies, sequencing of many cohorts, and environmental approaches, there is still no certainty of what are the causal factors of CAKUT. Sequencing studies demonstrate that the number of mutations associated with CAKUT are low, and that cohort size is an important factor. The sequencing results vary from one study to the other, and there are few single inherited gene mutations that lead to renal malformations. Most studies also lack further statistical analysis and functional studies to support the true pathogenicity of the mutations. There are several genes that have been shown to be important during kidney development, but have yet to be linked to CAKUT. For this reason, it is important to continue sequencing patients for new candidate genes.

For my thesis project, I sequenced patients with renal dysplasia, agenesis, and hypoplasia for mutations in claudins, proteins that have been found to have an important role in epithelial barrier and tubule formation, as well as in tissue morphogenesis during development (Bagnat et al., 2007; Moriwaki et el., 2007; Sun et al., 2015; Baumholtz et al., 2017). Claudins are essential

for the formation and maintenance of tight junctions, and have been shown to regulate morphogenesis in different epithelial structures. In order to understand the role and the interactions of claudins in the tight junction, it is necessary to first understand the tight junction and its components.

1.3 Tight Junctions

Tight junctions are the most apical junctional complex that comprises the contact points between epithelial cells. They were first identified by electron microscopy (EM) (Farquhar and Palade, 1963). In freeze-fracture electron micrographs, tight junctions appear as continuous intramembranous strands or fibrils in the protoplasmic (P) face (Staehelin, 1973). These apical "kissing points," are important for regulating cell polarity, paracellular transport and permeability, as well as cell adhesion (Frömter and Diamond, 1972).

1.3.1 Tight Junctions and Polarity

Cell polarity allows the organization of the cytoskeleton and the membrane. It prevents the mixing of apical and basal components by forming compartments along the apical and basal side of the cell (Saitou et al., 1998). Tight junctions are the fence mechanism that prevents the mixing of lipid and protein components in the plasma membrane, by restricting them to either the apical or basolateral domain to maintain cell polarity (Schneeberger and Lynch, 1992). Tight junctions also act as gates to regulate the paracellular movement of ions and molecules.

A structure such as the nephric duct, is built by mesenchymal cells that acquire polarization, and epithelialize into a tube with a single lumen. Apical-basal polarity of epithelial cells in the nephric duct, acquired during MET, helps the formation of the central lumen (Andrew and Ewald, 2010). Different molecular signalling cues drive epithelialization, maintaining the structure of the nephric duct as it elongates and forms the lumen. Once the nephric duct is polarized, it will start to elongate. The elongation process is induced by dividing cells and migratory cells with forward-oriented protrusions (Guioli et al., 2007).

During branching morphogenesis, bifurcation of the ureteric bud occurs by elongation of the bud into a continuous epithelium with an open luminal space (Sawyer et al., 2010). Cell polarity regulates apical constriction through different pathways. It requires the localization of

GTPase RhoA at the apical side, which activate ROCK, phosphorylating myosin regulatory light chains. Myosin induces the contraction of the actin cytoskeleton, which results in reduction of the surface area at the apical side, resulting in apical constriction (Martin and Goldstein, 2014).

1.3.2 Tight Junctions and Permeability

Tight junctions regulate permeability of epithelial cell layers and act as barriers controlling the movement of water and ions through the paracellular space between epithelial cells (Van Meer and Simons, 1986). While there are other transporters and proteins in the apical and basolateral membrane necessary for active transport across the cell, the tight junctions control paracellular transport (Weber, 2012). Claudins, tight junction membrane proteins, have been shown to have an important role in determining the characteristics and permeability of the barrier and the different selectivity properties between epithelial cell layers in different tissues (Angelow et al., 2008).

Tight junctions regulate ion conductance through pores that can open and close. Several proteins within the tight junction complex form channels that are selective to specific anions or cations, allowing the flow of specific molecules across the paracellular space (Van Itallie and Anderson, 2006). Altering the protein composition of the tight junction has major effects on permeability and barrier properties of the tight junction that do not necessarily disrupt its structural composition (Weber, 2012). Tight junctions are dynamic in their functionality and capable of making a distinction in charge and size when regulating the passage of ions and molecules through the paracellular space.

1.3.3 Tight Junctions and Adherens Junctions

In epithelial cells, cell-to-cell contact is achieved through different cell adhesion proteins at the junctions. Cadherins, a calcium dependent type-1 transmembrane protein, are necessary for the assembly of adherens junctions and desmosomes. Both are contact points between cells located below the tight junction (Geiger, 1987). Adherens junctions mediate cell adhesion through interaction of cadherin family members, such as transmembrane glycoproteins like E-cadherins and α-catenins (Hartsock and Nelson, 2008). To ensure stable interactions, cadherins

accumulate at the adherens junction and then spread laterally to help form the mature adherens junction (Yap et al., 1998).

There are other protein complexes that form and maintain adherens junctions. For instance, nectins, which recruit cadherins, are calcium-independent cell adhesion molecules that contain three immunoglobin domains. It has been shown that nectins form cell-to-cell contacts and then recruit cadherins to form the adherens junction. Nectins have also been shown to mediate the formation of tight junctions (Takai et al., 2003; Yano et al., 2017). Other proteins include GTPases, such as TARA, an actin-binding protein that activates TRIO. TRIO then activates Rac, which induces actin polymerization, a process that is also induced by other protein complexes such as ARP2/3 (Anderson and Van, 2009).

Adherens junctions and tight junctions are comprised of protein complexes. Contact points between epithelial cells are achieved through extracellular domains of transmembrane proteins and their intracellular link to the actin cytoskeleton. Transmembrane proteins participate in signalling pathways, including the regulation of gene transcription (Hartsock and Nelson, 2008). In order for the tight junction to assemble, the adherens junction needs to form first, due to E-cadherin recruitment promoting actin organization and apical-basal polarity (Gumbiner et al., 1988).

1.3.4 Tight Junction Proteins

1.3.4.1 ZO-1

The first protein identified to be part of the junctional complex, was Zona occludens-1 (ZO-1), a peripheral membrane protein (Stevenson et al., 1986). ZO proteins (ZO-1, ZO-2, and ZO-3) are characterized by a PDZ binding domain, a SH3 domain and a guanylate kinase homologous domain (Hartsock and Nelson, 2008). ZO-1 and ZO-3 have been shown to bind to α-catenin, while ZO-1 and ZO-2 bind directly to occludin, another tight junction protein. ZO proteins also bind to adherens junction proteins such as cadherins (Itoh et al., 1999), and some ZO proteins, such as ZO-1 can bind individually to ZO-2 or ZO-3, but there is no known complex formed between ZO-2 and ZO-3 (Utepbergenov et al., 2006). ZO proteins serve primarily as scaffolding proteins that link tight junction transmembrane proteins, such as claudins, occludins, and JAMs (junctional adhesion molecules) to the cytoplasmic cytoskeleton

and mediate the interaction with other cytoplasmic proteins (Rajasekaran et al., 1996; Haskins et al., 1998).

1.3.4.2 Occludin

Occludin was first characterized in the chicken as an integral membrane protein localized to the tight junction in epithelial and endothelial cells (Furuse et al., 1993). Occludin has a molecular mass of 60-65 kDa. It contains four transmembrane domains, NH_2- and COOH-cytoplasmic domains, and the COOH-terminal tail contains a ZO-1 binding site. There are two isoforms that result from alternative splicing of the same transcript (occludin and occludin 1B). There are no differences in their tissue distributions, however, they differ in their functionality and are distinctly regulated (Muresan et al., 2000).

It was previously shown that occludin was involved in both barrier, as well as cell adhesion functions of the tight junction (Balda et al., 1996; Van Itallie and Anderson, 1997). However, later studies showed that *Occludin* null-mice had no barrier dysfunction in tight junctions. These mice did show other phenotypes, including growth retardation, gastric epithelium inflammation and hyperplasia, absence of cytoplasmic granules in duct cells of the salivary gland, and calcification in the brain and testicle atrophy (Saitou et al., 2000).

Even though occludins have a role in cell adhesion, they are not necessary for tight junction formation (Wong and Gumbiner, 1997). Evidence for this statement comes from a study done using embryonic stem cells deficient in occludin. Once these cells were put in suspension culture, both the wildtype and occludin-deficient cells formed cystic embryoid bodies in a similar time period. Analyses showed that there was no difference in the composition of the tight junction between wildtype and occludin-deficient cells, and in both cell lines, ZO-1 localized to the tight junction (Saitou et al., 1998).

1.3.4.3 JAMs

Junctional adhesion molecules (JAMs) are transmembrane glycoproteins that localize to the tight junction. JAMs are part of the immunoglobulin superfamily, with two immunoglobulin-like domains, one transmembrane domain, and one cytoplasmic tail containing a PDZ domain (Garrido-Urbani et al., 2014). Through the PDZ binding domain, JAMs interact with polarity

complex proteins and interact with other tight junction associated proteins, regulating the acquisition of cell polarity (Liang et al., 2000). In a study in 2001, JAMs were found to bind to ZO-1 and PAR3, a polarity protein, directly through its PDZ binding domain. Similar to occludin, JAMs fail to induce tight junction formation when introduced in L fibroblasts (Itoh et al., 2001). In another study, JAMs were shown to participate in cell-to-cell adhesion as well as in the regulation of leukocyte migration in the immune system (Liu et al., 2000).

1.4 Claudins

Claudins are a family of integral transmembrane proteins important in regulating tissue morphogenesis during embryonic development. Of all the proteins that comprise the tight junction, claudins are the only ones necessary to form and maintain the tight junction (Furuse et al., 1998). Claudins determine the permeability and barrier properties of the tight junction. Some claudins are known to form channels to allow the passage of specific ions, and others help seal the paracellular space by acting as a barrier. Depending on the claudin composition, the tight junction becomes ′leaky′ or ′tight′ to the pass of specific ions and molecules.

1.4.1 Claudin Structure

To date there have been 24 family members identified in humans, 25 in mice, and 17 in chicken. Claudins range in size from 18 to 27 kDa, and contain two extracellular loops, four transmembrane domains, and N-terminal and C-terminal cytoplasmic domains. The first extracellular loop contains approximately 50 residues, including a highly conserved motif that regulates ion-selectivity. The second extracellular loop is shorter, between 16 and 33 amino acids, and interacts both, homotypically and heterotypically with other claudins (Furuse et al., 1999). The four hydrophobic transmembrane domains contribute to *cis*-interactions within the apical membrane, and the C-terminal tail allows for interaction with other proteins at the tight junction cytoplasmic plaque. The C-terminus contains a terminal peptide sequence YV that binds to the PDZ domain of other proteins (Figure 5). Including ZO-1, ZO-2 and ZO-3, which links the tight junction to the actin cytoskeleton (Krause et al., 2008; Findley and Koval, 2009).

1.4.2 Claudin Post-translational Modifications

1.4.2.1 Phosphorylation

Claudins are regulated through different mechanisms. Posttranslational modifications, such as phosphorylation have been shown to regulate claudin localization and tight junction assembly. Non-conserved residues in the C-terminal tail of claudins are phosphorylated by different kinases. For instance, phosphorylation by Protein Kinase A decreases the assembly of Claudin-3 into tight junctions (D'Souza et al., 2005), but it is necessary for the assembly of Claudin-16 into the tight junction (Banan et al., 2005). While phosphorylation of Claudin-1 by aPKC and PKA was found to induce its assembly into the tight junction (French et al., 2009), dephosphorylation of Claudin-1 by PP2A (protein phosphatase 2) increases barrier permeability (Nunbhakdi-Craig et al., 2002). In another study, overexpression of Claudin-1 on the right side of the embryo alters the direction of heart looping, a mechanism driven by PKC phosphorylation in the C-terminal tail of Claudin-1 (Simard et al., 2006).

Phosphorylation of claudins is important for tight junction formation, maintenance, and permeability. For example, phosphorylation by myosin light chain kinase (MLCK) and rho kinases is associated with changes in the permeability properties of tight junctions (Turner et al., 1999). EphA2 was shown to phosphorylate a tyrosine in the Claudin-4 tail, decreasing its interaction with ZO-1 and hence reducing Claudin-4 localization to the tight junction and enhancing paracellular permeability (Tanaka at el., 2005). The outcome of phosphorylation is dependent on the Claudin that is being modified, the position of the amino acid and the kinase involved.

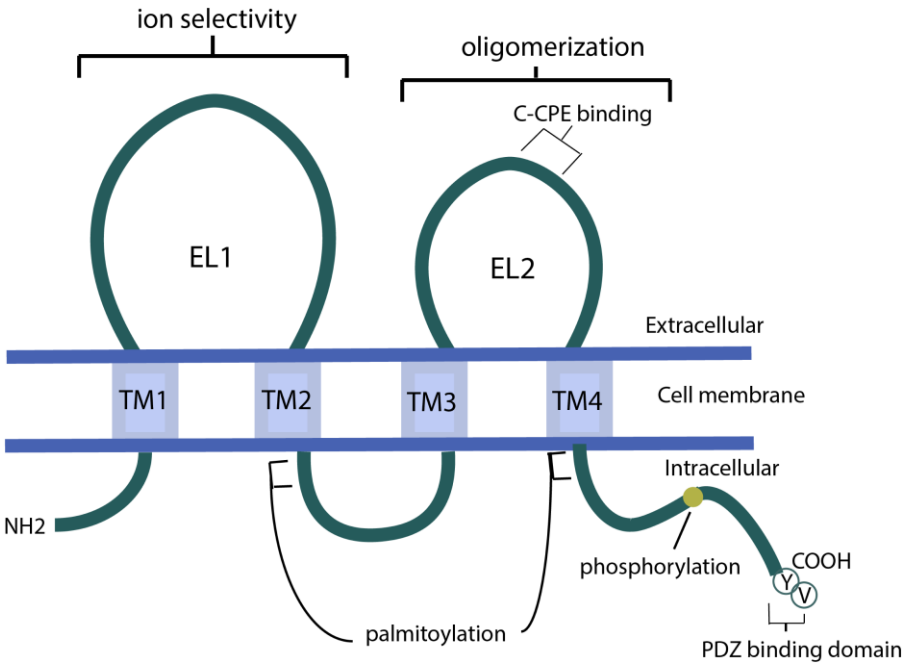

Figure 5. Schematic of Claudin Structure

Claudins are composed of two extracellular loops (EL1 and EL2), four transmembrane domains (TM1, TM2, TM3, TM4), and N-terminal (NH2) and C-terminal (COOH) cytoplasmic domains. EL1 has conserved amino acids that regulate ion selectivity, while EL2 participates in oligomerization with other claudins and in some members it is has a sequence recognized by C-CPE (C-terminal domain of *Clostridium perfringens* enterotoxin). The C-terminal tail interacts with other tight junction proteins, contains phosphorylation sites (yellow), and a binding domain (YV) for PDZ binding proteins. Palmitoylation sites are located in the intracellular domains.

1.4.2.2 Palmitoylation

Palmitoylation is the addition of a fatty acid such as palmitic acid to cysteine residues. Palmitoylation can influence claudin protein interactions andtight junction localization. For instance, Claudin-14 has different sites of palmitoylation at cysteines after the second and fourth transmembrane domains (Van Itallie et al., 2005). Mutating the cysteines in Claudin-14 did not affect the ability of the protein to localize to cell-cell contacts, but it did not localize properly to the tight junction. Palmitoylation occurs in other claudins as well, Claudin-1, -2, -3, and -4, where it is required for their localization to the tight junction (Van Itallie et al., 2005).

1.4.3 Claudin Interactions

As mentioned above, claudins have residues that can be modified to affect their interactions with other proteins and/or promote the integration of claudins within tight junctions. Claudin posttranslational modifications can also regulate paracellular permeability, or tight junction formation. The following are some of the interactions that occur between claudins and other proteins required to maintain tight junction function. Claudin PDZ binding motifs allow for the interaction with scaffolding proteins associated with the tight junction. Through this domain, most claudins interact with ZO-1 and ZO-2 (claudin-8 can also interact with ZO-3), linking the tight junction to the actin cytoskeleton (Figure 6). Other tight junction-associated proteins include MUPP1, multi-PDZ domain protein 1, which interacts with Claudin-1, -3, -8, and -14 (Jeansonne et al., 2003; Hamazaki et al., 2002). MUPP1 contains 13 PDZ binding domains, and has been found to also interact with JAMs through these domains. By immunofluorescence analysis, MUPP1 localizes exclusively to the tight junctions in polarized epithelial cells. Due to its localization and binding affinities, MUPP1 is thought to act as a scaffold protein recruiting claudins and JAMs to the tight junction (Hamazaki et al., 2002). A third protein interactor of claudins is occludin. According to a study that developed a peptide designed with the last part of the residues in the first extracellular loop of Claudin-1 was able to disrupt the tight junction and increase paracellular permeability *in vivo*. It was observed that this Claudin-1-derived peptide interacted with both Claudin-1, and occludin (Mrsny et al., 2008).

Claudin family members participate in homo- and heterotypic interactions in both *cis* and *trans* (Furuse et al., 1999). *Cis* interactions occur between claudins on the lateral side of the same

cell, and *trans* occur between claudins on opposing cells. Examples of *cis* heterotypic interactions are Claudin-16 with -19 and between Claudin-4 and -8 (Hou et al., 2010). Knock-down of *Claudin-19* and *Claudin-16* in mice demonstrated them to be interacting partners necessary for their assembly into the tight junction (Hou et al., 2009). In mouse kidney inner medullary collecting duct cells (mIMCD-3), Claudin-4 acts as a paracellular chloride channel and interacts with Claudin-8. When Claudin-8 is depleted from the tight junction, Claudin-4 fails to assemble into the tight junction, which leads to a reduction in chloride conductance (Hou et al., 2010).

Trans interactions have also been shown between different claudins. Heterotypic interactions are rare among claudins, but homotypic interactions occur between Claudin-1, -2, and -3. These interactions occur through both the first and the second extracellular loops (Furuse, et al., 1999). Studies showed that changing a single amino acid in a highly conserved region in the first extracellular loop of Claudin-3 to make it a Claudin-4 amino acid, induced heterotypic binding between two claudins, which do not normally interact. Suggesting that conserved residues in the first extracellular loop are capable of controlling claudin-claudin interactions (Daugherty et al., 2007).

Amino acids in the second extracellular loop have been shown to be important for claudin-claudin interactions. The second extracellular loop is involved in tight junction assembly through the trans interactions of claudins. Interactions between claudins in tight junctions (Piontek et al., 2008), as well as claudin composition, and pore formation control barrier properties and selectivity (Mrsny et al., 2008). This may explain why claudins have different expression patterns in different epithelial tissues during development. Here are some of the most important expression patterns of claudins in development, and their functions in the kidney.

1.4.4 Claudins in Development

Claudins are expressed throughout development and in adult life in different epithelial tissues, such as the testes, gall bladder, lungs, liver, and skin among others. Different groups of claudins are expressed in different tissues, and the combination of claudins present in an epithelial layer determines its barrier properties (Furuse et al., 2002). In the kidney, each nephron

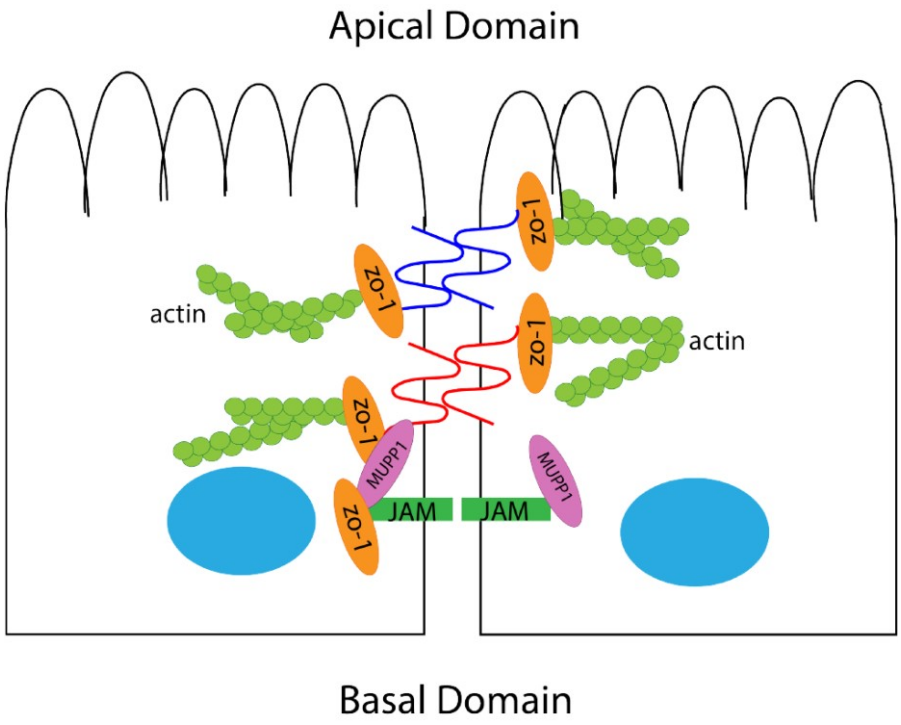

Figure 6. Claudin Protein Interactions at the Tight Junction

Diagram shows the claudin interactions at the tight junction. Claudins (red and dark blue) interact through the C-terminal tail with PDZ domain adaptor proteins such as MUPP1 (pink) and ZO-1 (orange). PDZ adaptor proteins help link the tight junction to the actin cytoskeleton. Tight junction protein JAM (dark green) also interacts with MUPP1 and ZO-1. Cell nucleus is light blue.

segment has a particular combination of claudins. At the proximal end the paracellular space is more permeable as it allows the reabsorption of different ions, in contrast, at the distal part of the nephron, the paracellular space becomes tighter to prevent the loss of important ions. For instance, Claudin-2 forms a cation pore in the proximal tubule, where it regulates sodium reabsorption. Claudin-8, however, is a sealing claudin, expressed in the distal tubule and collecting duct, preventing the loss of sodium and potassium that are actively transcellularly transported (Angelow et al., 2008). Alternative splicing of some claudins yields two different isoforms with different properties. For example, Claudin-10a is anion-selective and expressed in the renal tubules in the cortex, while Claudin-10b is cation selective and expressed in the medulla. The importance of claudins in regulating the permeability and barrier properties in the renal tubules is supported by knock-out and knock-down of claudins in mouse models.

1.4.5 Claudin Knock-out Models

A summary of the claudin knock-out mouse models is provided in Table 2. Knock-out and knock-down mouse models for *Claudins-4, -10, -14, -16*, and *-19* have been the only ones shown to have an important role in physiology of the kidney (Fujita et al., 2012; Breiderhoff et al., 2012; Ben-Yosef et al., 2003; Hou et al., 2007; Hou et al., 2005).

Claudin-4 null mice designed by Fujita and colleagues develop hydronephrosis (accumulation of urine that swells up the kidney) at 10 months of age (Fujita et al., 2012). These mice had an increase in the urinary excretion of calcium and chloride, suggesting a role of Claudin-4 for the paracellular reabsorption of these ions. The tight junction structure was not affected, but the level of Claudin-8 at the tight junction was decreased and that of Claudin-3 was increased (Fujita et al., 2012). Mice with a *Claudin-10* deletion develop nephrocalcinosis determined by medullary calcium deposits. Hypomagnesemia (low level of magnesium in the blood) was also detected, due to the altered paracellular permeability in the thick ascending limb (TAL) of the kidney where Claudin-10 is expressed (Breiderhoff et al.,2012).

The generation of a *Claudin-14* null mouse helped to understand the importance of this Claudin in the kidney. Claudin-14 is expressed in the TAL in mouse kindey and it acts as a Claudin-14 can interact with Claudin-16 and with itself, but not with Claudin-19 (Gong et al., 2012). Claudin-16 and -19 are known to interact in the TAL, and Claudin-14 is able to integrate

into this complex to block the paracellular cation channel formed by Claudin-16 and -19 that is necessary for calcium reabsorption. Claudin-14 levels also increase under a calcium rich diet. Under this dietary condition, Claudin-14 knock-out mice develop hypermagnesaemia, and low levels of calcium in the urine, demonstrating the importance of Claudin-14 for calcium and magnesium homeostasis in the kidney (Gong et al., 2012).

Using RNA interference, Hou and colleagues generated a *Claudin-16* knock-down mouse model (Hou et al., 2007). Claudin-16 deficient mice develop nephrocalcinosis and urinary wasting of magnesium and calcium, a characteristic seen in a rare human syndrome known as familial hypomagnesemia with hypercalciuria and nephrocalcinosis (FHHN). The loss of Claudin-16 decreases the cation selectivity of the tight junctions in the TAL (Hou et al., 2007). Similar to Claudin-16, Claudin-19 facilitates calcium reabsorption in the TAL. siRNA knock-down of *Claudin-19* in mice resulted in decreased Claudin-16 in tight junctions in the TAL, without decreasing its expression level. Deficiency of *Claudin-16* produced a loss of Claudin-19 at the tight junction. It was shown that Claudin-16 oligomerizes with Claudin-19 and their interaction is necessary for their assembly into the tight junction in the TAL (Hou et al., 2009). Claudin-19 deficient mice exhibit similar urinary wasting as that observed in Claudin-16 knock-out mice, replicating FHHN (Hou et al., 2007). Given the importance of claudins in the kidney, this led to the search for mutations in claudin loci in patients with CAKUT.

Claudin	Phenotypes	Reference
Claudin-1	Water loss and dehydration through epidermis	Furuse et al., 2002
Claudin-2	Hypercalciuric	Muto et al., 2010
Claudin-4	Urothelial Hyperplasia and hydronephrosis	Fujita et al., 2012
Claudin-5	Defects in blood brain barrier	Nitta et al., 2003
Claudin-7	Chronic dehydration and salt wasting	Tatum et al., 2010
Claudin-8 (conditional KO)	Hypotension, hypokalemia, and metabolic alkalosis	Gong Y et al., 2015
Claudin-9	Deafness-loss of sensory hair cells	Nakano et al., 2009
Claudin-10	Hypermagnesemia and nephrocalcinosis	Breiderhoff et al., 2012
Claudin-11	Male sterility and deafness	Tiwari-Wooddruff et al., 2001. Gow et al., 2004. Furuse et al., 2009
Claudin-14	Hypermagnesemia, hypocalciuria, and hypomagnesiuria	Ben-Yosef et al., 2003. Gong et al., 2012
Claudin-15	Mega-intestine phenotype	Tamura et al., 2008
Claudin-16 (knock-down)	Hypomagnesemia, hypocalciuria, and nephrocalcinosis	Hou et al., 2007
Claudin-18	Impaired alveolarization and increased alveolar fluid clearance	Lafemina et al., 2014. Li et al, 2014. Hayashi et al., 2012
Claudin-19 (knock-down)	Hypomagnesemia, hypocalciuria, and nephrocalcinosis	Miyamoto et al., 2005. Will et al., 2010

Table 2. Mouse Phenotypes in Claudin Knock-out and Knock-down Models

1.4.6 Human Mutations in *CLDN* Loci are Associated with Kidney Disease

Several claudins have been implicated in human diseases. To date there have been 28 different mutations found in *CLDN16* in patients with familial hypomagnesemia, hypercalciuria and nephrocalcinosis (FHHNC) (Günzel et al., 2009). Most mutations in CLDN16 are found in the first and second extracellular loops in conserved amino acids (Kang et al., 2005). CLDN16 is expressed in the thick ascending limb of the loop of Henle and the distal convoluted tubule, where it is involved in calcium and magnesium reabsorption. FHHNC is characterized by urinary wasting of magnesium and calcium, deposition of calcium in the kidneys, and in some cases renal failure.

Mutations in *CLDN19* have also been found in patients with FHHNC with ocular defects (Konrad et al., 2006). The main clinical features observed in these patients are hypomagnesimia, renal failure, and ocular anomalies. Claudin-19 is highly expressed in renal tubules, in the thick and thin ascending limb, as well as in the retina. The mutations found in *CLDN19* appear to interfere with protein trafficking and the assembly of Claudin-19 into the tight junction (Konrad et al., 2006).

Mutations in *CLDN14* have also been found in patients with kidney disease. Claudin-14 interacts with Claudin-16 and 19 to decrease the paracellular permeability to sodium. Claudin-14 regulates calcium reabsorption and it is expressed in the thick ascending limb (Gong et al., 2012). In a genome-wide association study with a cohort from The Netherlands, common and synonymous variants in *CLDN14* were associated with a higher risk for developing kidney stones and with reduced bone mineral density (Thorleifsson et al., 2009). Mutations in *CLDN14* were also identified in patients with a rare autosomal non-syndromic deafness (DFNB29) (Wilcox et al., 2001).

Claudin mutations in patients with kidney disease has shed light on the importance of the different claudin expression patterns in the TAL of the nephron for the homeostasis of reabsorption of ions and urine production. They also implicate the importance of certain residues for claudin interactions, assembly to the tight junction, and trafficking in the TAL.

Human mutations and knock-out/knock-down mouse models have shown that claudins regulate permeability properties. However, none of the knock-out or knock-down mouse models have morphological or developmental kidney phenotypes. This might be due to functional redundancy in the claudin family, in which case more than one claudin would need to be removed in order to replicate a CAKUT phenotype. For this reason, our lab has taken an approach to remove a subset of claudins from the tight junction using the C-CPE peptide.

1.5 C-CPE

Clostridium perfringens is a bacteria that causes food poisoning in humans by forming a pore in the epithelium of the intestine (Katahira et al., 1997; Lindström et al., 2011). *Clostridium perfringens* enterotoxin (CPE) binds to receptors in the tight junctions of the intestine. Claudins have been previously identified to be one of these receptors. CPE binds to the second extracellular loop of a subset of claudins, including Claudin-3, -4, -6, -7, -8, -14, with different affinities (Fujita et al., 2000; Winkler et al., 2009; Robertson et al., 2010). Once it binds to a claudin, it forms a complex that creates a pore, damaging cell permeability and causing calcium influx, inducing cell death (Lindström et al., 2011). CPE is a protein with a molecular weight of around 35 kDa, its C-terminus contains a claudin binding domain and its N-terminal domain regulates membrane permeability. In brief, the COOH- domain binds to claudins and facilitates formation of a pore through its NH_2- domain (Fujita et al., 2000).

In the search for a tool that can modify tight junction barriers at the cellular level to increase or decrease epithelial permeability for drug target delivery, several studies have focused on a peptide that can bind directly to claudins without causing cell death. C-CPE (C-terminal domain of the CPE) was first identified in 1997, by separating the N-terminal region from the C-terminal region of CPE (Katahira et al., 1997). The C-terminal domain in C-CPE binds to the second extracellular loop of claudins and is able to remove them from the tight junction without causing cell death (Kondoh et al., 2006). When C-CPE was used to target Claudin-4 and -6 in the mouse, blastocyst formation was inhibited due to a decrease in hydrostatic pressure (Moriwaki at al., 2007). However, neither Claudin-4 nor -6 null mice exhibit a blastocyst phenotype, which supports the idea of functional redundancy among claudin family members (Fujita et al., 2012) (Anderson et al., 2008).

Our group has used C-CPE to remove claudins from tight junctions in cells and in the chick embryo, as a tool to examine the role of claudins in epithelial barrier formation and development. In claudin-transfected HEK293 cells treated with C-CPE, claudins are removed from the tight junction after 5 hours of treatment (Baumholtz unpublished). When measuring TER (transepithelial resistance) in MDCK cells, C-CPE affects tight junction maintenance. Other experiments in our laboratory using C-CPE have also helped demonstrate the importance of claudins in development.

For instance, targeted removal of Claudin-3, -4, and -8 in the neural and non-neural ectoderm with C-CPE caused open neural tube in chick embryos (Baumholtz et al., 2017). In the kidney, culturing mouse kidney explants in media containing C-CPE caused a decrease in branching morphogenesis (Figure 7) (Khairallah, 2013). In the nephric duct, C-CPE soaked agarose beads were implanted adjacent to 10^{th} somite into the chick embryo. C-CPE inhibited the elongation of the nephric duct (Figure 8) (Simard, 2014). These studies with C-CPE demonstrate a role for claudins in nephric duct elongation and ureteric bud branching. For this reason, we sequenced patients with kidney malformations in the search for CLDN mutations.

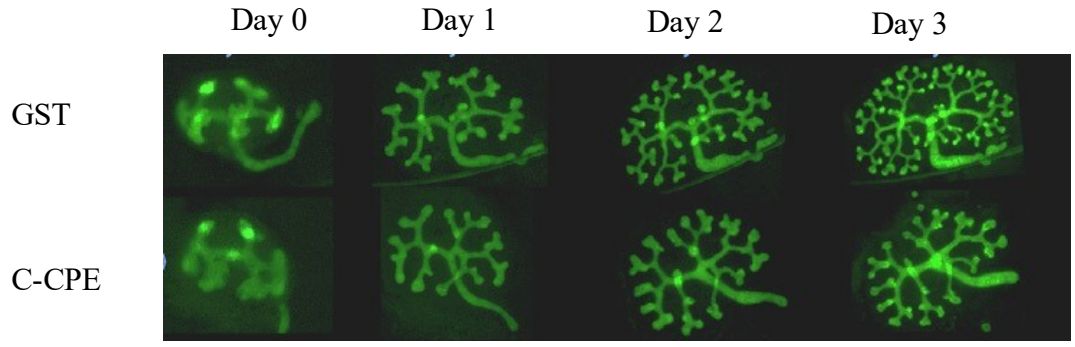

Figure 7. C-CPE Treatment Inhibits Branching Morphogenesis in Explanted Mouse Kidneys

Hoxb7/GFP+/- transgenic E12.5 mouse kidneys cultured in media with C-CPE and GST (control). To obtain embryos that expressed green fluorescent protein (GFP) in the nephric duct, the ureteric bud, and ureteric bud derivatives, *Hoxb7/GFP*+/- transgenic males were mated with CD1 females. After Day 1 there starts to be a delay in branching, with less branching points (ureteric buds). This defect becomes more prominent by Day 3. The C-CPE treated kidney has less branching tips and less branching events compared to the GST treated kidney (Khairallah, 2013).

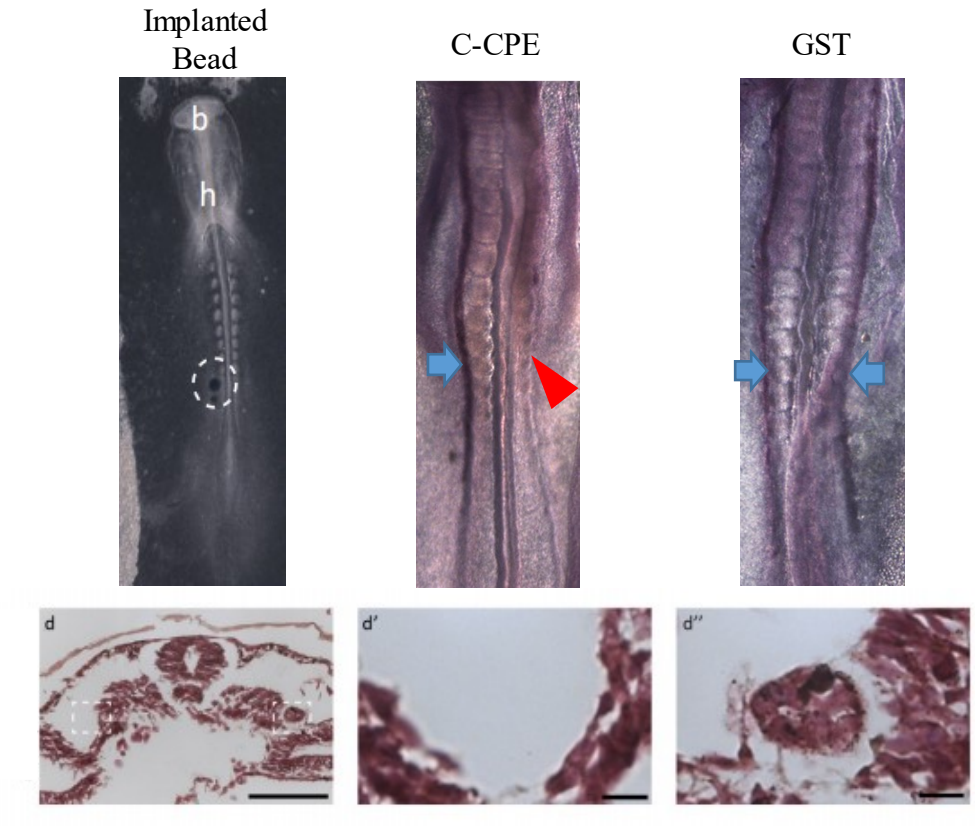

Figure 8. C-CPE Soaked Bead Treatment Inhibit Chick Nephric Duct Elongation

In the left panel on the top a whole HH10 chick embryo with C-CPE soaked bead (white dashed circle) adjacent to the 10th somite in the left duct, ventral view. *Lim1* mRNA antisense probe was used as a marker of the nephric duct. In the middle a whole embryo at HH12 after incubation at 39°C with C-CPE soaked bead for 24h. Only the right side nephric duct (red arrowhead) (dorsal view) was treated with the bead. *In situ* hybridization with *Lim1* shows no staining on the right duct compared to the left duct (blue arrow). In the top right panel a GST soaked bead treated embryo at HH12 after incubation at 39°C with bead for 24h. Only the right duct (dorsal view) was treated. *In situ* hybridization with *Lim1* shows staining of both ducts (blue arrows). (d) Transverse section through whole embryo at HH12 with absent left duct. (d') Magnification of the left duct in transverse section showing complete absence of duct tissue. (d'') Magnified image of the right duct (Simard, 2014).

1.6 Hypothesis and Objectives

1.6.1 Hypothesis

Claudins are necessary to establish and maintain tight junctions in epithelial structures during kidney development by playing a role in regulating epithelial cell organization. C-CPE experiments have demonstrated that claudins are important in regulating nephric duct elongation and branching morphogenesis. Based on these data, I hypothesize that C-CPE-sensitive claudins expressed in the nephric duct and ureteric bud are important for kidney development. Consequently, *CLDN* sequence variants in patients with congenital kidney malformations will disrupt nephric duct elongation and ureteric bud branching resulting in kidney malformations.

1.6.2 Objectives

1.6.2.1 Objective 1: Characterization C-CPE-Sensitive Claudins

To address the hypothesis, I first performed whole mount *in situ* hybridization to characterize the expression pattern of C-CPE-sensitive claudins in the chick nephric duct. In order to address branching morphogenesis, I used the mouse as a model, due to the easy visualization of branching in the embryonic kidney. Only Claudin-4 and -14 antisense probes were analyzed in the mouse embryos to complete data generated by a previous graduate student in the laboratory. To assess protein expression in the nephric duct, I performed Claudin-3 immunofluorescence in sections from chick embryos.

1.6.2.2 Objective 2: Analysis of *CLDN* Sequence Variants in Patients with Kidney Malformations

In order to search for potentially deleterious variants in humans, a cohort of 96 patients from the NIH-sponsored Chronic Kidney Disease in Children (CKiD) study was exon-sequenced using next-generation technologies. DNA samples were obtained from 96 children between the ages of 1 and 16. Each patient had either kidney dysplasia, hypoplasia, or agenesis. Common, rare and novel variants were gathered; rare and novel variants were validated and analyzed through mutation assessment *in silico* prediction software.

1.6.2.3 Objective 3: Functional Studies of CLDN Variants

Two of the variants that were predicted to be detrimental for the protein function were tested. To test the functionality of the variants I cloned them into an RCAS vector. RCAS is an avian retroviral vector derived from a strain of Rous sarcoma virus (Hughes, 2004). Retroviral particles overexpressing the variants and the wildtype claudins were injected directly into cells adjacent to the 10^{th} somite of the chick embryo. An empty GFP-expressing RCAS was used as a control. Elongation of the duct was assessed using an antisense riboprobe to *Lim1*.

CHAPTER II: Materials and Methods

2.1 Preparation of Sense and Antisense Riboprobes

Sense and antisense riboprobes for *in situ* hybridization analysis were made using linearized DNA. Plasmids containing chick or mouse claudin cDNA were digested with specific restriction enzymes to linearize the plasmid as shown in Table 3. Sense and antisense riboprobes were made using RNA polymerase T7, T3 or Sp6 according to the construct. Gene transcription for the riboprobe preparation was done by a setting up a reaction with 2µl of 10X transcription buffer, 2µl of 100Mm DTT (dithiothreitol), 0.5µl of RNaseOUT (Thermo Fisher), 2µl of DIG (digoxigenin-UTP) RNA labelling mix 10X (Roche), 1µg of the linearized DNA, 1µl of the RNA polymerase and RNase free water. The reaction was left in a 37°C water bath for 2h, and then 1µl of RNase-free DNase (Promega) was added to the solution and the incubated for 10 more minutes at 37°C. To precipitate the RNA 1µl of 0.5M EDTA, 1.3µl of 7.5M LiCl and 55µl of 100% ethanol were added to the riboprobe solution and left at -80°C for 1h. Then, it was centrifuged at 13000rpm at 4°C for 30 minutes. The pellet was left to dry and resuspended in 20µl of 0.1M DTT. The 20µl were then added to a hybridization solution (50% formamide, 5X saline sodium citrate buffer (SSC) pH5, 50µg/ml yeast tRNA, 1% sodium dodecyl sulfate (SDS) and 50µg/ml heparin). The amount of hybridization solution added was determined by running 1µl of the riboprobe solution in a 1% agarose gel.

2.2 Collection of Mouse and Chick Embryos for Whole Mount *In Situ* Hybridization

Mouse embryos were collected from CD1 pregnant mice at embryonic day (E) 10.5, E13.5 and E16.5. Embryos were dissected in a petri dish containing a 1X PBS (phosphate buffered saline) solution and rinsed twice. Fertilized chicken eggs (Couvoir Simetin, St-Canut, Quebec) were incubated at 39°C until they reached the desired stage at which point embryos were removed from the egg. Both mouse and chick embryos were fixed overnight at 4°C in 4% PFA (paraformaldehyde)-PBS. They were then washed twice for 5 minutes in 1X PBT (phosphate buffered saline with 0.1% Tween-20) and then dehydrated in consecutive 5-10 minute washes of PBT:methanol (3:1, 1:1, 1:3) and a final wash of 100% methanol. The dehydrated embryos were stored in methanol at -20°C.

cDNA insert	Plasmid vector	Antisense Riboprobe		Sense Riboprobe	
		Restriction Enzyme	RNA Polymerase	Restriction Enzyme	RNA Polymerase
Chick *Claudin-1*	pBluescript KS	NotI	T3	XhoI	T7
Chick *Claudin-3*	pBluescript KS	XhoI	T7	NotI	T3
Chick *Claudin-4*	pCanHA3	BamHI	Sp6	NotI	T7
Chick *Claudin-8*	pSC-A vector	BamHI	T3	HindIII	T7
Chick *Claudin-14*	pSC-A vector	BamHI	T3	HindIII	T7
Mouse *Claudin-4*	pSC-A vector	BamHI	T3	HindIII	T7
Mouse *Claudin-14*	pSC-A vector	BamHI	T3	HindIII	T7

Table 3. Restriction Digest Enzyme for the Linearization of Chick and Mouse Claudin cDNA Vectors and RNA Polymerase Used for Riboprobe Synthesis

2.3 Whole Mount *In Situ* Hybridization

In situ hybridization was performed according to a previous described procedure (Collins and Ryan, 2011). Embryos were rehydrated in consecutive 5-10 minute washes of PBT:methanol (1:3, 1:1, 3:1), and then twice for 5 minutes in PBT. Treatment of embryos with proteinase K (10µg/ml) was done according to the embryo stage as shown in Table 4. After treatment, embryos were washed twice in PBT-glycine for 5 minutes. They were then fixed in 4% PFA with glutaraldehyde (80µl of glutaraldehyde per 10ml of 4% PFA) for 20 minutes on ice, followed by two 5 minute washes with PBT. After, they were washed with hybridization solution (50% formamide, 5X SSC pH5, 50µg/ml yeast tRNA, 1% SDS and 50µg/ml heparin) for 5 minutes at room temperature followed with 1h incubation with fresh hybridization solution at 65°C. The hybridization solution was replaced with the digoxygenin-labelled antisense or sense riboprobe and embryos were incubated at 65°C overnight. On the second day, the embryos were washed 3 times for 20 minutes at 65°C with 50% formamide, 5X SSC pH5, 1% SDS and 3 times for 20 minutes at 65°C with 50% formamide, 2X SSC pH5. Embryos were then washed 3 times for 10 minutes at room temperature in TBST (Tris-buffered saline plus Tween-20; 140mM NaCl, 3mM KCl, 3mM Tris-HCl, pH7.5 and 0.1% Tween-20) plus 2mM levamisole. They were then incubated in a blocking solution of 10% normal sheep serum in TBST for 1-2 hours at room temperature. While the embryos were blocking, the antibody mix was prepared as follows. 0.0375g of chick/mouse powder was incubated in 6.25ml TBST for 30 minutes at 65°C and then chilled on ice. 62.5µl sheep serum and a 1:2000 dilution of anti-dioxigenin-AP antibody were added to the embryo powder in TBST and incubated for 1h at 4°C while shaking. The antibody mix was then centrifuged at 4°C for 10 minutes and the supernatant was removed. Next, 18.75ml of TBST and 187.5µl of sheep serum were added to the supernatant. The blocking solution was then removed and the final antibody mix was added to the embryos and left overnight at 4°C. On the third day, embryos were washed 3 times for 5 minutes in TBST with 2mM levamisole and then 5 times for 1 hour each at room temperature. This was followed by three 10-minute washes with NTMT (0.1M NaCl, 0.1M Tris-HCl, pH9.5, 50mM MgCl2 and 0.1% Tween-20). Colour development was done by adding 2.5µl of BCIP (5-Bromo-4-chloro-3'- indolyphosphate p-toluidine) and 2.5µl of NBT (nitro-blue tetrazolium chloride) to 1ml of NTMT solution. Colour development was allowed to proceed until there was tissue specific purple staining.

Embryo Stage	Proteinase K (time of incubation)
Chick HH10-HH12	3 min
Chick HH13-HH15	4-5 min
Chick HH16-HH18	6-8min
Chick HH19-HH20	9-10min
Mouse E10.5	12 min
Mouse E13.5 (kidney)	5 min
Mouse E16.5 (kidney)	8 min

Table 4. Duration of Proteinase K Treatment in Chick and Mouse Embryos

Incubation times for Proteinase K treatment during day 1 of whole mount *in situ* hybridization for the different embryonic stages of chick and mouse.

2.4 Paraffin Sectioning

After *in situ* hybridization, the embryos were photographed and then dehydrated in consecutive 20 minute washes of 50%, 70% and 95% ethanol-PBS, followed by 2 times 30-minute washes in 100% ethanol and 2 times 30 minute washes in xylene. Embryos were placed into moulds with paraffin in a vacuum oven for 1 hour and then transferred into new molds with fresh paraffin in which they were positioned and left to solidify. 10µm sections were collected using a Leica RM2155 microtome. Sections were placed in a 39-41°C water bath and then transferred to microscope slides. The slides were left on a heating plate overnight to dry. Sections were washed 2 times for 10 minutes in xylene and then coverslipped using Permount. Imaging of the sections was done using Zeiss Axiophot microscope with AxioCamMRc with Axiovision v4.7.1.0 software.

2.5 Cryosectioning

Chick embryos were rinsed twice with PBS and fixed for 6 hours at 4°C in 4% PFA-PBS or 1 hour in 10% trichloroacetic acid (TCA). Next, embryos were put into 5% sucrose-PBS solution at room temperature for 20 minutes to 1 hour until they sunk and then transferred to 30% sucrose-PBS solution for 2 hours at room temperature for younger embryos (HH10-14) or overnight at 4°C for older embryos (HH15-HH20). The next day the embryos were placed in a 1:1 solution of 30% sucrose and OCT (optimal cutting temperature) matrix for 1 hour at room temperature. Then the embryos were embedded in OCT and left on an ethanol-dry ice bath to solidify. 16µm sections were collected using a Leica CM3050 cryostat and placed onto microscope slides. The slides were left to dry for 2 hours and placed at -80°C for long-term storage or left at room temperature and coverslipped with Glycerol gelatin mounting solution (Sigma-Aldrich) for imaging.

2.6 Exon Sequencing

Exon sequencing was performed on 96 patients with congenital kidney malformations from the NIH-sponsored Chronic Kidney Disease in Children (CKiD) study. Parallel amplification and library preparation were performed through the 48.48 Fluidigm Access Array

Integrated Fluidic Circuit (IFC) for 23 human *CLAUDIN* genes. Each sample had a specific barcode and primer pairs were designed within 50 base pairs of flanking sequence outside of the exon coding sequence. Each gene was covered by one to three overlapping primer pairs, generating amplicons of 300 to 400 base pairs (shown in Table 5). Amplicon libraries were pooled and subjected to Illumina MiSeq sequencing.

2.7 Molecular Cloning

Selected variants identified in patient DNA sequences were first cloned into pSC-A and then subcloned into pcDNA3.1, then the Slax adaptor plasmid and at last, the Replication-competent ASLV long terminal repeat (RCAS) vector. Cloning of the full length of Claudin-8 and -14 into a pSC-A-amp/kan vector was done using StrataClone PCR Cloning Kit (Agilent). The coding sequences were PCR (polymerase chain reaction) amplified. The *CLDN8* forward primer contained EcoRI and NdeI sites (5′-GCGGAATTCCATATGGCAACCCATGC-3′) and the reverse primer contained a BamHI site (5′-CGGGATCCCTACACATACTGACTTCTGG-3′). For PCR amplification 50ng/µl of DNA and 3µl of 6mM of primer were used with an annealing temperature of 53°C and a 45 second extension time. The *CLDN14* forward primer contained NcoI sites (5′-GCGGAATTCACCATGGCCAGCACG-3′) and the reverse primer contained an EcoRI site (5′-CGGGATCCGGACTCACACGTAGTCG-3′). For PCR amplification 50ng/µl of DNA and 3µl of 6mM of primer were used with an annealing temperature of 56°C and a 45 second extension time. Using the same primers, *CLDN8* and *CLDN14* were cloned into FLAG-HA-pcDNA3.1 (Addgene). Cloning from pcDNA3.1 into the Slax Nde or Nco adaptor plasmid was done by restriction digest using either Nde or Nco sites that were added during PCR amplification. Digestion and cloning from the Slax vector into the RCAS vector was done using ClaI enzyme (Invitrogen).

2.8 Preparation of Retroviral Particles

Transfection of virus, viral supernatant production, and titration of virus were done as previously described by Logan and Tabin (Logan and Tabin, 1998). DF-1 (chicken embryonic fibroblasts) cells were thawed and seeded on a 6-well plate in 2ml DMEM 10% FBS cell culture

media with 1% penicillin and streptomycin. Once the cells reached 70-80% confluency, the DMEM 10% FBS media was replaced with new media. One hour later the cells were transfected with the RCAS vector containing the *CLDN* variant cDNA. 500ng/µl of DNA (*CLDN* variant and wildtype in RCAS vector) were added to 25µl of DMEM 10% FBS with antibiotics and 1µl of P300 Lipofectamine reagent (Invitrogen), according to manufacturer's instructions. In a separate tube, 1µl of Lipofectamine 3000 was added to 25µl of DMEM with no FBS and no antibiotics. This last solution containing the Lipofectamine was then added to the DNA with the reagent and the media, incubated for 15 minutes, and then added to the media in the 6-well plate. After 24 hours, when the cells were 90-100% confluent, they were trypsinized and passaged to a 10cm plate with 10ml 10% FBS DMEM media plus antibiotics. 50µl of trypsinized cells were seeded on a 6-well plate for staining with the AMV-3C2 (avian myoblastosis virus) monoclonal mouse antibody used to identify cells infected with the avian sarcoma virus.

After 24 hours the cells on the 6-well plate were washed 3 times with PBS and then fixed in 4%PFA/PBS for 12 minutes. After fixing the cells were washed three times with PBS, and blocked using 10% normal goat serum in 0.3% TritonX-100 /PBS for one hour. Blocking solution was replaced with the primary 3C2 monoclonal antibody (Developmental Studies Hybridoma Bank, U. Iowa), which recognizes cells infected with the virus, diluted 1:100 in 5% normal goat serum and 0.3% TritonX-100/PBS, and the cells were incubated with the primary antibody for 45 minutes at room temperature. They were then washed three times for 5 minutes with PBS. The secondary antibody, biotinylated anti-mouse IgG (Vector Labs) was added at a 1:400 dilution and incubated for 30 minutes. During the incubation of the secondary antibody, the A/B solution (Vectastain Kit, Vector Labs) was prepared by adding 2 drops of solution A and 2 drops of solution B to 10ml of PBT and left standing for 30 minutes. After removing the secondary antibody, the cells were washed three times for 5 minutes with PBS, and the A/B solution was added to each well and incubated for 30 minutes. Cells were then washed three times for 5 minutes with PBS and 500µl of DAB (3,3'-diaminobenzidine) solution, prepared according to manufacturer's instructions, was added to each well. Brown staining of cells indicated the presence of the retroviral particles.

Once the cells in the 10cm plate reached 80% confluency, they were split into two 15cm plates. After two days, the media was replaced with new DMEM 10% FBS plus antibiotics. Once the cells reached 80% confluency, they were left 48 hours more to reach superconfluency. Once

this occurred, media was changed to 12ml of DMEM 2% FBS without antibiotics. 24h later, the media was collected in a 50ml tube, frozen at -80°C and replaced with fresh 12ml DMEM 2% FBS without antibiotics. Media collection was repeated for two more days.

After three days of collection, the frozen media containing the viral particles was thawed and filtered through a 0.45um cellulose acetate filter (Corning). The filtered supernatant was then placed in ultra-centrifuge tubes (Beckman Coulter) in a SW-32 swinging-bucket rotor (L80 ultracentrifuge) and centrifuged at 21,900rpm for 3 hours at 4°C. The supernatant was carefully removed and then the tubes were placed upright to allow media on the sides to drain to the bottom and overlie the pellet of retrovirus particles. The tubes were covered and stored at 4°C overnight. The pellets with the viral particles were resuspended in 100µl total volume of DMEM, aliquoted and stored at -80°C.

2.9 Injection of Retroviral Particles

Stage HH10 chick embryos were collected on filter paper supports and cultured *ex ovo* on agar-albumin plates as previously described (Collins and Ryan, 2011). Briefly, fertilized eggs were incubated at 39°C until they reached stage HH10. The egg was cracked into a 10cm glass petri dish and the thick albumen was removed from the surface of the embryo using KimWipes. A filter paper support was placed over the center of the yolk and the embryo was attached to the center of the support. The rest of the yolk was removed with scissors. The filter paper with the embryo was placed on agar-albumen plates with the ventral side facing up. 1µl of Fast Green was added to a thawed aliquot of retroviral particles. The retrovirus was injected adjacent to the 10^{th} somite of the embryo on the left side using a pulled glass capillary needle (1mm x 500mm) and a Narishige IM 300 microinjector. Embryos were then incubated for 12 hours in a humidified incubator at 38°C to reach stage HH12. After incubation, embryos were fixed in 4% PFA overnight. Whole mount *in situ* hybridization was performed using an RCAS *env* ripobrobe to confirm that the viral particles were present only in the left nephric duct, the site of injection. The *Lim1* antisense riboprobe was used to assess nephric duct elongation.

Fragment	F primer sequence	R primer sequence	Position in build hg19	Fragment size
CLDN1E01	CCATGGAATCACACAACAGAA	AACTCTCCGCCTTCTGCAC	chr3:190039682-190040052	371
CLDN1E02	TGTTTGCAGTTTGCCTTAGA	TTCCATTTTTCTCTTGTTGGTC	chr3:190030547-190030886	340
CLDN1E03	ATGGCACTAGCAGGACTTTG	TGGACTTCTAATCTCCCTAATACC	chr3:190027878-190028192	315
CLDN1E04	TCCATTTTCGGTTTGTTTCA	CAGAAATCTTAAAGTACTTCCCAAGG	chr3:190026019-190026376	358
CLDN2E02_001	GGTGTTCAAGGAGCAAGAGC	GGAGGAGATTGCACTGGATG	chrX:106171383-106171734	352
CLDN2E02_002	GCATCACCCAGTGTGACATC	ATGAGCAGGAAAAGCAGAGG	chrX:106171637-106172017	381
CLDN2E02_003	TTCTTCCCTGTTCTCCCTGA	CATCCTTGGCAATTCAACCT	chrX:106171965-106172350	386
CLDN3E01_001	GGTGGTGGTGTTGGTGGT	CCAAGGCCAAGATCACCAT	chr7:73183665-73184045	381
CLDN3E01_002	CACCACGGGGTTGTAGAAGT	CTTCATCGGCAGCAACATC	chr7:73183927-73184281	355
CLDN3E01_003	AGCAGCGAGTCGTACACCTT	CCGTCGGTGAGTCAGTCC	chr7:73184171-73184510	340
CLDN4E01_001	AGCCTTCCAGGTCCTCAACT	CCTCCAGGCAGTTGGTACAC	chr7:73245495-73245859	365
CLDN4E01_002	CATCATCGTGGCTGCTCTG	AGCAGAGAGGAACAGAGTGGA	chr7:73245792-73246193	402
CLDN5E02_001	CCCCAGGCTTATCCAACG	GAGGCGTGCTCTACCTGTTT	chr22:19511057-19511417	361
CLDN5E02_002	GACAATGTTGGCGAACCAG	GTCCGCAGCGTTGGAGAT	chr22:19511350-19511773	424
CLDN5E02_003	GCACGCCAGGATCAGACC	CCCTAACTTCAGCTGCCAGA	chr22:19511704-19512077	374
CLDN6E01_001	GCCTCCGCATTAGTTCCATA	CATTACATGGCCCGCTACTC	chr16:3065069-3065440	372
CLDN6E01_002	TTCTTGGTAGGGTACTCAGAGG	CACGTGCCCTCTGTGTCAT	chr16:3065370-3065784	415
CLDN6E01_003	TCCTCCACACAGGTGGTACA	TGCTTCTGTCCCAAACACAG	chr16:3065694-3066063	370
CLDN7E01	CCAGCCGACCACTTCCTC	CGTTTGTTTTACTGTAGGGTCTCC	chr17:7165005-7165421	417
CLDN7E02	TCAGTATAGTGAGGCCCCAAA	GGCCCAGGTCTTGGACAC	chr17:7164066-7164458	393
CLDN7E03	GGACAGGAACAGGAGAGCAG	CCATCTGGGAGGAGCAAG	chr17:7163769-7164121	353
CLDN7E04	AGGCCCTTTCAGGCATCTA	CCCTTTGATCCCTACCAACA	chr17:7163631-7163984	354
CLDN8E01_001	CAAAGTTTCTTTGGGGTCCA	GTGGTGCTCATCCCTGTGA	chr21:31587477-31587850	374
CLDN8E01_002	AGAGCTTCTCCAAGCTCACG	ACTGTGGATGAATTGCGTGA	chr21:31587750-31588097	348
CLDN8E01_003	AGCCAGCAGGGAATCATAGA	CTGGCCAGAAGTAGCAAAGC	chr21:31588028-31588403	376
CLDN9E01_001	GGGGCTGAGAAGACCTAACC	GGCGAGGAGGAGGATGAC	chr16:3063334-3063747	414
CLDN9E01_002	TGTACCACGTGTGTGGAGGA	ATCAGGCCAAGGTCGAAAG	chr16:3063673-3064081	409
CLDN9E01_002r	AAGGCCCGTATCGTGCTC	ATCTGGTCATCAGGCCAAG	chr16:3063703+3064089	387
CLDN10E01_001	ACAGGGCATGGGTGTGAG	AGGGAAGGAGGGCTGAGG	chr13:96204832-96205268	437
CLDN10E02	TTTTTGGAAAACAAACATCCA	TGAGCACAGCCCTAACAAAT	chr13:96212286-96212646	361
CLDN10E03	TTTGGCTGGGATTGTATTCAT	TGCATATTTTGCGTATGTGG	chr13:96212519-96212893	375
CLDN10E04	TTGGGATGGTCTAATGGCTA	CAGGTCATTTTTGTCTCTTTTTC	chr13:96229286-96229619	334

CLDN10E05	ACTTCTTGGGGCAAGAGGAG	AATTATGGGAGGGCCTTGAT	chr13:96230002-96230353	352
CLDN11E01	GTACCTGGGCAGGCACTGT	TATCCCGCTCTCTACCCAGA	chr3:170136776-170137141	366
CLDN11E02	AGAAGGAGGAAGGGAGATGG	CTTCACTTGGCTTCCTTTCA	chr3:170140850-170141228	379
CLDN11E03	TGGAAGCCACAAGTGTGTGTA	CACACTGTGACGAGCAAACC	chr3:170150214-170150618	405
CLDN12E04_001	TCTGACTGACAGTACTCCACAAG	CTGAAGGCAGTGTTGCACAT	chr7:90041958-90042331	374
CLDN12E04_002	AGTTTGCCCTACCCCTCAG	TGGGTGGATGGGAGTACAAT	chr7:90042250-90042636	387
CLDN12E04_003	TTTGAGCCAGTCTTTTCATTTG	TTGGCTTCATTGATTGGTCA	chr7:90042483-90042842	360
CLDN14E01_001	CTGCCTCCATTGACAGTCC	TCCTGGACCACCAACGAC	chr21:37833204-37833585	382
CLDN14E01_002	GGAGATGAAGCCCAGGTACA	TCCTACCTGAAAGGGCTCTG	chr21:37833484-37833861	378
CLDN14E01_003	ATCGGTAGATCTGGCACTGG	TCGGTGACAGAAATAAGTGCAT	chr21:37833789-37834156	368
CLDN15E01	TGCATCCTCACGGAAGTACC	TTCCAGTTCCCTAGGGGTTC	chr7:100880558-100880933	376
CLDN15E02	TCTGGGGAGTACAGATGAGG	GATGGGAAAGGCTGACAAC	chr7:100877397-100877757	361
CLDN15E03	CAGGATGGAGATCAGTGAGG	CTGCTCTGGGACTTGGTG	chr7:100875944-100876315	372
CLDN15E04	TAGGCGTTTCTGCCGTATTT	GGCTGGCGTCTCACTTGT	chr7:100875698-100876049	352
CLDN15E05	CGGCCCCTGAGGTTACTA	CCTCACTGATCTCCATCCTG	chr7:100875598-100875963	366
CLDN16E01	CCACCCGAAACACACTCAG	GGCCTGGATCATGAAAAGAA	chr3:190105843-190106268	426
CLDN16E02	GGCTTCAATTGTCAGTGCTT	TTTTCTGTCCCTTTCCCTTC	chr3:190119939-190120280	342
CLDN16E03	AGGGGTACTTATGTTCAAGTTCAT	AGCAGCTTCAGCACAACTCT	chr3:190122398-190122800	403
CLDN16E04	TGTAGCATCCTCCCTTTCTTT	TGCCCTTGAACAATTGGA	chr3:190126079-190126437	359
CLDN16E05	TTTCCCAAGTTCACTGAGTTCT	AAAGAAAAAGTATAGGAGAATCAAACA	chr3:190127643-190127985	343
CLDN17E01_001	GCAAGTTCTCCTGCCTCAC	GTGAGCTGGACAGCCAATA	chr21:31538170-31538527	358
CLDN17E01_002	GATGGCTGGGTTGTAGAAATC	TTTGAGAGGCTCTGGGAAG	chr21:31538477-31538809	333
CLDN17E01_003	ACAAGGAGCTATAGAACTTGCATT	GTTAGGCCAAGTTCAGTCACA	chr21:31538725-31539099	375
CLDN18E01	CACCAGCCTCTCAGAGAAAA	GTTTCCTCTCCACCTCCAAT	chr3:137717613-137717985	373
CLDN18E02	TTTGTCTGCTTGTGTCTTGC	TTGGACCTCCACACTCAGAT	chr3:137742466-137742806	341
CLDN18E03	CAATATTCTGCAGCCTACTCATC	ATGGCATGGTTGTCTCTGAT	chr3:137743342-137743695	354
CLDN18E04	ACCATATTGACAGCCACCAT	GGCTGAAATATTCCCATTCTG	chr3:137748607-137748929	323
CLDN18E05	CAAAGACATCTACAATCATGGAAT	AGACTGAGGCTAAGACCATTTG	chr3:137749771-137750145	375
CLDN19E01	CTGTTCCCACCTCCCATCT	CTGCCTCTGACCCTCCTTCT	chr1:43205468-43205863	396
CLDN19E02	GTGCAGAGGCCTAAAGACAA	CTCTCAAGCTGGGCTCCT	chr1:43203975-43204346	372
CLDN19E03	TCCAGTGGACAAAGGTCAGT	GGAGACAGCAACCCCATT	chr1:43203835-43204158	324
CLDN19E04	CCTGCCTCTGGTGTCTCTCT	CCTGATGCCACTCTCCCTAC	chr1:43201351-43201730	380
CLDN19E05	GACAGACCGAATGATACCATGA	GCCACCTACACAGATGGTGA	chr1:43200644-43200995	352
CLDN20E02_001	AGAATTCTGACAGCCATCATTG	TGTCCCCTCCTAAGCGAGTA	chr6:155596787-155597184	398

CLDN20E02_002	GCTTTGGGGATCTGCACTT	GCACCCAAAAGTTCCATTTC	chr6:155597127-155597552	426
CLDN20E02_004	TCATTTCTGCAATGCTGTTG	AAACATGGAAACAATAATGGAAA	chr6:155597356-155597730	375
CLDN22E01_001	GGGACATCCTACCAAATCCA	TGATCCTGGGAGGAATTCTG	chr4:184240642-184241016	375
CLDN22E01_002	TCTCATCCCAGAACTCCTGAA	CTTTGCTGGGATGGGTTTTA	chr4:184240918-184241322	405
CLDN22E01_003	ACACAGGTTTGCCAGAGTCC	ACCTTGGCATTACTGGTTGG	chr4:184241208-184241586	379
CLDN23E01_001	CGACAGCGGAGAAGGAAG	CACGAAGTTGGGCTCGTC	chr8:8559854-8560244	391
CLDN23E01_002	GTCCTGGGGCTTCTGCTG	GGCCGTCGCTGTAGTACTTG	chr8:8560182-8560590	409
CLDN23E01_003	AGCAGCGTCAGCACCATC	GAAAGGCAGATTTCCATCCA	chr8:8560515-8560908	394
CLDN24E01_001	ACATCTCTGGCCTTGTCG	TTTGAGAATTGGAGAGAGTCAGA	chr4:184242894-184243268	375
CLDN24E01_002	CAGAATTCCTCCCAGAATGA	TGGCTTTAATCTTTAGAACAGCA	chr4:184243205-184243578	374
CLDN24E01_003	TGGCAAATAAGTTGTAATAATGGA	AGCCCTCTTTGTTCATCCTT	chr4:184243487-184243879	393
CLDN25E01_001	TTGGACACACCCTCTAAACC	CTCCCAAATCCCCATGAT	chr11:113650325-113650673	349
CLDN25E01_002	TGGGTCTGCTCCTGTGTTAC	GGAGACTGGAAGGAGGGTAG	chr11:113650578-113650931	354
CLDN25E01_003	GTCTCCTGGGAAGGACTTTG	GGCAGAAGCCAGTCCTAGAT	chr11:113650873-113651221	349
CLDN25E01_004	TATTTTCCTGGCTCTTGGTG	AAAAATACATTTGTTAGACACTGTGC	chr11:113651036-113651398	363

Table 5. Primer Sequences for Amplification of Claudin Exons

Forward and reverse primers used to amplify all 23 claudins to generate amplicons between 300 to 400 base pairs.

CHAPTER III: Results

3.1 Expression of C-CPE-Sensitive Claudins in Chick and Mouse Nephric Duct and Mouse Ureteric Bud

3.1.1 *Claudin-1* mRNA Expression in the Chick Nephric Duct

Whole mount *in situ* hybridization was performed to determine at what stage and in which region of the nephric duct claudins where first expressed. The expression patterns of the C-CPE-sensitive claudins *Claudin-3, -4, -8* and *-14* and *Claudin-1* were analyzed from stages HH10 to HH20. At HH10, between the 6th and 10th somite, mesenchymal cells aggregate within the intermediate mesoderm. At HH12-13, mesenchymal cells epithelialize adjacent to the 16th somite. At HH14-15, the nephric duct continues to epithelialize and elongate and by HH17, it becomes an epithelial tube (Obara-Ishihara et al., 1999).

Lim1 is a transcription factor expressed in a subset of intermediate mesoderm cells that will give rise to the nephric duct (Kobayashi et al., 2005). I performed *in situ* hybridization on chick embryos HH8-HH20 using a *Lim1* antisense riboprobe to compare its expression to the selected claudins. *Lim1* expression was detected as early as HH8 (Figure 9a), and was expressed in the mesenchymal precursor cells of the duct at HH10, within the intermediate mesoderm, somites 8 to 10 (Figure 9b) (Obara-Ishihara et al., 1999; Attia et al., 2012). *Lim1* expression was seen at HH12 (Figure 9c) when the nephric duct is first discerned as an epithelial structure, and it continued to be expressed at HH14-HH16 (Figure 9d and 9e) and at HH17 (Figure 9f).

Claudin-1 was expressed in the nephric duct at HH12 to HH20 and not in the intermediate mesoderm at HH10 as observed for *Lim1*. At HH10, *Claudin-1* was only expressed in the neural tube, the ectoderm and endoderm (Figure 10a). In the nephric duct, *Claudin-1* was expressed at HH12 at the level of the 16th somite (Figure 10 b'' and b'''). At HH17, *Claudin-1* was expressed along the entire duct. It was observed at the most anterior region, at the level of the heart (Figure 10c, c') and at the most posterior region, inserting into the cloaca (Figure 10c''). At this stage *Claudin-1* was also seen in the pronephric tubules adjacent to the anterior duct (Figure 10c'). By HH20, when the nephric duct has completely elongaed, *Claudin-1* was expressed in the mesonephric tubules (Figure 10d"). *Claudin-1* sense riboprobe was used as a control and revealed no specific staining at stages HH10 to HH20 (Figure A1).

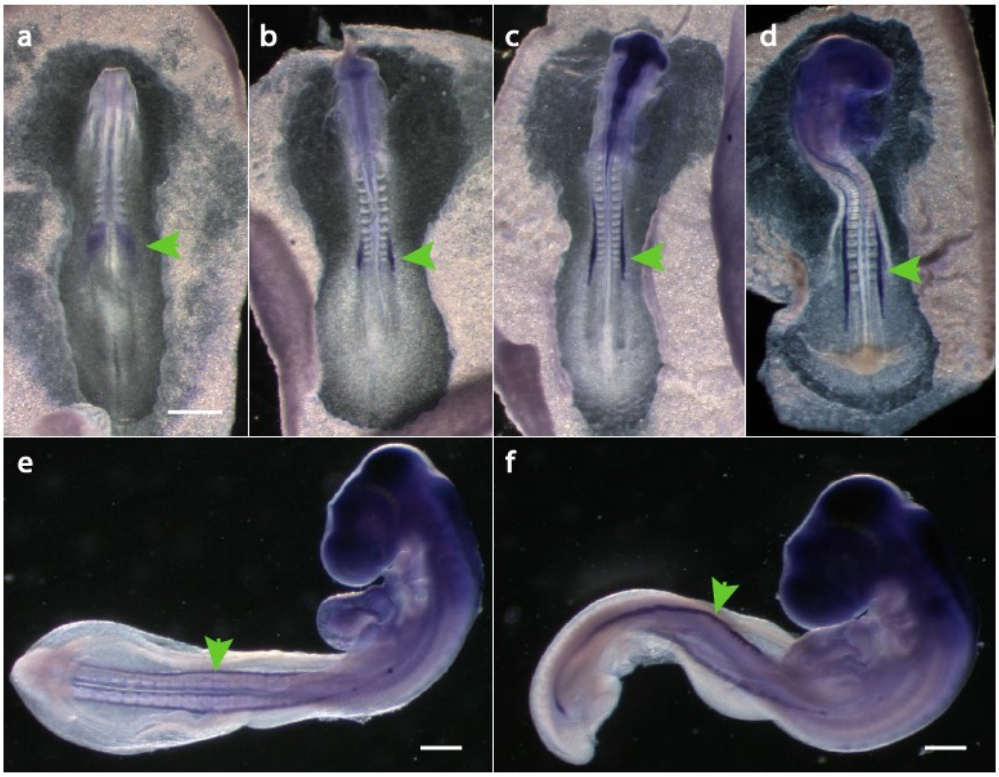

Figure 9. *Lim1* mRNA Expression in the Nephric Duct of Chick Embryos

In situ hybridization of *Lim1* in (a) HH8 and (b) HH10 chick embryos with *Lim1* expression in the intermediate mesoderm in the precursors cells of the nephric duct. At HH12 (c), HH14 (d), HH16 (e), and HH17 (f) *Lim1* was expressed in the nephric duct of chick embryos. Green arrowheads indicate the expression in the intermediate mesoderm and the nephric duct. Scale bar, 1mm.

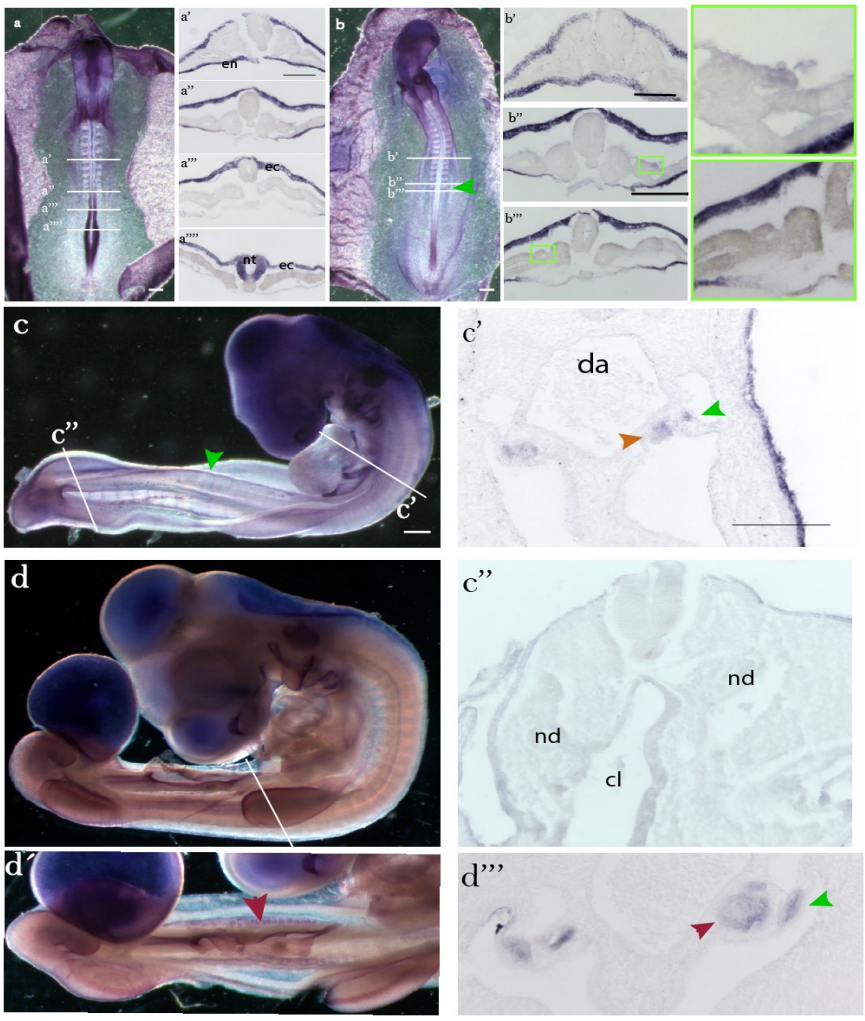

Figure 10. *Claudin-1* mRNA Expression in the Chick Nephric Duct

Whole mount *in situ* hybridization of *Claudin-1* in HH10 (a) HH12 (b), HH17 (c) and HH20 (d) embryos. (a', a'', a''', a'''') Transverse sections from anterior to posterior regions at the level of the white lines of a HH10 embryo (a) showed no nephric duct. Transverse sections from HH12 embryo (b) showed *Claudin-1* expression in the nephric duct at the level of the 16th somite (indicated by green arrowhead) (b'', b'''). Magnified images of the nephric duct shown in the green squares. *Claudin-1* was not expressed when there was no epithelialized duct in anterior regions (b'). Transverse sections at the level of the white lines of HH17 embryo (c) show *Claudin-1* expressed in the anterior region of the nephric duct (shown by green arrowhead) (c') and at the most posterior region where the duct inserts into the cloaca (c''). Pronephric tubules (orange arrowhead) expressed *Claudin-1*. (d, d''') HH20 *Claudin-1* whole mount and transverse section at the level of the white line show expression in mesonephric tubules (purple arrowhead) and nephric duct (green arrow). (d') Ventral view of *Claudin-1* expression in a HH20 chick embryo. Mesonephric tubules (purple arrowhead) are observed along the nephric duct. Scale bar, 100 µm. Abbreviations: en, endoderm; ec, ectoderm; nt, neural tube; da, dorsal aorta; cl, cloaca; nd, nephric duct.

3.1.2 *Claudin-3* mRNA Expression in the Chick Nephric Duct

Similar to *Claudin-1*, *Claudin-3* was first observed at HH12 (Figure 11a). *Claudin-3* was expressed in the nephric duct adjacent to the 16th somite (Figure 11a'''). At a more anterior region at the level of the 2nd somite, *Claudin-3* was not observed in the intermediate mesoderm (in the mesenchymal cells precursors to the nephric duct) (Figure 11a''). *Claudin-3* expression was observed along the entire anterior-posterior region of the duct at stages HH16 and HH20 (Figure 11b and c). It was observed approximately at the level of the first somites adjacent to the dorsal aorta as shown in the whole mount (Figure 11c) and the transverse section (Figure 11c') down throughout the nephric duct up until its insertion into the cloaca (Figure 11c'''). *Claudin-3* sense riboprobe was used as a control and showed nonspecific signal compared to the antisense riboprobe HH10 to HH20 (Figure A2).

3.1.3 *Claudin-4* mRNA Expression in the Chick Nephric Duct

In situ hybridization with an antisense riboprobe for chick *Claudin-4* showed low levels of expression in the nephric duct in whole mounts at HH12, HH14, and HH16 (Figure 12). Transverse sections (Figure 12a, b and c) revealed lower expression of *Claudin-4* in the nephric duct compared to *Claudin-1* or *Claudin-3*. *Claudin-4* expression began when the nephric duct starts to form at HH12 (Figure 12a'). *In situ* hybridization was performed with a *Claudin-4* sense riboprobe as well and showed no specific signal in the chick embryos stages HH10 to HH20 (Figure A3).

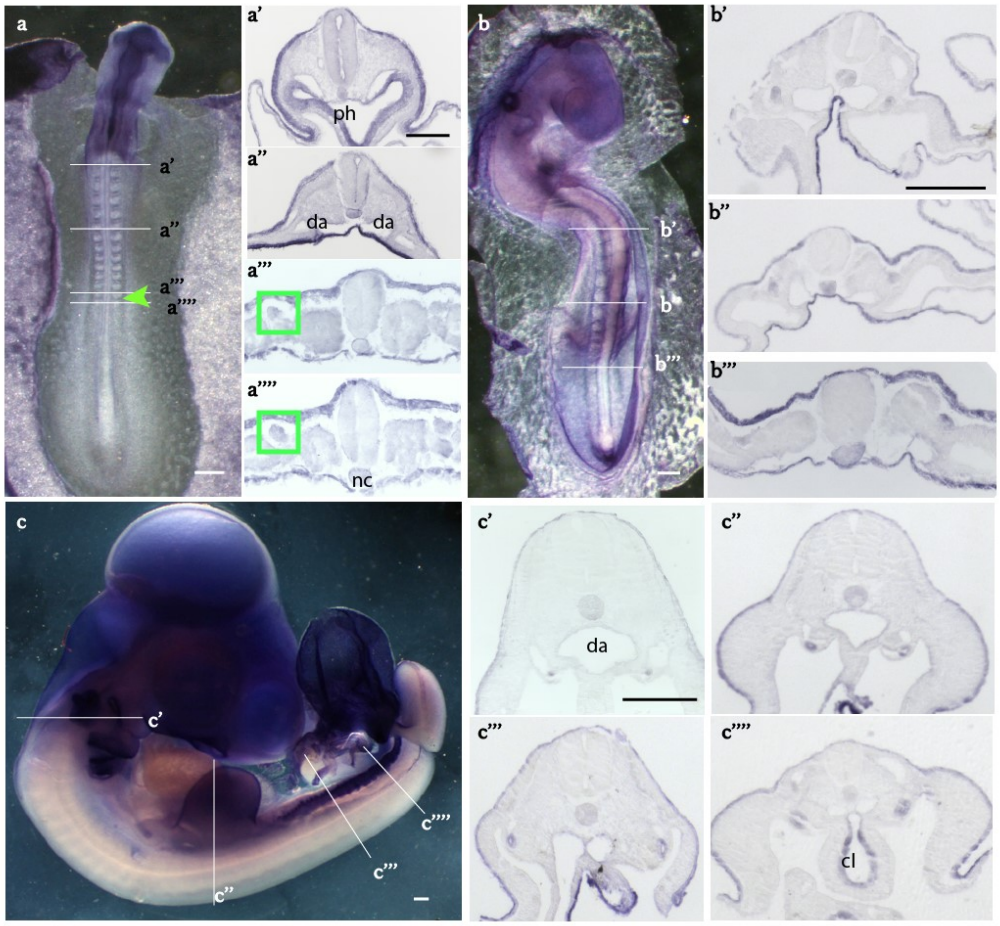

Figure 11. *Claudin-3* mRNA Expression in the Chick Nephric Duct

Whole mount *in situ* hybridization of *Claudin-3* in HH12 (a), HH16 (b) and HH20 (c) chick embryos. (a') Transverse section at the level of the pharynx of the embryo defined by the white line. No nephric duct is seen in this region (a''). (a''', a'''') *Claudin-3* was expressed in the nephric duct (green squares) in transverse sections at the level of the 16th somite (indicated by green arrowhead) in HH12 embryo. (b', b'', b''') *Claudin-3* expression in the nephric duct shown in transverse sections from the region indicated by the white lines on HH16 embryo (b). *Claudin-3* expression in the nephric duct at HH20 from the most anterior region of the duct extending to the level of the cloaca (c', c'', c'''). Scale bar, 100 µm. Abbreviations: ph, pharynx; nc, notochord; da, dorsal aorta; cl, cloaca.

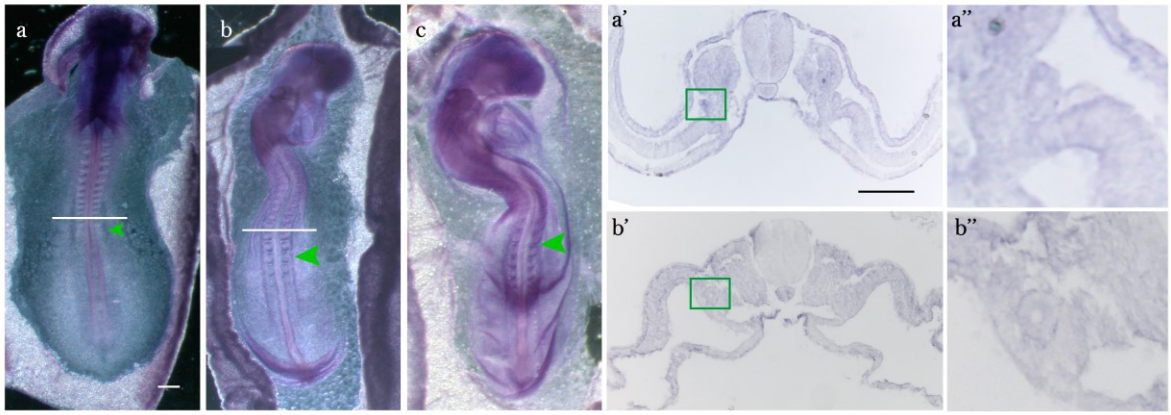

Figure 12. *Claudin-4* mRNA Expression in the Chick Nephric Duct

Whole mount *in situ* hybridization of *Claudin-4* antisense riboprobe in chick embryos at HH12 (a), HH14 (b) and HH16 (c). *Claudin-4* expression in the nephric duct (green square) shown in transverse sections at the region indicated by the white line. (a', b') *Claudin-4* expression in the nephric duct at H12, HH14 and HH16 and in (a'', b'') magnified images of the nephric duct indicated by the green square. Nephric duct expression in the whole mount indicated by green arrowhead. *Claudin-4* was also observed in the somites at these stages. Scale bar, 100 μm.

3.1.4 *Claudin-8* and *-14* Are not Expressed in the Chick Nephric Duct

Analysis of *in situ* hybridization experiments using antisense riboprobes for *Claudin-8* and *Claudin-14* revealed that they were not expressed in the nephric duct (Figure 13 and 14). From stages HH12 to HH20, neither *Claudin-8* nor *-14* expression was detected in the duct. *Claudin-8* was previously reported to be expressed in the mouse nephric duct (Khairallah, 2013), while *Claudin-14* has been shown to be expressed both in the mouse and chick at later stages during kidney development, but not in the nephric duct (Khairallah, 2013). *In situ* hybridization was performed using sense riboprobes for both *Claudin-8* and *-14* in order to prove that the staining seen with the antisense riboprobes was specific (Figure A4 and A5).

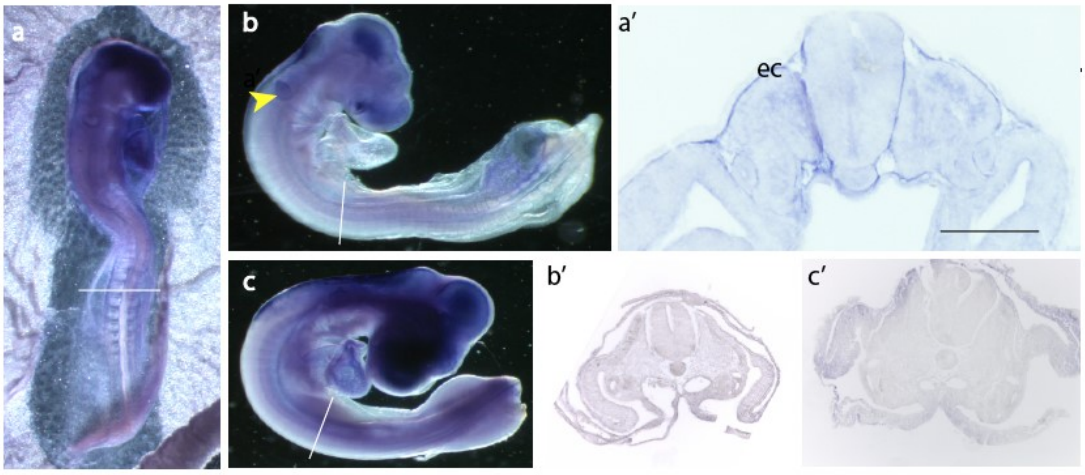

Figure 13. Whole Mount *In situ* Hybridization with *Claudin-8* Antisense Riboprobe in Chick

Chick embryo whole mounts at HH14 (a), HH17 (b) and HH18 (c). *Claudin-8* was not expressed in the nephric duct. (a', b', c') Transverse sections on the whole embryos were taken at the regions shown by the white lines. *Claudin-8* is expressed in the otic vesicle (yellow arrowhead) and the ectoderm (ec) as shown in a'. Scale bar, 100 μm.

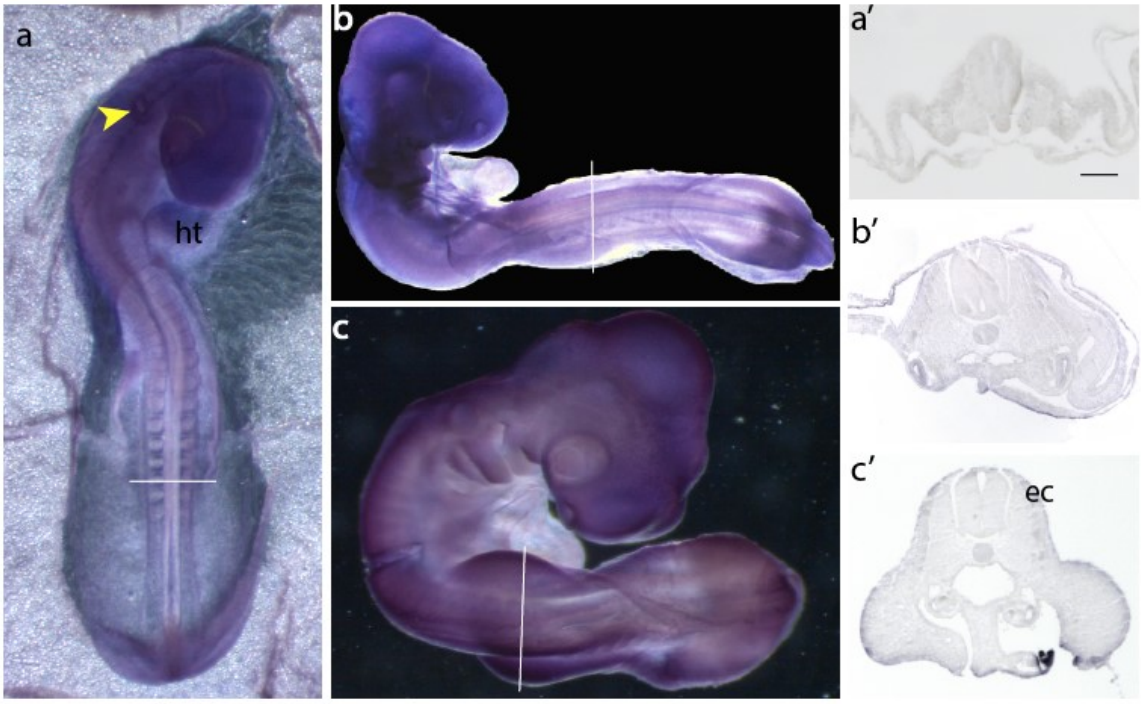

Figure 14. Whole Mount *In situ* Hybridization with *Claudin-14* Antisense Riboprobe in Chick

Whole mount *in situ* hybridization of chick embryos at HH16 (a), HH17 (b) and HH19 (c) had no *Claudin-14* expression in the nephric duct. (a', b', c'). Transverse sections of whole mount embryos at the regions indicated by the white lines. *Claudin-14* is expressed in the otic vesicle (yellow arrowhead), and the ectoderm (ec) as shown in c'. Scale bar, 100 μm.

3.1.5 *Claudin-4* mRNA Expression in the Mouse Nephric Duct and Ureteric Bud

To examine claudin expression in the metanephric kidney during ureteric bud branching I used the mouse as a model to observe branching morphogenesis. I performed *in situ* hybridization to examine two C-CPE-sensitive claudins, *Claudin-4* and *Claudin-14,* in the mouse nephric duct and during the first branching events of the ureteric bud. Embryos were dissected at E10.5 when the nephric duct has reached the cloaca and the ureteric bud outgrowth emerges. *In situ* hybridization was also performed at E13.5, after the completion of two to three rounds of ureteric bud branching, and at a later stage of branching at E16.5.

Claudin-4 was expressed in the nephric duct in mouse embryos. The expression pattern was similar to the one observed in the chick nephric duct, in that Claudin-4 showed less intensity compared to *Claudin-1* and *-3* (Figure 15a''). *Claudin-4* was expressed in the ureteric bud tips at E13.5 and the ureteric tips and trunks at E16.5. *Claudin-4* was also in the ureter.

3.1.6 *Claudin-14* Is Not Expressed in the Mouse Nephric Duct and Ureteric Bud

Claudin-14 was previously reported to be expressed within tubular kidney structures in later stages after E16.5 in the mouse kidney (Khairallah, 2013). In order to asses if *Claudin-14* was expressed at earlier stages, *in situ* hybridization in whole mount mouse embryos at E10.5 and mouse embryonic kidneys at E13.5 and E16.5 was performed. The results showed that *Claudin-14* was not expressed at E13.5 or E16.5 in mouse embryonic kidneys (Figure 16), or in the mouse nephric duct at E10.5, similar to what was seen in the chick.

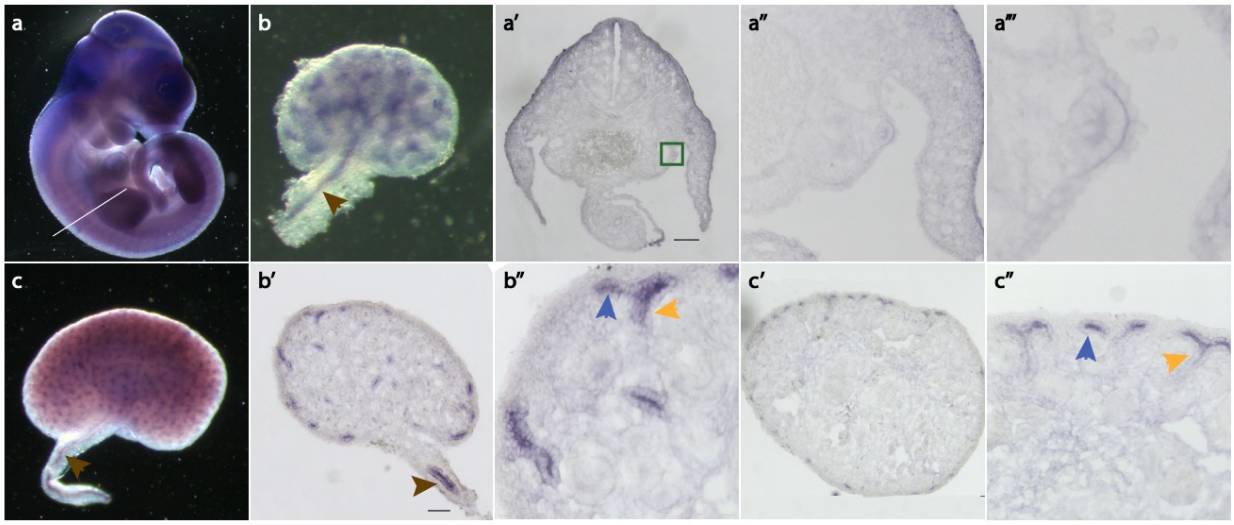

Figure 15. *Claudin-4* mRNA Expression in the Mouse Nephric Duct and Ureteric Bud

Whole mount *in situ* hybridization of *Claudin-4* antisense riboprobe in E10.5 (a) embryos and mouse embryonic kidneys at E13.5 (b) and E16.5 (c). (a') *Claudin-4* expression in the nephric duct shown by transverse section in the region indicated by the white line. (a'', a''') Magnified images of the nephric duct (green square). (b) Mouse embryonic kidney at E13.5 with *Claudin-4* expression in the ureteric bud tips and trunks, and in the ureter. (b', b'') *Claudin-4* expression in transverse section and magnified image of E13.5 kidney. (c) *Claudin-4* was also expressed in E16.5 mouse kidney in the ureteric bud tips and trunks, as well as in the ureter. Ureter is indicated by brown arrowhead (b, b', c) the ureteric bud tip by the blue arrowheads (b'', c'') and ureteric bud trunk by yellow arrowheads (b'', c''). Scale bar, 100 μm.

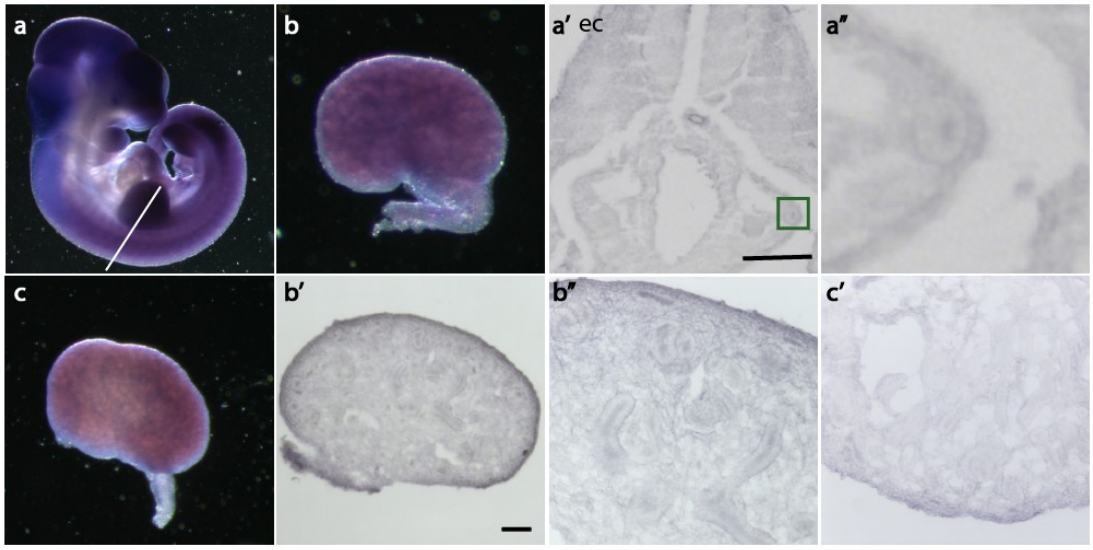

Figure 16. Whole Mount *In situ* Hybridization with *Claudin-14* Antisense Riboprobe in Mouse

Whole mount *in situ* hybridization using *Claudin-14* mouse antisense riboprobe in E10.5 (a) embryos and E13.5 (b) and E16.5 (c) mouse embryonic kidneys. (a') Transverse section in the region indicated by the white line. No expression of *Claudin-14* in the nephric duct. (a'', a''') Magnified images of the nephric duct (green square). (b) Mouse embryonic kidney E13.5. (b', b'') Transverse section and magnified image of E13.5 kidney. (c) E16.5 mouse embryonic kidney. *Claudin-14* was only expressed in the ectoderm (ec) at E10.5 (a'). Scale bar, 100 μm.

3.2 Human Cohort Sequencing Analysis

3.2.1 The CKiD Cohort

The CKiD cohort includes approximately 600 children between 1 and 16 years old with different causes of chronic kidney disease with a mild to moderate kidney function with an estimated glomerular filtration rate (GFR) between 30 and 90ml/min/1.73m^2. 96 children with either renal dysplasia, hypoplasia, or agenesis were selected. There is no access to other demographic data, including ethnicity, gender or family history of these children with CAKUT.

3.2.2 CKiD Cohort and Analysis for Claudin Variants

To better understand the role that claudins play in the development of the kidney. I hypothesized that damaging variants in claudins might alter nephric duct elongation and/or ureteric bud branching and lead to CAKUT. Therefore, DNA samples from 96 CAKUT patients in the CKiD cohort were sequenced using next-generation technology. The entire family of claudins were exon-sequenced to determine if the patients carried any claudin variants, including in the C-CPE-sensitive family members described above.

Exon sequences were analysed using IGV (Integrative Genomics Viewer) software, a visualization software that color codes a change in a nucleotide base. Two specific cut-offs were used to record variants. First, a mean coverage of the total number of reads per base of 100x, and second, a minimum of 25% of reads with a change of base were necessary to call a variant (Nicolaou, et al., 2016).

79 variants in the 23 CLDNs were identified. Forty-two of the 79 nucleotide variants were synonymous mutations. Of these, 17 were common, 16 were rare and 9 were novel. Common variants had a minor allele frequency (MAF) greater than 1%, rare variants had a MAF less than or equal to 1%, and novel variants were absent from ExAC (Exome Aggregation Consortium) (Lek et al., 2016) (http://exac.broadinstitute.org). ExAC is a browser that contains a consortium of large-scale sequencing projects from around the globe representing 60,000 individuals with no severe pediatric diseases.

From the 37 non-synonymous variants, 17 common, 16 rare and 4 novel were detected. A summary of the analysis of variants is shown in a workflow chart in Figure 17. Only 17 of the 20

non-synonymous rare and novel variants were confirmed through Sanger sequencing, the other three were false positives. The chromatographs of all 17 wildtype and variant sequences are shown in Figure 18 and 19. The location of all the confirmed non-synonymous variants and their corresponding amino acid location is shown in Figure 20.

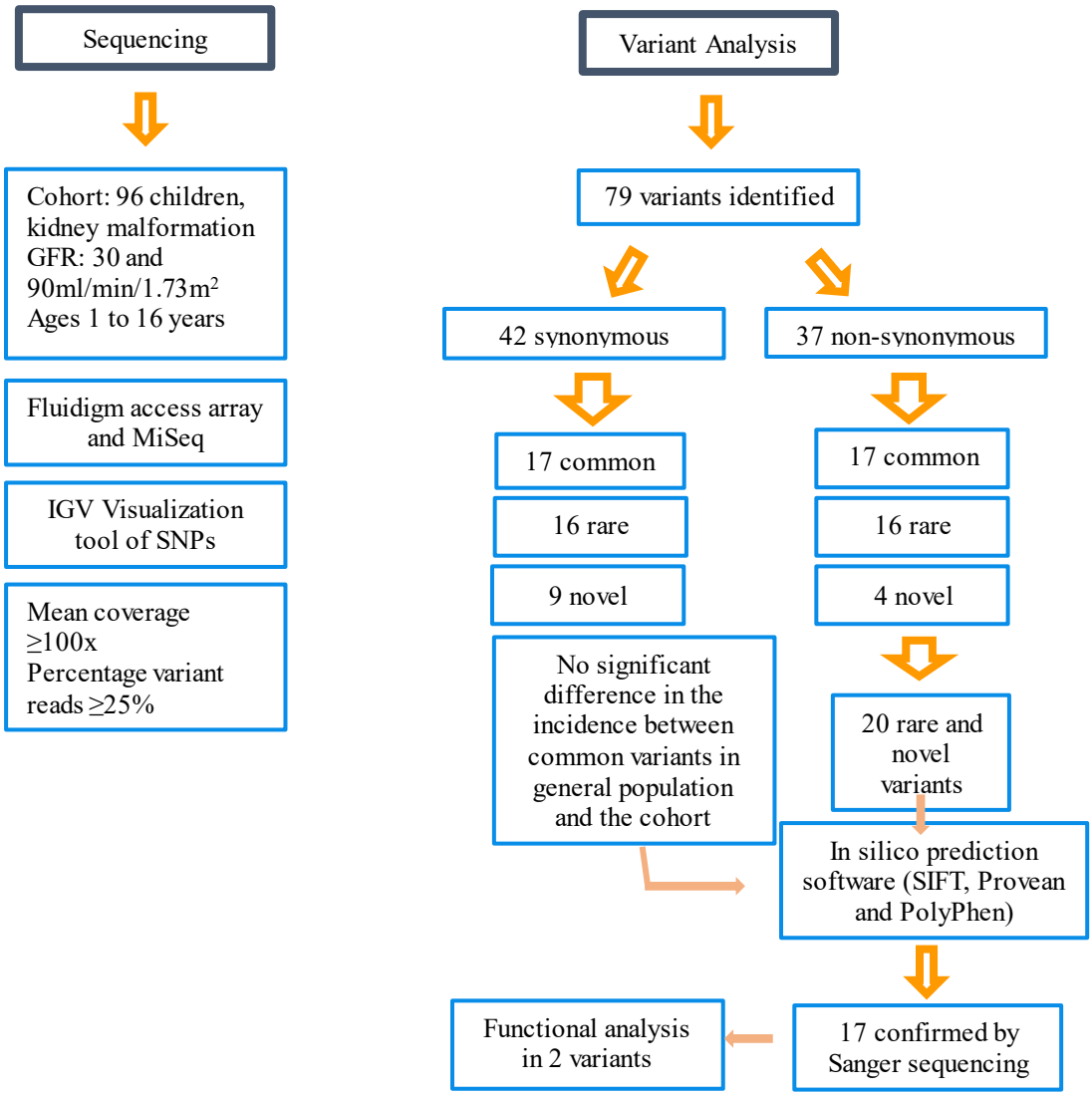

Figure 17. Chart Workflow of Claudin Variant Analysis of CKiD Cohort

Sequencing on 96 children from the CKiD cohort using Fluidigm access array paired with MiSeq next-generation sequencing. Nucleotide changes were visualized using IGV at a mean coverage of ≥100x. Variants in the CKiD cohort were classified into non-synonymous and synonymous and common, rare or novel. Common variants were compared using the ExAC browser. From the 17 confirmed variants, 2 were selected for functional analysis.

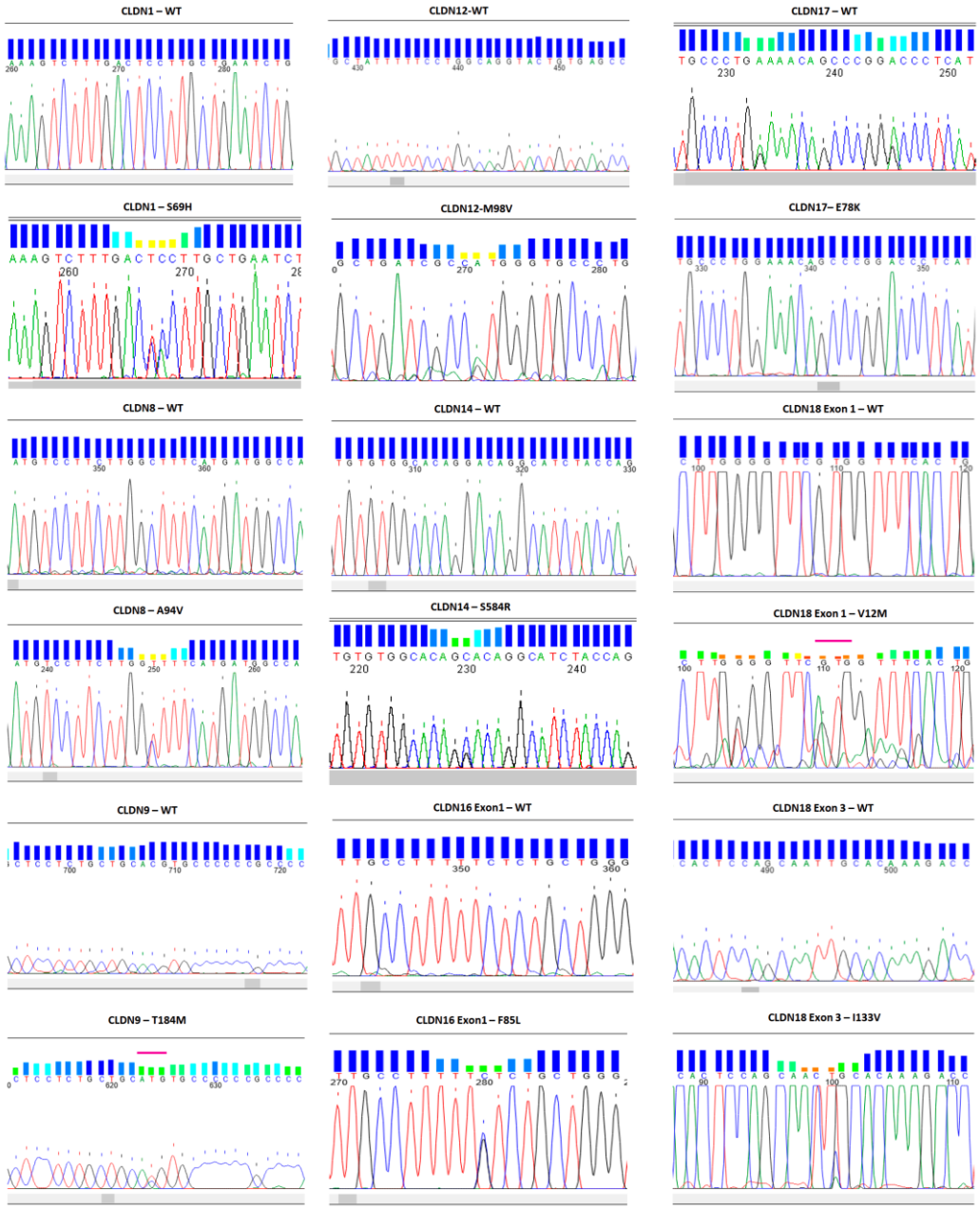

Figure 18. Chromatographs of Rare and Novel Non-synonymous Variants in CKiD Cohort: Claudins 1-18

Variants were confirmed through Sanger sequencing as shown by the chromatograms. Genes are read in the direction at which they are translated. The mutation is indicated by a change in color or a purple line (when the change in color is not clear). Claudin-17 chromatogram shows both the rare variant (*CLDN17*-E78K) and the common (*CLDN17*-A82T) variants.

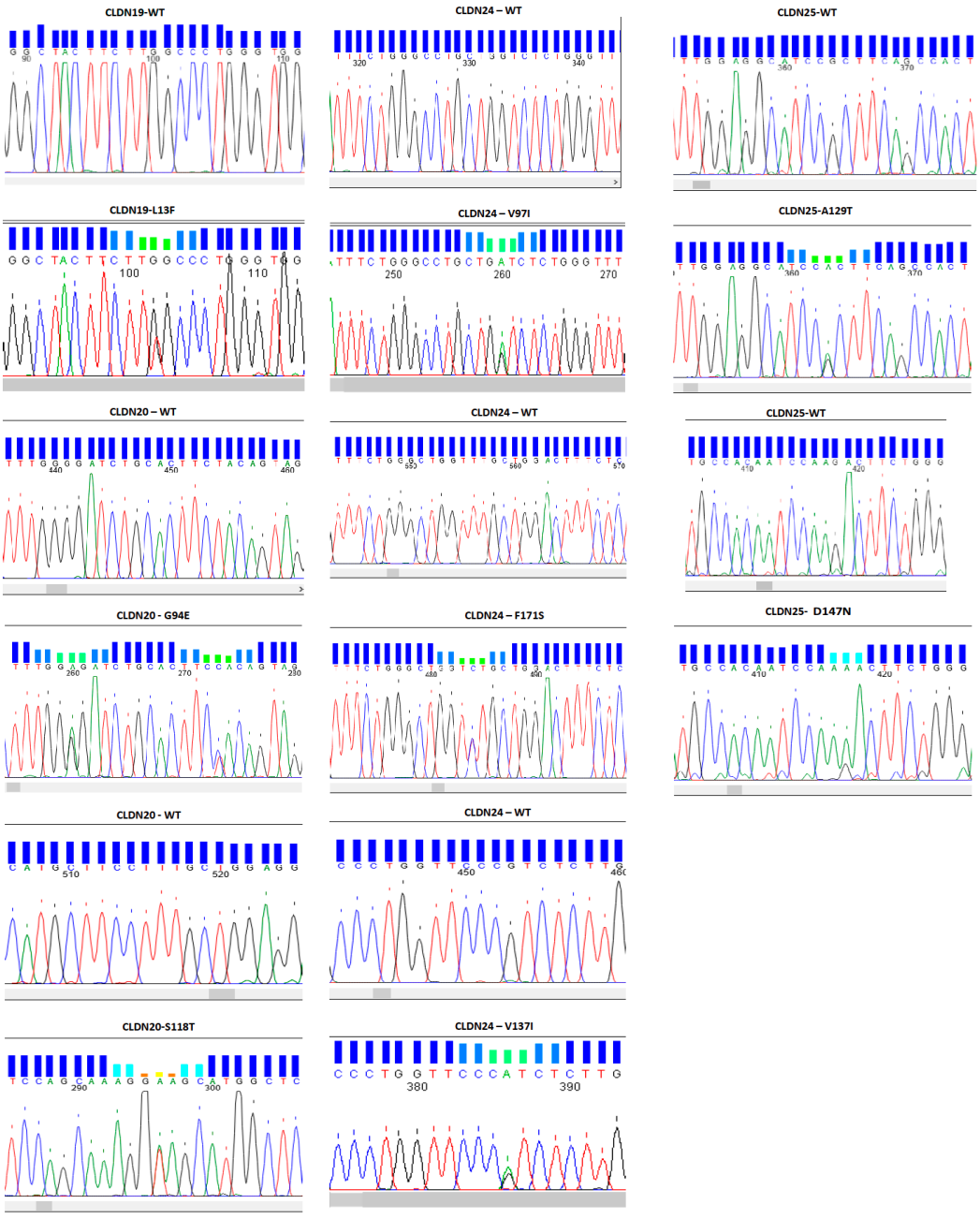

Figure 19. Chromatographs of Rare and Novel Non-synonymous Variants in CKiD Cohort: Claudins 19-25

Variants were confirmed through Sanger sequencing as shown by the chromatograms. Genes are read in the direction at which they are translated. The mutation is indicated by a change in color or a purple line (when the change in color is not clear). Claudin-20 chromatogram shows both the rare variant (*CLDN20*-G94E) and the common (*CLDN20*-S98S) variants.

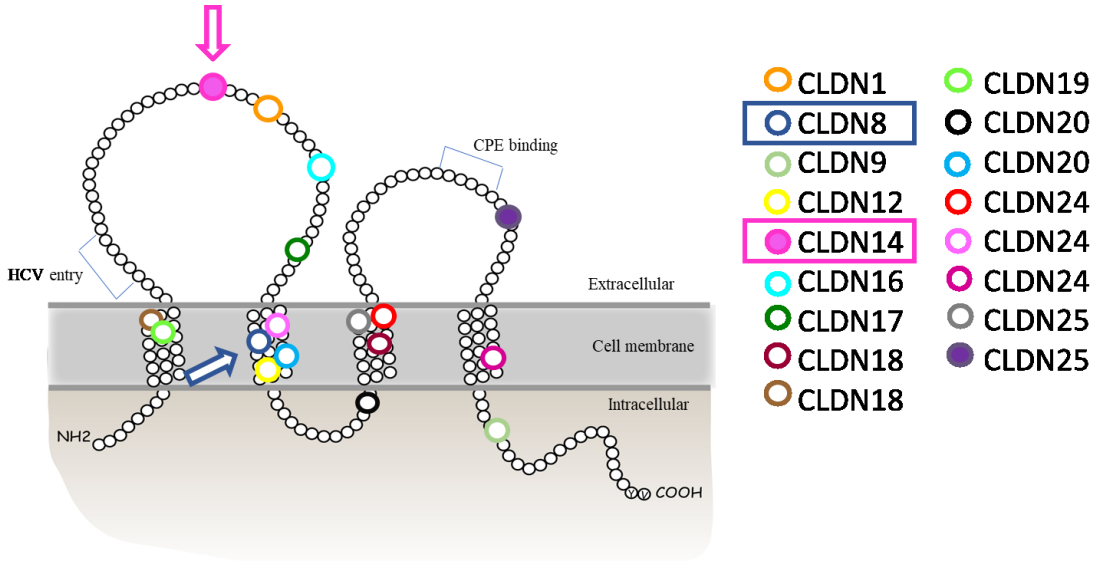

Figure 20. Localization of Non-Synonymous Mutations to Claudin Protein Domains

The diagram shows the location of each of the non-synonymous rare (empty circle) and novel (solid colored circle) variants found in the CKiD cohort within the claudin protein structure. Three variants are localized in the first transmembrane domain, 4 are in the first extracellular loop, 1 is in the intracellular loop, three are in the third transmembrane domain, 1 is in the fourth transmembrane domain and 1 is found in a cytoplasmic C-terminal tail. Two variants: Claudin-8 A94V and Claudin-14 S58R were selected for functional analysis.

I compared the MAF of the common variants in the CKiD cohort to the general population using the ExAC database (Lek et al., 2016). According to statistical analyses using the chi-squared test, there were no significant differences between the MAF of the cohort and the population (Table 6). SIFT (Sorting Intolerant from Tolerant) (Vaser et al., 2015) (http://sift.jcvi.org/) and Provean (Protein Variation Effect Analyzer) (Choi et al., 2012) (http://provean.jcvi.org/) were used as *in silico* prediction software to assess if amino acid changes were deleterious for protein function based on the nucleotide change and the evolutionary conservation of the amino acid at a specific position. All common variant scores were neutral and tolerated, which means the amino acid changes were not predicted to have a negative effect on the function of the claudin as shown in Table 6.

For the remainder of my analysis, I focused on the non-synonymous rare and novel variants. All 20 rare and novel synonymous variants were analysed *in silico* using PolyPhen and SIFT prediction software to predict if the variant could be detrimental to protein function and structure (Table 7). PolyPhen (Polymorphism Phenotyping) (Adzhubei et al., 2010) (http://genetics.bwh.harvard.edu/pph2/) and SIFT both use the evolutionary conservation of the amino acid across species as well as the location of the amino acid on the protein, to assess the effect on protein structure and function. The SIFT score considers a variant damaging when the score ranges from 0.0 to 0.05, and tolerated when the score is from 0.05 to 1.0. In PolyPhen, it is the opposite, scores from 0.0 to 0.05 are tolerated, while scores from 0.05 to 1.00 are defined as 'possibly damaging' to 'damaging'. The list of variants and their predicted socres using PolyPhen and SIFT are shown in Table 7.

3.2.3 Rare and Novel *CLDN* Variants in CKiD Cohort

All of the rare mutations occurred in a heterozygous state. Six of the 17 non-synonymous rare mutations were found in two patients. The remaining variants were found in one patient each. In *CLDN1* a rare heterozygous variant, S69H (MAF=0.003%), was localized in the first extracellular loop and was found only in one patient. According to the prediction software PolyPhen (Adzhubei et al., 2010) and SIFT (Vaser et al., 2015), the change from a polar amino acid to a positively charged histidine could affect protein stability. A change to a histidine at this

position signifies a loss of a phosphorylation site, making the substitution from a serine to a histidine potentially a deleterious change for the protein.

The CLDN8 p.A94V variant with a MAF of 0.4% was detected in two patients. The variant is located in the second transmembrane domain. Given that both alanine and valine are non-polar amino acids it might not be detrimental for the protein function. However, the alanine at position 94 is a highly conserved amino acid among human, mouse and chick species. Given the previously reported expression patterns of *Claudin-8* in the mouse nephric duct and the fact that Claudin-8 is a C-CPE sensitive claudin, this variant was selected for functional analysis (See Results Section 3.6).

CLDN9 p.T184M is a rare variant (MAF=0.002%) in the cytoplasmic tail. The threonine at this position is a putative phosphorylation site for cdc2, as predicted by NetPhos3.1 (Blom et al., 1999), a server that predicts serine, threonine and tyrosine phosphorylation sites in eukaryotic proteins. Cdc2, cyclin-dependant protein kinase, is important for cell cycle progression. The substitution of the threonine for a non-polar amino acid might alter a phosphorylation site in the tail which in turn might affect its interaction with other proteins.

CLDN12 p.V98M is a rare variant, MAF of 0.3%, and it localizes to the second transmembrane domain. It was predicted to be benign by both PolyPhen (Adzhubei et al., 2010) and SIFT (Vaser et al., 2015). The methionine is a hydrophobic amino acid. Since valine is also a hydrophobic amino acid, this substitution is not likely to alter the folding of the protein.

CLDN14 p.S58R is a novel variant that localizes to the first extracellular loop. It is predicted to be deleterious by both PolyPhen (Adzhubei et al., 2010) and SIFT (Vaser et al., 2015). The change from a serine to an arginine has the potential to change in the structure of the protein, changing a non-charged amino acid for a positively charged one. A change in the charge of a residue in the first extracellular loop, which controls the ion selectivity of the claudin, could have a detrimental effect on permeability. Serine 58 is also predicted to be a phosphorylation site in CLDN14 according to NetPhos3.1. Based on the role of Claudin-14 in the mouse and the discovery of *CLDN14* mutations in human patients (Dimke et al., 2013; Gong et al., 2012; Thorleifsson et al., 2009), this variant was selected for follow up functional analysis.

CLDN16 p.F85L is a rare variant with a MAF of 0.3%, located in the first extracellular loop of CLDN16. The phenylalanine residue at position 85 is a poorly conserved amino acid between mouse, human and chick. Also, phenylalanine and leucine are both non-polar amino acids. For these reasons, both PolyPhen (Adzhubei et al., 2010) and SIFT (Vaser et al., 2015) predicted that this variant is benign and has no effect on protein function.

CLDN17 p.E75K (MAF=0.14) is a rare variant in the first extracellular loop of the protein. It was detected in a single patient. The substitution of glutamic acid modifies a negatively charged polar amino acid to a positively charged lysine. This change in charge is likely to affect the ion selectivity of the CLDN17 first extracellular loop. Also it may lead to the possibility of a change in the protein structure by altering its hydrophilic interactions, which can affect protein folding.

Two rare mutations were found in *CLDN18*: CLDN18 p.V12M, MAF=1%, is situated in the first transmembrane domain and p.I133V, MAF=0.1%, is situated in the third transmembrane domain. Both variants were found in two patients. The amino acid changes can potentially affect the assembly of the domains of the protein into the membrane, as well as the *cis*-interaction with other claudins. Variant V12M was predicted to be benign, since both valine and methionine are hydrophobic residues. On the other hand, variant I133V was predicted to be deleterious even though the amino acid change does not affect hydrophobicity, perhaps because it does affect a conserved amino acid between mouse, chick and human species.

CLDN19 p.L13F is a rare variant with a MAF of 0.3% in the first transmembrane domain. It was predicted to be deleterious by PolyPhen (Adzhubei et al., 2010) and SIFT (Vaser et al., 2015). Leucine and phenylalanine are both non-polar amino acids, suggesting that this substitution is unlikely to have an effect on the localization of the protein to the tight junction. However, it was predicted to be detrimental due to conservation of this leucine residue in human, mouse and chick.

CLDN20 p.G94E (MAF=1%), is located in the second transmembrane domain. The change of a glycine for glutamic acid is considered detrimental according to PolyPhen (Adzhubei et al., 2010) and SIFT (Vaser et al., 2015) given that glycine at this position is conserved in some species, including human and mouse. A change from a non-polar residue to a negatively charged

side chain can have drastic effects on protein interactions by affecting protein folding. However, this mutation has a minor allele frequency of 1% which also means that there are a higher number of people in the general population (compared to other mutations) with this variant, making it a potential risk factor more than a causal variant. A second rare variant in CLDN20, p.S118T (MAF=0.11%), occurs in the intracellular loop. It was not predicted to be deleterious by either PolyPhen (Adzhubei et al., 2010) or SIFT (Vaser et al., 2015). Serine and threonine are both polar amino acids without a charged chain, suggesting that there might not be any interference with the protein function. However, serine is predicted to be a phosphorylated site.

Three rare heterozygous variants were found in CLDN24: pV97I (MAF=0.6%), p.V137I (MAF=0.04%) and p.F171S (MAF=0.9%). Variants V97I and F171S, were found in two patients, one of whom also carried the CLDN8 p.A94V variant, while V137I was found in one patient. V97I is located in the second transmembrane domain, V137I is in the third transmembrane domain, and F171S maps to the fourth transmembrane domain. The substitution of valine at position 97 for an isoleucine does not change the hydrophobicity of the side chain, and it is a poorly conserved amino acid, making it a benign mutation. On the other hand, F171S was predicted to be deleterious by both prediction software. Substitution of the hydrophobic phenylalanine with the polar serine may alter the protein structure by shifting its accessibility to solvents and thus, the ion permeability of the claudin. A valine substitution for an isoleucine does not affect the charge of the side chain, and for this reason it was predicted to be benign.

The rare variant CLDN25 p.A129T had a MAF of 0.05% is located in the third transmembrane domain. The amino acid modification was predicted to be deleterious. A change from an alanine to a threonine changes a hydrophobic to a polar amino acid, and it introduces a potential phosphorylation site that could alter protein folding. A novel variant, p.D147N, was also found in *CLDN25,* located in the second extracellular loop of the protein. The variant was predicted to be benign by both PolyPhen and SIFT due to the fact that the residue is poorly conserved. However, it does have the potential to affect insertion of the claudin into the membrane or interactions with other proteins because the modification changes a non-polar uncharged amino acid to a negatively charged polar amino acid. A substitution in the second extracellular loop of the claudin could also affect its interaction with other claudin proteins (Furuse et al., 1999).

CLAUDIN	Common Variant	MAF	MAF (ExaC)	Chi²	SIFT	PROVEAN	Heterozygous (%)	Homozygous (%)
CLDN1	G123G	0.77	0.83	0.0268	Tolerated	Neutral	14.58	15.10
	G122G	0.015	0.014	0.9061	Tolerated	Neutral	1.56	0.00
	A36A	0.036	0.045	0.54746	Tolerated	Neutral	3.65	0.00
CLDN3	Y164Y	0.046	0.0057	1.19E-13	Tolerated	Neutral	0.52	2.08
CLDN4	I40I	0.032	0.0000082	0.000	Tolerated	Neutral	35.93	0.00
CLDN6	I1443V	0.42	0.3614	0.09098	Tolerated	Neutral	22.39	9.89
	I86I	0.015	0.01092	0.5864	Tolerated	Neutral	0.52	0.52
	V130L	0.036	0.0138	0.00836	Tolerated	Neutral	3.65	0.00
	L89L	0.026	0.042	0.269048	Tolerated	Neutral	2.60	0.00
	V136V	0.02	0.0104	0.18978	Tolerated	Neutral	2.08	0.00
CLDN7	V197A	0.6	0.65	0.146349	Tolerated	Neutral	20.83	22.92
CLDN8	S151P	0.26	0.297	0.26185	Tolerated	Neutral	17.71	4.17
	T129A	0.041	0.053	0.45796	Tolerated	Neutral	4.17	0.00
CLDN12	D62D	0.036	0.019	0.084456	Tolerated	Neutral	3.65	0.00
CLDN14	T21T	0.015	0.039	0.085836	Tolerated	Neutral	1.56	0.00
	T4M	0.031	0.04	0.524518	Tolerated	Neutral	3.13	0.00
	T229T	0.197	0.168	0.28245	Tolerated	Neutral	15.63	2.08
	R81R	0.234	0.216	0.54445	Tolerated	Neutral	19.27	2.08
	Y211Y	0.016	0.0062	0.09704	Tolerated	Neutral	1.56	0.00
CLDN15	P202P	0.14	0.224	0.00524	Tolerated	Neutral	8.85	2.60
CLDN16	A56P	0.224	0.1945	0,.30337	Tolerated	Neutral	18.23	2.08
	R55*DEL	0.224	0.0000082	0.000	Tolerated	Neutral	20.31	0.00
CLDN17	A82T	0.078	0.0943	0.44242	Tolerated	Neutral	6.77	0.52
CLDN18	S214S	0.067	0.122	0.02150	Tolerated	Neutral	6.77	0.00
	M149L	0,068	0.1148	0.040629	Tolerated	Neutral	7.29	0.00
CLDN20	S16S	0.656	0.661	0.88363	Tolerated	Neutral	21.88	17.71
	S98S	0.343	0.333	0.768748	Tolerated	Neutral	25.00	4.69
CLDN22	L177P	0.0156	0.00948	0.381510	Tolerated	Neutral	1.56	0.00
CLDN23	V210M	0.104	0.207	0.00042	Tolerated	Neutral	10.42	0.00
	P232S	0.161	0.409	2.75E-12	Tolerated	Neutral	13.02	2.08
	R81R	0.026	0.0337	0.5543	Tolerated	Neutral	2.60	0.00
CLDN24	Q207H	0.223	0.285	0.05702	Tolerated	Neutral	18.23	2.08
	I131V	0.0156	0.0111	0.55174	Tolerated	Neutral	1.56	0.00
	L18F	0.213	0.767	1.09E-64	Tolerated	Neutral	15.10	25.52

Table 6. Common Non-Synonymous and Synonymous Variants in CKiD Cohort and ExAC

Comparison between the MAF (minor allele frequency) of the common non-synonymous and synonymous variants in the CKiD cohort and in the ExAC database, used as a reference for the general population. According to the Chi^2 analysis there was no significant difference found between the MAF of these two groups. SIFT and Provean scores for the variants are tolerated or neutral. Percentages of how many patients out of 96 were heterozygous and how many were homozygous for the common variant are shown in the last two columns.

CLAUDIN	Variant	Patient	MAF (ExAC) in %	SIFT	PolyPhen
CLDN1	S69H	E12	0.003	0.041	1.00
CLDN8	A94V*	A1 and B12	0.4	0.002	0.997
CLDN9	T184M	A2	0.002	0.008	0.978
CLDN12	M98V	D4	0.3	1.00	0.00
CLDN14	S58R	A4	NOVEL	0.00	1.00
CLDN16	F85L*	D10 and H5	0.3	1.00	0.061
CLDN17	E78K	E11	0.14	0.004	0.955
CLDN18	I133V*	E6 and G2	0.1	0.039	0.924
	V12M*	A5 and C9	1	0.084	0.045
CLDN19	L13F	D6	0.3	0.002	0.998
CLDN20	S118T	H4	0.11	0.063	0.028
	G94E	C6	1	0.004	1.00
CLDN24	F171S*	H11 and B12	0.9	0.022	0.964
	V97I*	H11 and B12	0.6	0.207	0.248
	V137I	F10	0.04	0.006	0.990
CLDN25	D147N	E10	NOVEL	0.126	0.242
	A129T	C7	0.05	0.010	1.00

Table 7. Rare and Novel Non-Synonymous Variants in CKiD Cohort

Rare and novel non-synonymous CLDN variants found in patients with kidney malformations. All variants were confirmed by Sanger sequencing. All patients were heterozygous. * Indicates variants that were found in two patients, the rest were only found in one patient. MAF (minor allele frequency) in the ExAC database is given as a percentage. All variants were subjected to *in silico* predictions (PolyPhen and SIFT) to assess their mutagenic effect and a score was given based on how detrimental the substitution was for the protein function. The scores in red indicate those variants predicted to be deleterious, those with no color were predicted to be benign.

3.3 Retroviral Injections in Chick Embryos

In order to investigate the function of the variants I used the RCAS system to infect cells in the nephric duct. The rare variant in *CLDN8* (A94V) and the novel variant in *CLDN14* (S58R) were selected for functional analysis given that they are both C-CPE-sensitive claudins. CLDN8 p.A94V was found in two patients, one of whom also carried two mutations in *CLDN24*. Even though *Claudin-8* was not expressed in the chick nephric duct, it is expressed in the mouse nephric duct. *Claudin-8* is also expressed in the collecting ducts in the adult mouse kidney (Khairallah, 2013). In cells, Claudin-8 mediates paracellular Cl- reabsorption, and it interacts with Claudin-4, to recruit Claudin-4 to the tight junction. It has been shown that Claudin-8 deletion in the kidney causes hypotension and an increase in urinary salt excretion (Hou et al., 2010). *Claudin-14* is expressed in the thick ascending limb of Henle's loop (Dimke et al., 2013). Intronic polymorphisms in *CLDN14* that increase mRNA and protein expression are associated with a risk for kidney stones (Ure, et al., 2017). As mentioned in the Introduction, Claudin-14 is also important for calcium homeostasis in mice (Gong et al., 2012).

The nephric duct in HH10 chick embryos was injected with retroviral (RCAS) expression vectors at the level of the 10th somite. The RCAS vector contained the wildtype or the variant sequences of *CLDN8* (A94V) and *CLDN14* (S58R). After incubation, embryos were collected at HH12-14 when the nephric duct starts to form. This approach allows for all cells of the intermediate mesoderm and subsequently, the duct, to be infected with the viral expression vector carrying the claudin wildtype or variant sequence.

First, to assess that the virus was being injected into the right location within the embryo, *in situ* hybridization with an antisense riboprobe targeting the viral mRNA that encodes an envelope protein made by the virus, was performed. Figure 21 shows *env* mRNA transcripts on the injected side (dorsal right), for both the wildtype and variant of *CLDN8* and *CLDN14*. However, not all embryos examined were positive for *env* mRNAs on the injected side. In the injected CLDN8 WT embryos, 9 out of 12 embryos were positive for *env* mRNA transcripts on the injected side of the duct (Figure 21a). In embryos injected with the CLDN8 variant A94V, 12 out of 14 had *env* mRNAs detected in the injected duct (Figure 21b). 8 out of 12 embryos injected with the CLDN14 WT were *env*-positive in the injected duct (Figure 21c), and 10 out of 13 injected embryos with CLDN14 variant S58R had *env* mRNA detected in the injected duct

(Figure 21d). These results indicate that there is a 70 to 80% success rate of injections. The rest of the embryos were negative for *env* mRNA on both the injected and uninjected sides.

In situ hybridization with *Lim1* antisense showed that some embryos had different nephric duct elongation patterns. Compared to the uninjected side and to the embryos injected with the CLDN8 WT (Figure 22a), *Lim1* expression was interrupted in the duct infected with the retroviral particles carrying the CLDN8 variant A94V (Figure 22b). An underdeveloped duct was also observed in a second RCAS CLDN8 A94V variant embryo (Figure 22c). However, these patterns were only seen in two out of five embryos. RCAS CLDN14 WT embryos had normal expression patterns of *Lim1* (Figure 22d), while one of the six CLDN14 variant S58R embryos had abnormal *Lim1* expression (Figure 22e).

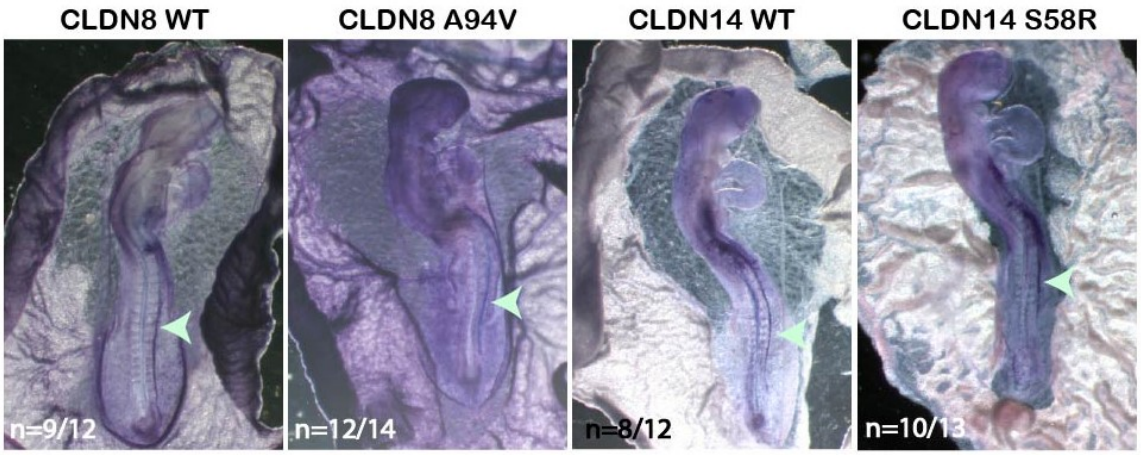

Figure 21. RCAS *env In situ* Hybridization of 24h Cultured Embryos After Retroviral Particle Injection at HH10

Whole mount *in situ* hybridization using antisense RCAS *env* riboprobe in HH14 (a) and HH15 (b, c, d) embryos, 24h after injection with retroviral particles. Embryos were injected with retroviral particles into the condensing mesenchyme adjacent to somite 10. (a) RCAS CLDN8 WT embryos showed RCAS infection in the duct on the side of the injection in 9 out of 12 embryos. (b) Embryos injected with retroviral particles encoding CLDN8 A94V also showed positive *RCAS* expression in the injected nephric duct in 12 out of 14 embryos. (c) RCAS CLDN14 WT embryos showed RCAS infection in the duct on the side of the injection in 8 out of 12 embryos. (d) RCAS CLDN14 variant S58R embryos showed RCAS infection in the duct on the side of the injection in 10 of the 13 embryos injected. Green arrows indicate positive RCAS infection on the injected nephric duct (dorsal view). n= number of positive embryos/total number of embryos inejcted. Scale bar, 100 mm.

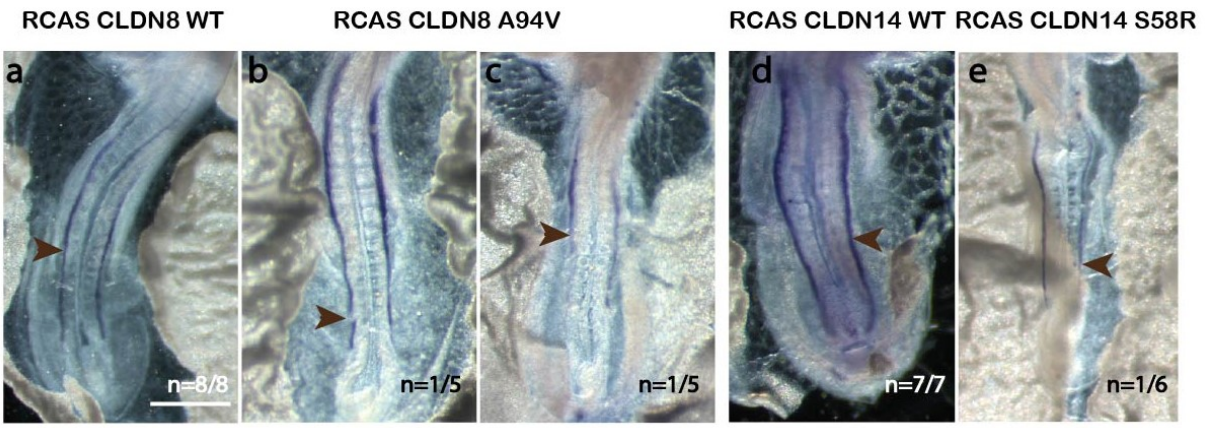

Figure 22. *Lim1 In situ* Hybridization of 24h Cultured Embryos After Retroviral Particle Injection at HH10

Whole mount *in situ* hybridization using antisense *Lim1* riboprobe in HH14 embryos (a, b, c, d, e), 24h after injection with viral particles. Embryos were injected with retroviral particles into the intermediate mesoderm adjacent to somite 10. (a) *Lim1* expression was normal in RCAS CLDN8 WT embryos in both the injected and uninjected ducts. (b) *Lim1* expression was normal in RCAS CLDN8 A94V injected embryos in the injected and uninjected ducts. However the injected duct is interrupted (shown by brown arrow). (c) A second embryo injected with retroviral particles encoding RCAS CLDN8 A94V showed aberrant *Lim1* expression in the injected duct (brown arrow). (d) *Lim1* expression was normal in RCAS CLDN14 WT injected embryos in both the injected and uninjected ducts. (e) *Lim1* expression was interrupted in the injected duct with retroviral particles expressing RCAS CLDN14 S58R. Brown arrows indicate injected side and phenotype. n= number of embryos with the same expression pattern/total number of embryos injected. Scale bar, 100 mm.

CHAPTER IV: Discussion

Claudins are necessary to form and maintain the tight junction, as well as to mediate protein interactions that link the tight junction to the actin cytoskeleton (Hartsock and Nelson, 2008). Claudins are implicated in barrier permeability properties in the kidney, by regulating transport of ions in different segments of the nephron (Breiderhoff et al., 2012; Günzel et al., 2009; Hou et al., 2009). Knock-out and knock-down mouse models implicate roles for claudins in renal barrier function; alerting claudin expression can alter homeostatic balance of ions leading to renal diseases (Ben-Yosef et al., 2003; Gong et al., 2012).

Although many claudins are expressed during kidney development, before the presence of a urine filtrate, their function is unknown. Single knock-out and knock-down mouse models of claudins do not yield any phenotype in early kidney formation. However, some studies have demostrated that claudins play a role in epithelial morphogenesis. For instance, claudins have been shown to be important during neural tube formation in the chick (Baumholtz et al., 2017). In another study, overexpression of Claudin-3 increased tubule formation during branching morphogenesis in mouse inner medullary collecting duct cell line (mIMCD-3) (Haddad et al., 2011). A study in *Xenopus* shows that knock-down of *XClaudin-6* prevents differentiation of the pronephros. Reduced *XClaudin-6* prevented the maintenance of the apical-basal polarity and caused a defect in cell adhesion, interfering with tubule formation (Sun et al., 2015). These studies suggest a role for claudins in formation of epithelial structures in early embryo development.

4.1 *Claudin-1* and *-3* Are Expressed in the Chick Nephric Duct and *Claudin-4* Is Expressed in the Chick Nephric Duct and Mouse Ureteric Bud

The first objective of my thesis was to define when a subset of claudins were first turned on during early kidney development. I characterized their expression patterns during nephric duct development in the chick and the mouse. Previous work in the laboratory showed that *Claudin-1*, *-3*, and *-4* are expressed in the chick nephric duct (Collins et al., 2013; Simard 2014) and *Claudin-3*, *-4*, *-6*, *-7* and *-8* are expressed in the mouse nephric duct and in the ureteric bud epithelial lineages (Haddad et al., 2011; Khairallah et al., 2013). In the developed kidney, *Claudin-1* (Kiuchi-Saishin et al., 2002), *-2* (Enck et al., 2001), *-3, -4, -6* (Abuazza et al., 2006),

-7, -8 (Li et al., 2004), *-9* (Abuazza et al., 2006), *-10, -11, -14, -16* and *-19* (Kiuchi-Saishin et al., 2002; Angelow et al., 2007; Khairallah et al., 2013) are expressed in different nephron segments (Angelow et al., 2008). Here, I showed that *Claudin-1* is also expressed in the pronephros at HH17 and in the mesonephros at HH20 (Figure 10). The expression of different claudins in different species in the pronephros might suggest that claudin function is evolutionary conserved. XClaudin-6 mediates cell adhesion and polarity in the formation of pronephros in *Xenopus*, raising the possibility that Claudin-1 and Claudin-6 could play a role in formation and maintenance of the epithelium in the pronephros as well as the mesonephric tubules, and the metanephric kidney. The chick genome does not have *Claudin-6*, which is why it is not implicated in the formation of tubular structures in the chick, but it might have a conserved role in mouse and human.

I showed that *Claudin-1* and *Claudin-3* expression in the chick nephric duct started at HH12 once the nephric duct was epithelialized at the level of the 16th somite, contrary to Liml, which started to be express earlier, at the level of the 6th somite. *Lim1* expression was broader than *Claudin-1* and *-3* in the structures giving rise to the kidney, which means that *Lim1* is expressed in cells of the intermediate mesoderm that give rise to the nephric duct and in the nephric duct itself, while *Claudins* were only expressed once the duct starts to form a lumen. After HH12 and by HH14-15 the expression of *Claudin-1* and *-3* in the embryo starts to increase. This suggests that the increased claudin expression correlates with the epithelialization of the nephric duct. When cells undergo MET, claudins are turned on to form tight junctions allowing cell adhesion and cell polarization to occur.

Claudin-4 was expressed in the nephric duct in both chick and mouse embryos. However, it was expressed at a lower level than *Claudin-1* and *-3*. From transverse sections, it appeared as if not all cells of the duct expressed *Claudin-4*. Previous work showed that removing *Claudin-4* from the nephric duct with a C-CPE Claudin-4-specific variant disrupted nephric duct elongation, contrary to Claudin-3-specific C-CPE variants, which did not abrogate nephric duct elongation (Simard, 2014). This suggests that Claudin-4 plays a more important role than Claudin-3 during nephric duct elongation. Here, I also showed that *Claudin-4* is expressed in the ureteric bud tips, the ureteric bud trunks and the ureter in E13.5 and E16.5 mouse embryos. These results implicate *Claudin-4* in ureteric bud formation and branching.

My *in situ* hybridization analysis of the C-CPE-sensitive claudins also revealed that *Claudin-8* is not expressed in the chick nephric duct. In the adult kidney, *Claudin-8* is expressed in the distal nephron in the convoluted tubule and in the collecting duct. Tissue specific knock-out of *Claudin-8* in the collecting duct causes hypotension and metabolic alkalosis, probably due to disrupted barrier function resulting from the lack of interaction between Claudin-4 and -8 (Gong Y et al., 2015). This study indicates that interaction between Claudin-4 and Claudin-8 is important in maintaining the paracellular channel transport in the developed nephron.

Claudin-14 was not expressed in the chick or mouse nephric duct nor during ureteric bud branching. Claudin-14 is required in the adult nephron, where it acts as a paracellular cation barrier. Based on the mouse knock-out model (Ben-Yosef et al., 2003), the human mutations associated with kidney stones (Thorleifsson et al., 2009), and its expression patterns in the distal convoluted tubule and collecting duct (Kirk et al., 2010), Claudin-14 is essential to maintain the permeability properties in different nephron segments in the adult kidney.

The expression patterns of claudins in early kidney development, which seemed to be conserved between species, indicates a role in the formation of the epithelium of the pronephros, the mesonephros, the nephric duct, and the collecting duct system. This led to the hypothesis that claudin sequence variants found in patients with kidney malformation will disrupt nephric duct elongation and/or ureteric bud branching.

4.2 Common Variants in the CKiD Cohort

The incidence of claudin variants in the general population was determined using the ExAC database (Lek et al., 2016). None of the individuals included in the ExAC database have severe pediatric disease. There was no significant difference in the MAF of the common variants in the CKiD cohort as compared to the ExAC. This suggests that none of the common variants are causal of kidney malformations.

Nonetheless, common variants could be potential risk factors for kidney malformations. Although they are not disease-causing, common variants affect susceptibility. Common variants on a *CLDN* allele that are in *cis* with rare and/or novel variants may have an additive effect, contributing to kidney malformations. For instance, if Claudin-4 and -6 have similar functions, a

mutation in only *Claudin-4* might not give rise to a kidney phenotype. However, when combined with one or more common mutations in *Claudin-6*, a deleterious phenotype may be observed.

4.3 Rare and Novel Non-Synonymous Variants in the CKiD Cohort

Fifteen rare and two novel claudin variants were found in 96 patients in a heterozygous state in different locations within the different functional domains of the claudin proteins (Figure 20). The location within each of the domains of the protein can suggest how they might perturb claudin function. Variants affecting residues within the transmembrane domains could affect how claudins insert into the membrane, since the four domains anchor the protein within the phospholipid bilayer. They can potentially also lead to loss of a transmembrane domain. There were two rare variants (CLDN19 p.L13F and CLDN18 p.V12M) in the first transmembrane domain, four (CLDN8 p.A94V, CLDN12 p.V98M, CLDN20 p.G94E, CLDN24 p.V97I) in the second, three in the third one (CLDN18 p.I133V, CLDN24 p.V137I, CLDN25 p.A129T), and one in the fourth transmembrane domain (CLDN24 p. F171S).

In the kidney, claudin barrier properties are important for paracellular transport of nutrients, waste and water within the different segments of the nephron (Günzel et al., 2009; Gong et al., 2012; Van Itallie and Anderson, 2006). The ion selectivity of the barrier is largely determined by the first extracellular loop, while the second extracellular loop is involved in claudin-claudin interactions between cells. Variants in the second extracellular loop could disrupt claudin interactions with other claudins, whereas variants in the first extracellular loop could affect the permeability properties of the tight junction, by altering residues that contribute to ion selectivity of the tight junction. There were three rare variants and one novel located in the first extracellular loop. One rare variant was found in CLDN1 (p.S69H), a novel variant in CLDN14 (p.S58R), a second rare variant in CLDN16 (p.F85L), and a third rare variant in CLKDN17 (p.E75K). Both CLDN14 and 16 have been previously linked with transport of ions in the kidney (Dimke et al., 2013; Hou et al., 2007). Only one CLDN had a mutation in the second extracellular loop, CLDN25, p.D147N a novel variant.

Variants in the C-terminal tail can affect claudin localization to the tight junction if they disrupt a phosphorylation consensus sequence (Tanaka et al., 2005). They can also modify interactions with PDZ binding proteins, which could lead to alterations in the communication

with the actin cytoskeleton, affecting cell shape changes. Only one rare variant in CLDN9 (p.T184M) was located in the C-terminal tail, in a putative phosphorylation site for cdc2, predicted by NetPhos3.1 (Blom et al., 1999). There was also one variant found in the intracellular domain in CLDN20 (p. S118T). Although there is not that much known about the function of the intercellular domain, it contains palmitoylation sites that appear to be required for the assembly of claudins in the tight junction (Van Itallie et al., 2005).

Although all patients were heterozygous for both the rare and the novel variants, this sequence variation can have a significant effect on protein function. Compared to deletions or insertions, point mutations of an amino acid might not seem to be as detrimental. However, with heterozygous missense sequence variations, the aberrant protein may compete with the "wild-type" claudin to localize to the membrane. The variant protein may also disrupt the interactions of the wild-type claudin with other claudins or other tight junction proteins. Disruption of the hydrophobic interactions, as well as change of amino acids affecting protein structure might have a deleterious impact on the protein's function.

For my functional studies, I prioritized two variants that were found in patients with more than one claudin variant, novel variants, and C-CPE-sensitive claudin variants. CLDN8 p.A94V was selected because this variant was found in two patients, one of whom had two other mutations in CLDN24 and a common variant in CLDN6. The CLDN8 p.A94V variant was predicted to be deleterious and has a low MAF in the ExAC database (Lek et al., 2016). The second variant chosen for functional assessment was CLDN14 p.S58R because it is a novel variant predicted to be deleterious. Both CLDN8 and CLDN14 are C-CPE-sensitive claudins, and previous work shows that C-CPE disrupts nephric duct elongation and branching morphogenesis (Simard, 2014; Khairallah, 2013). For future studies, the next variants to be prioritized for analyses will be the rare variants in CLDN24 (p.V97I and p.F171S) that were also found in one of the patients carrying the p.A94V CLDN8 variant. Variants found in more than one patient (p.F85L in CLDN16, p.I133V in CLDN18, p.V12M in CLDN18), and the novel variant in CLDN25 (p.D147N) will also be prioritized.

In vivo studies in the chick showed that the nephric duct was appropriately targeted in approximately 70-80% of the embryos injected with the retroviral particles (RCAS CLDN8 WT

and p.A94V, and with RCAS CLDN14 WT and p.S58R). Embryos injected with RCAS CLDN8 A94V retroviral particles had defects in *Lim1* expression (n=2/5). The observations that the success rate of the injections was close to 80% and that 40% of the embryos have a phenotype suggest that CLDN8 A94V might disrupt nephric duct development. The embryos injected with the RCAS CLDN14 p.S58R variant had disrupted *Lim1* expression in only 1 out of 6 embryos, suggesting that nephric duct development is affected in ~one-third of the properly targeted nephric ducts. To further confirm the results, more round of injections and analysis of the embryo sections are needed.

4.4 CAKUT

Although sequencing CAKUT patients has helped in the discovery of new variants, there is still uncertainty in the strength of these studies in the absence of rigorous functional analysis in the kidney. Most studies have focused on candidate genes that have been previously linked with CAKUT (Heidet et al., 2017; Weber et al., 2006). Additionally, in the majority of cohort studies patients have mild kidney function, or a combination of both mild and severe kidney function (Thomas et al., 2011; Nicolaou et al., 2015 Weber et al., 2006). For this reason, the best option is for cohort studies to focus only on patients that have been rigorously phenotyped, or in babies or children in early childhood that have CAKUT and are in need for dialysis. Sequencing of these patients will identify variants that are associated with severe congenital renal diseases and are not the result of environmental factors.

Claudins play important roles in the maintenance and formation of epithelial structures. I demonstrated that in the nephric duct, claudins are expressed once the lumen starts to form. The conserved expression of claudins in early kidney development in different species suggests an evolutionary conserved function. I also showed that overexpression of claudin variants can have an effect on nephric duct elongation. However, claudin variants could be acting as risk factors for CAKUT rather than causal mutations. Together these results implicate claudins in epithelial morphogenesis during kidney development, and the association of mutations in these genes with congenital renal malformations.

CHAPTER V: Conclusions and Future Directions

In my thesis project I showed that expression of *Claudin-1* and *-3* starts at HH12 during epithelialization of the nephric duct. Once the nephric duct is fully developed, *Claudin-1* and *Claudin-3* are expressed along the entire anterior-posterior length of the duct up until its insertion into the cloaca. *Claudin-4* was expressed in the chick and mouse nephric ducts and in mouse embryonic kidney in the ureteric bud tips and trunks. To validate the expression patterns of *Claudin-1, -3* and *-4* it is necessary to look at their expression at the protein level in the nephric duct.

My preliminary results suggest that the rare CLDN8 p.A94V variant and the novel CLDN14 p.S58R variant disrupt nephric duct elongation. By increasing the success rate of the injections, I will be able to better assess the effect of the variants and further characterize their phenotype. The variants can also be functionally tested *in vivo* by electroporation with a CLDN-IRES-GFP RCAS vector into the nephric duct using GFP to track the elongation of the nephric duct in live imaging.

When assessing CLDN variants in patients with kidney malformations, common, rare, and novel variants were found. Even though there was no significant difference between the incidence of common variants in the general population and the cohort, it will be interesting to apply further statistical tests to measure the cumulative effect of common and rare variants. It would also be useful to do whole-genome or whole-exome sequencing of patients with early onset CAKUT to look for mutations in claudin variants, as well as for mutations in genes that have not been previously linked with CAKUT.

Nephric duct elongation and ureteric bud branching require cell-to-cell contacts and cell-to-cell communication for the formation and maintenance of the epithelium. During kidney development, mesenchymal cells that undergo MET acquire tight junctions. After the acquisition of cell contact points, cells can synchronize movements that help the formation of tubular structures as well as tissue movements. These tissue movements are driven by individual cell shape changes that occur at the level of the cytoskeleton and are communicated between cells in the epithelium.

Communication between the cytoskeleton and the membrane is essential for the regulation of cell shape changes in epithelial cell layers. Claudins are essential to maintain contact points between cells, as well as supporting the interactions with the actin cytoskeleton that help in cell rearrangements (Hartsock and Nelson, 2008; Itoh et al., 1999). Based on my results, and on published data, we know that claudins help form and maintain epithelial integrity through cell-to-cell contacts allowing for the formation of an organized epithelium. During kidney development these cell rearrangements are essential for the formation and the maintenance of the epithelium in the nephric duct and the collecting duct system.

References

Abuazza, G., Becker, A., Williams, S.S., Chakravarty, S., Truong, H.-T., Lin, F., Baum, M., 2006. Claudins 6, 9, and 13 are developmentally expressed renal tight junction proteins. American journal of physiology. Renal physiology *291*, F1132-F1141.

Adzhubei, I.A., Schmidt, S., Peshkin, L., Ramensky, V.E., Gerasimova, A., Bork, P., Kondrashov, A.S., Sunyaev, S.R., 2010. A method and server for predicting damaging missense mutations. Nature Methods *7*, 248.

Anderson, J.M., Van Itallie, C.M., 2009. Physiology and Function of the Tight Junction. Cold Spring Harbor Perspectives in Biology *1*, a002584.

Anderson, W.J., Zhou, Q., Alcalde, V., Kaneko, O.F., Blank, L.J., Sherwood, R.I., Guseh, J.S., Rajagopal, J., Melton, D.A., 2008. Genetic targeting of the endoderm with claudin-6(CreER). Developmental Dynamics *237*, 504-512.

Andrew, D.J., Ewald, A.J., 2010. Morphogenesis of epithelial tubes: Insights into tube formation, elongation, and elaboration. Developmental Biology *341*, 34-55.

Angelow, S., Ahlstrom, R., Yu, A.S.L., 2008. Biology of claudins. American Journal of Physiology - Renal Physiology *295*, F867-F876.

Angelow, S., El-Husseini, R., Kanzawa, S.A., Yu, A.S.L., 2007. Renal localization and function of the tight junction protein, claudin-19. American Journal of Physiology-Renal Physiology *293*, F166-F177.

Atsuta, Y., Takahashi, Y., 2015. FGF8 coordinates tissue elongation and cell epithelialization during early kidney tubulogenesis. Development (Cambridge, England) *142*, 2329-2337.

Atsuta, Y., Takahashi, Y., 2016. Early formation of the Müllerian duct is regulated by sequential actions of BMP/Pax2 and FGF/Lim1 signaling. Development *143*, 3549-3559.

Attia, L., Yelin, R., Schultheiss, T.M., 2012. Analysis of nephric duct specification in the avian embryo. Development (Cambridge, England) *139*, 4143-4151.

Aue, A., Hinze, C., Walentin, K., Ruffert, J., Yurtdas, Y., Werth, M., Chen, W., Rabien, A., Kilic, E., Schulzke, J.-D., Schumann, M., Schmidt-Ott, K.M., 2015. A Grainyhead-Like 2/Ovo-Like 2 Pathway Regulates Renal Epithelial Barrier Function and Lumen Expansion. Journal of the American Society of Nephrology: JASN *26*, 2704-2715.

Bagnat, M., Cheung, I.D., Mostov, K.E., Stainier, D.Y.R., 2007. Genetic control of single lumen formation in the zebrafish gut. Nature Cell Biology *9*, 954.

Baker, P.C., Schroeder, T.E., 1967. Cytoplasmic filaments and morphogenetic movement in the amphibian neural tube. Developmental Biology *15*, 432-450.

Balda, M.S., Whitney, J.A., Flores, C., González, S., Cereijido, M., Matter, K., 1996. Functional dissociation of paracellular permeability and transepithelial electrical resistance and disruption of the apical-basolateral intramembrane diffusion barrier by expression of a mutant tight junction membrane protein. The Journal of Cell Biology *134*, 1031-1049.

Banan, A., Zhang, L.J., Shaikh, M., Fields, J.Z., Choudhary, S., Forsyth, C.B., Farhadi, A., Keshavarzian, A., 2005. θ Isoform of Protein Kinase C Alters Barrier Function in Intestinal Epithelium through Modulation of Distinct Claudin Isotypes: A Novel Mechanism for Regulation of Permeability. Journal of Pharmacology and Experimental Therapeutics *313*, 962-982.

Barbacci, E., Reber, M., Ott, M.O., Breillat, C., Huetz, F., Cereghini, S., 1999. Variant hepatocyte nuclear factor 1 is required for visceral endoderm specification. Development *126*, 4795-4805.

Baumholtz, A.I., Gupta, I.R., Ryan, A.K., 2017. Claudins in morphogenesis: Forming an epithelial tube. Tissue Barriers, e1361899.

Baumholtz, A.I., Simard, A., Nikolopoulou, E., Oosenbrug, M., Collins, M.M., Piontek, A., Krause, G., Piontek, J., Greene, N.D.E., Ryan, A.K., 2017. Claudins are essential for cell shape changes and convergent extension movements during neural tube closure. Developmental Biology *428*, 25-38.

Ben-Yosef, T., Belyantseva, I.A., Saunders, T.L., Hughes, E.D., Kawamoto, K., Van Itallie, C.M., Beyer, L.A., Halsey, K., Gardner, D.J., Wilcox, E.R., Rasmussen, J., Anderson, J.M., Dolan, D.F., Forge, A., Raphael, Y., Camper, S.A., Friedman, T.B., 2003. Claudin 14 knockout mice, a model for autosomal recessive deafness DFNB29, are deaf due to cochlear hair cell degeneration. Human Molecular Genetics *12*, 2049-2061.

Bertram, J.F., Douglas-Denton, R.N., Diouf, B., Hughson, M.D., Hoy, W.E., 2011. Human nephron number: implications for health and disease. Pediatric Nephrology *26*, 1529.

Blake, J., Rosenblum, N.D., 2014. Renal branching morphogenesis: Morphogenetic and signaling mechanisms. Seminars in Cell & Developmental Biology *36*, 2-12.

Blom, N., Gammeltoft, S. and Brunak, S. (1999). Sequence and structure-based prediction of eukaryotic protein phosphorylation sites. J Mol Biol *294*, 1351-1362.

Bouchard, M., Souabni, A., Mandler, M., Neubüser, A., Busslinger, M., 2002. Nephric lineage specification by Pax2 and Pax8. Genes & Development *16*, 2958-2970.

Breiderhoff, T., Himmerkus, N., Stuiver, M., Mutig, K., Will, C., Meij, I.C., Bachmann, S., Bleich, M., Willnow, T.E., Müller, D., 2012. Deletion of claudin-10 (Cldn10) in the thick ascending limb impairs paracellular sodium permeability and leads to hypermagnesemia and nephrocalcinosis. Proceedings of the National Academy of Sciences *109*, 14241-14246.

Brophy, P.D., Ostrom, L., Lang, K.M., Dressler, G.R., 2001. Regulation of ureteric bud outgrowth by Pax2-dependent activation of the glial derived neurotrophic factor gene. Development *128*, 4747-4756.

Bulum, B., Özçakar, Z.B., Üstüner, E., Düşünceli, E., Kavaz, A., Duman, D., Walz, K., Fitoz, S., Tekin, M., Yalçınkaya, F., 2013. High frequency of kidney and urinary tract anomalies in asymptomatic first-degree relatives of patients with CAKUT. Pediatric Nephrology *28*, 2143-2147.

Capone, V.P., Morello, W., Taroni, F., Montini, G., 2017. Genetics of Congenital Anomalies of the Kidney and Urinary Tract: The Current State of Play. International Journal of Molecular Sciences *18*, 796.

Choi, Y., Sims, G.E., Murphy, S., Miller, J.R., Chan, A.P., 2012. Predicting the Functional Effect of Amino Acid Substitutions and Indels. PLOS ONE *7*, e46688.

Cieply, B., Farris, J., Denvir, J., Ford, H., Frisch, S.M., 2013. Epithelial-mesenchymal transition and tumor suppression are controlled by a reciprocal feedback loop between ZEB1 and Grainyhead-like-2. Cancer research *73*, 6299-6309.

Collins, M.M., Baumholtz, A.I., Ryan, A.K., 2013. Claudin family members exhibit unique temporal and spatial expression boundaries in the chick embryo. Tissue Barriers *1*, e24517.

Collins, M.M., Ryan, A.K., 2011. Manipulating Claudin Expression in Avian Embryos, in: Turksen, K. (Ed.), Claudins: Methods and Protocols. Humana Press, Totowa, NJ, pp. 195-212.

Costantini, F., Kopan, R., 2010. Patterning a Complex Organ: Branching Morphogenesis and Nephron Segmentation in Kidney Development. Developmental Cell *18*, 698-712.

Costantini, F., Shakya, R., 2006. GDNF/Ret signaling and the development of the kidney. BioEssays *28*, 117-127.

Dart, A.B., Ruth, C.A., Sellers, E.A., Au, W., Dean, H.J., 2015. Maternal Diabetes Mellitus and Congenital Anomalies of the Kidney and Urinary Tract (CAKUT) in the Child. American Journal of Kidney Diseases *65*, 684-691.

Daugherty, B.L., Ward, C., Smith, T., Ritzenthaler, J.D., Koval, M., 2007. Regulation of Heterotypic Claudin Compatibility. Journal of Biological Chemistry *282*, 30005-30013.

Davidson AJ., 2009. Mouse kidney development. In: StemBook [Internet]. Cambridge (MA): Harvard Stem Cell Institute; 2008. Available from: https://www-ncbi-nlm-nih-gov.proxy3.library.mcgill.ca/books/NBK27080/ doi: 10.3824/stembook.1.34.1

Davies, R.R., 1999. Multiple roles for the Wilms' tumor suppressor, WT1. Cancer research *59*.

Davis, T.K., Hoshi, M., Jain, S., 2014. To Bud or not to Bud: The RET perspective in CAKUT. Pediatric nephrology (Berlin, Germany) *29*, 597-608.

Dimke, H., Desai, P., Borovac, J., Lau, A., Pan, W., & Alexander, R. T., 2013. Activation of the Ca2+-sensing receptor increases renal claudin-14 expression and urinary Ca2+excretion. The American Journal of Physiology, *304(6)*, F761–F769.

Dressler, G.R., 2006. The Cellular Basis of Kidney Development. Annual Review of Cell and Developmental Biology *22*, 509-529.

Dressler, G.R., Deutsch, U., Chowdhury, K., Nornes, H.O., Gruss, P., 1990. Pax2, a new murine paired-box-containing gene and its expression in the developing excretory system. Development *109*, 787-795.

D'Souza, T., Agarwal, R., Morin, P.J., 2005. Phosphorylation of Claudin-3 at Threonine 192 by cAMP-dependent Protein Kinase Regulates Tight Junction Barrier Function in Ovarian Cancer Cells. Journal of Biological Chemistry *280*, 26233-26240.

Ebnet, K., Suzuki, A., Ohno, S., Vestweber, D., 2004. Junctional adhesion molecules (JAMs): more molecules with dual functions? Journal of Cell Science *117*, 19-29.

Edghill, E.L., Stals, K., Oram, R.A., Shepherd, M.H., Hattersley, A.T., Ellard, S., 2013. HNF1B deletions in patients with young-onset diabetes but no known renal disease. Diabetic Medicine *30*, 114-117.

Egger, G., Liang, G., Aparicio, A., Jones, P.A., 2004. Epigenetics in human disease and prospects for epigenetic therapy. Nature *429*, 457-463.

Enck, A.H., Berger, U.V., Yu, A.S.L., 2001. Claudin-2 is selectively expressed in proximal nephron in mouse kidney. American Journal of Physiology-Renal Physiology *281*, F966-F974.

Farquhar, M.G., Palade, G.E., 1963. Junctional Complexes in Various Epithelia. The Journal of Cell Biology *17*, 375-412.

Findley, M.K., Koval, M., 2009. Regulation and roles for claudin-family tight junction proteins. IUBMB life *61*, 431-437.

French, A.D., Fiori, J.L., Camilli, T.C., Leotlela, P.D., O'Connell, M.P., Frank, B.P., Subaran, S., Indig, F.E., Taub, D.D., Weeraratna, A.T., 2009. PKC and PKA Phosphorylation Affect the Subcellular Localization of Claudin-1 in Melanoma Cells. International Journal of Medical Sciences *6*, 93-101.

Frömter, E.E., Diamond, J., 1972. Route of passive ion permeation in epithelia. Nature: New biology *235*, 9-13.

Fujita, H., Hamazaki, Y., Noda, Y., Oshima, M., Minato, N., 2012. Claudin-4 Deficiency Results in Urothelial Hyperplasia and Lethal Hydronephrosis. PLoS ONE *7*, e52272.

Fujita, K., Katahira, J., Horiguchi, Y., Sonoda, N., Furuse, M., Tsukita, S., 2000. Clostridium perfringens enterotoxin binds to the second extracellular loop of claudin-3, a tight junction integral membrane protein. FEBS Letters *476*, 258-261.

Furuse, M., Hata, M., Furuse, K., Yoshida, Y., Haratake, A., Sugitani, Y., Noda, T., Kubo, A., Tsukita, S., 2002. Claudin-based tight junctions are crucial for the mammalian epidermal barrier: a lesson from claudin-1–deficient mice. The Journal of Cell Biology *156*, 1099-1111.

Furuse, M., Hirase, T., Itoh, M., Nagafuchi, A., Yonemura, S., Tsukita, S., Tsukita, S., 1993. Occludin: a novel integral membrane protein localizing at tight junctions. The Journal of Cell Biology *123*, 1777-1788.

Furuse, M., Moriwaki, K., 2009. The Role of Claudin-Based Tight Junctions in Morphogenesis. Annals of the New York Academy of Sciences *1165*, 58-61.

Furuse, M., Sasaki, H., Fujimoto, K., Tsukita, S., 1998. A Single Gene Product, Claudin-1 or -2, Reconstitutes Tight Junction Strands and Recruits Occludin in Fibroblasts. The Journal of Cell Biology *143*, 391-401.

Furuse, M., Sasaki, H., Tsukita, S., 1999. Manner of Interaction of Heterogeneous Claudin Species within and between Tight Junction Strands. The Journal of Cell Biology *147*, 891-903.

Garrido-Urbani, S., Bradfield, P.F., Imhof, B.A., 2014. Tight junction dynamics: the role of junctional adhesion molecules (JAMs). Cell and Tissue Research *355*, 701-715.

Geiger, B.B., 1987. Molecular interactions in adherens-type contacts. Journal of cell science. Supplement *8*, 251-272.

Gong, Y., Renigunta, V., Himmerkus, N., Zhang, J., Renigunta, A., Bleich, M., Hou, J., 2012. Claudin-14 regulates renal Ca(++) transport in response to CaSR signalling via a novel microRNA pathway. The EMBO Journal *31*, 1999-2012.

Gong, Y., Wang, J., Yang, J., Gonzales, E., Perez, R., Hou, J., 2015. KLHL3 regulates paracellular chloride transport in the kidney by ubiquitination of claudin-8. Proceedings of the National Academy of Sciences of the United States of America *112*, 4340-4345.

Guioli, S., Sekido, R., Lovell-Badge, R., 2007. The origin of the Mullerian duct in chick and mouse. Developmental Biology *302*, 389-398.

Gumbiner, B., Stevenson, B., Grimaldi, A., 1988. The role of the cell adhesion molecule uvomorulin in the formation and maintenance of the epithelial junctional complex. The Journal of Cell Biology *107*, 1575-1587.

Günzel, D., Haisch, L., Pfaffenbach, S., Krug, S.M., Milatz, S., Amasheh, S., Hunziker, W., Müller, D., 2009. Claudin Function in the Thick Ascending Limb of Henle's Loop. Annals of the New York Academy of Sciences *1165*, 152-162.

Haddad, N., Andalousi, J.E., Khairallah, H., Yu, M., Ryan, A.K., Gupta, I.R., 2011. The tight junction protein claudin-3 shows conserved expression in the nephric duct and ureteric bud and promotes tubulogenesis in vitro. American Journal of Physiology - Renal Physiology *301*, F1057-F1065.

Hamazaki, Y., Itoh, M., Sasaki, H., Furuse, M., Tsukita, S., 2002. Multi-PDZ Domain Protein 1 (MUPP1) Is Concentrated at Tight Junctions through Its Possible Interaction with Claudin-1 and Junctional Adhesion Molecule. Journal of Biological Chemistry *277*, 455-461.

Hamburger, V., Hamilton, H.L., 1992. A series of normal stages in the development of the chick embryo. Developmental Dynamics *195*, 231-272.

Hammes, A., Guo, J.-K., Lutsch, G., Leheste, J.-R., Landrock, D., Ziegler, U., Gubler, M.-C., Schedl, A., 2001. Two Splice Variants of the Wilms' Tumor 1 Gene Have Distinct Functions during Sex Determination and Nephron Formation. Cell *106*, 319-329.

Harambat, J., van Stralen, K.J., Kim, J.J., Tizard, E.J., 2012. Epidemiology of chronic kidney disease in children. Pediatric Nephrology *27*, 363-373.

Hartsock, A., Nelson, W.J., 2008. Adherens and Tight Junctions: Structure, Function and Connections to the Actin Cytoskeleton. Biochimica et biophysica acta *1778*, 660-669.

Hartwig, S., Ho, J., Pandey, P., MacIsaac, K., Taglienti, M., Xiang, M., Alterovitz, G., Ramoni, M., Fraenkel, E., Kreidberg, J.A., 2010. Genomic characterization of Wilms' tumor suppressor 1 targets in nephron progenitor cells during kidney development. Development *137*, 1189-1203.

Haskins, J., Gu, L., Wittchen, E.S., Hibbard, J., Stevenson, B.R., 1998. ZO-3, a Novel Member of the MAGUK Protein Family Found at the Tight Junction, Interacts with ZO-1 and Occludin. The Journal of Cell Biology *141*, 199-208.

Heidet, L., Morinière, V., Henry, C., De Tomasi, L., Reilly, M.L., Humbert, C., Alibeu, O., Fourrage, C., Bole-Feysot, C., Nitschké, P., Tores, F., Bras, M., Jeanpierre, M., Pietrement, C., Gaillard, D., Gonzales, M., Novo, R., Schaefer, E., Roume, J., Martinovic, J., Malan, V., Salomon, R., Saunier, S., Antignac, C., Jeanpierre, C., 2017. Targeted Exome Sequencing Identifies PBX1 as Involved in Monogenic Congenital Anomalies of the Kidney and Urinary Tract. Journal of the American Society of Nephrology *28*, 2901-2914.

Hildebrandt, F., 2010. Genetic kidney diseases. The Lancet *375*, 1287-1295.

Hiruma, T., Nakamura, H., 2003. Origin and development of the pronephros in the chick embryo. Journal of Anatomy *203*, 539-552.

Hou, J., Renigunta, A., Gomes, A.S., Hou, M., Paul, D.L., Waldegger, S., Goodenough, D.A., 2009. Claudin-16 and claudin-19 interaction is required for their assembly into tight junctions and for renal reabsorption of magnesium. Proceedings of the National Academy of Sciences of the United States of America *106*, 15350-15355.

Hou, J., Renigunta, A., Yang, J., Waldegger, S., 2010. Claudin-4 forms paracellular chloride channel in the kidney and requires claudin-8 for tight junction localization. Proceedings of the National Academy of Sciences of the United States of America *107*, 18010-18015.

Hou, J., Shan, Q., Wang, T., Gomes, A.S., Yan, Q., Paul, D.L., Bleich, M., Goodenough, D.A., 2007. Transgenic RNAi Depletion of Claudin-16 and the Renal Handling of Magnesium. Journal of Biological Chemistry *282*, 17114-17122.

Hughes, S.H., 2004. The RCAS vector system. Folia biologica 50, 107-119. Hull, B.E., Staehelin, L.A., 1976. Functional significance of the variations in the geometrical organization of tight junction networks. Journal of Cell Biology *68*, 688-704.

Hwang, D.-Y., Dworschak, G.C., Kohl, S., Saisawat, P., Vivante, A., Hilger, A.C., Reutter, H.M., Soliman, N.A., Bogdanovic, R., Kehinde, E.O., Tasic, V., Hildebrandt, F., 2014. Mutations in 12 known dominant disease-causing genes clarify many congenital anomalies of the kidney and urinary tract. Kidney International *85*, 1429-1433.

Itoh, M., Furuse, M., Morita, K., Kubota, K., Saitou, M., Tsukita, S., 1999. Direct Binding of Three Tight Junction-Associated Maguks, Zo-1, Zo-2, and Zo-3, with the Cooh Termini of Claudins. The Journal of Cell Biology 147, 1351-1363.

Itoh, M., Morita, K., Tsukita, S., 1999. Characterization of ZO-2 as a MAGUK Family Member Associated with Tight as well as Adherens Junctions with a Binding Affinity to Occludin and α Catenin. Journal of Biological Chemistry *274*, 5981-5986.

Itoh, M., Sasaki, H., Furuse, M., Ozaki, H., Kita, T., Tsukita, S., 2001. Junctional adhesion molecule (JAM) binds to PAR-3 a possible mechanism for the recruitment of PAR-3 to tight junctions *154*, 491-498.

Ivanova, E., Chen, J.-H., Segonds-Pichon, A., Ozanne, S.E., Kelsey, G., 2012. DNA methylation at differentially methylated regions of imprinted genes is resistant to developmental programming by maternal nutrition. Epigenetics *7*, 1200-1210.

James, R.G., Schultheiss, T.M., 2003. Patterning of the Avian Intermediate Mesoderm by Lateral Plate and Axial Tissues. Developmental Biology *253*, 109-124.

Jeansonne, B.B., Lu, Q., Goodenough, D.A., Chen, Y.H., 2003.Claudin-8 interacts with multi-PDZ domain protein 1 (MUPP1) and reduces paracellular conductance in epithelial cells. Cellular and molecular biology 49, 13-21.

Jiang, D., Chen, J., Fan, Z., Tan, D., Zhao, J., Shi, H., Liu, Z., Tao, W., Li, M., Wang, D., 2017. CRISPR/Cas9-induced disruption of wt1a and wt1b reveals their different roles in kidney and gonad development in Nile tilapia. Developmental Biology *428*, 63-73.

Jin, M., Zhu, S., Hu, P., Liu, D., Li, Q., Li, Z., Zhang, X., Xie, Y., Chen, X., 2014. Genomic and Epigenomic Analyses of Monozygotic Twins Discordant for Congenital Renal Agenesis. American Journal of Kidney Diseases *64*, 119-122.

Joseph, A., Yao, H., Hinton, B.T., 2009. Development and morphogenesis of the Wolffian/Epididymal Duct, More Twists and Turns. Developmental biology *325*, 6-14.

Kang, J.H., Choi, H.J., Cho, H.Y., Lee, J.H., Ha, I.S., Cheong, H.I., Choi, Y., 2005. Familial hypomagnesemia with hypercalciuria and nephrocalcinosis associated with CLDN16 mutations. Pediatric Nephrology *20*, 1490-1493.

Katahira, J., Inoue, N., Horiguchi, Y., Matsuda, M., Sugimoto, N., 1997. Molecular Cloning and Functional Characterization of the Receptor for Clostridium perfringens Enterotoxin. The Journal of Cell Biology *136*, 1239-1247.

Khairallah, H. Claudins Are Required for Ureteric Bud Branching in the Mouse Embryonic Kidney. Thesis, 2013.

Khairallah, H., El Andalousi, J., Simard, A., Haddad, N., Chen, Y.-H., Hou, J., Ryan, A.K., Gupta, I.R., 2014. Claudin-7, -16, and -19 during mouse kidney development. Tissue Barriers *2*, e964547.

Kirk, A., Campbell, S., Bass, P., Mason, J., Collins, J., 2010. Differential expression of claudin tight junction proteins in the human cortical nephron. Nephrology Dialysis Transplantation *25*, 2107-2119.

Kiuchi-Saishin, Y., Gotoh, S., Furuse, M., Takasuga, A., Tano, Y., Tsukita, S., 2002. Differential Expression Patterns of Claudins, Tight Junction Membrane Proteins, in Mouse Nephron Segments. Journal of the American Society of Nephrology *13*, 875-886.

Kobayashi, A., Kwan, K.-M., Carroll, T.J., McMahon, A.P., Mendelsohn, C.L., Behringer, R.R., 2005. Distinct and sequential tissue-specific activities of the LIM-class homeobox gene Lim1 for tubular morphogenesis during kidney development. Development *132*, 2809-2823.

Kobayashi, H., Kawakami, K., Asashima, M., Nishinakamura, R., 2007. Six1 and Six4 are essential for Gdnf expression in the metanephric mesenchyme and ureteric bud formation, while Six1 deficiency alone causes mesonephric-tubule defects. Mechanisms of Development *124*, 290-303.

Kondoh, M., Takahashi, A., Fujii, M., Yagi, K., Watanabe, Y., 2006. A Novel Strategy for a Drug Delivery System Using a Claudin Modulator. Biological and Pharmaceutical Bulletin *29*, 1783-1789.

Konrad, M., Schaller, A., Seelow, D., Pandey, A.V., Waldegger, S., Lesslauer, A., Vitzthum, H., Suzuki, Y., Luk, J.M., Becker, C., Schlingmann, K.P., Schmid, M., Rodriguez-Soriano, J., Ariceta, G., Cano, F., Enriquez, R., Jüppner, H., Bakkaloglu, S.A., Hediger, M.A., Gallati, S., Neuhauss, S.C.F., Nürnberg, P., Weber, S., 2006. Mutations in the Tight-Junction Gene Claudin 19 (CLDN19) Are Associated with Renal Magnesium Wasting, Renal Failure, and Severe Ocular Involvement. The American Journal of Human Genetics *79*, 949-957.

Kreidberg, J.A., 2010. WT1 and kidney progenitor cells. Organogenesis *6*, 61-70.

Kreidberg, J.A., Sariola, H., Loring, J.M., Maeda, M., Pelletier, J., Housman, D., Jaenisch, R., 1993. WT-1 is required for early kidney development. Cell *74*, 679-691.

Lek, M., Karczewski, K.J., Minikel, E.V., Samocha, K.E., Banks, E., Fennell, T., O'Donnell-Luria, A.H., Ware, J.S., Hill, A.J., Cummings, B.B., Tukiainen, T., Birnbaum, D.P., Kosmicki, J.A., Duncan, L.E., Estrada, K., Zhao, F., Zou, J., Pierce-Hoffman, E., Berghout, J., Cooper, D.N., Deflaux, N., DePristo, M., Do, R., Flannick, J., Fromer, M., Gauthier, L., Goldstein, J., Gupta, N., Howrigan, D., Kiezun, A., Kurki, M.I., Moonshine, A.L., Natarajan, P., Orozco, L., Peloso, G.M., Poplin, R., Rivas, M.A., Ruano-Rubio, V., Rose, S.A., Ruderfer, D.M., Shakir, K., Stenson, P.D., Stevens, C., Thomas, B.P., Tiao, G., Tusie-Luna, M.T., Weisburd, B., Won, H.-H., Yu, D., Altshuler, D.M., Ardissino, D., Boehnke, M., Danesh, J., Donnelly, S., Elosua, R., Florez, J.C., Gabriel, S.B., Getz, G., Glatt, S.J., Hultman, C.M., Kathiresan, S., Laakso, M., McCarroll, S., McCarthy, M.I., McGovern, D., McPherson, R., Neale, B.M., Palotie, A., Purcell, S.M., Saleheen, D., Scharf, J.M., Sklar, P., Sullivan, P.F., Tuomilehto, J., Tsuang, M.T., Watkins, H.C., Wilson, J.G., Daly, M.J., MacArthur, D.G., Exome Aggregation, C., 2016. Analysis of protein-coding genetic variation in 60,706 humans. Nature *536*, 285.

Li, W.Y., Huey, C.L., Yu, A.S.L., 2004. Expression of claudin-7 and -8 along the mouse nephron. American Journal of Physiology - Renal Physiology *286*, F1063-F1071.

Li, Y., Manaligod, Jose M., Weeks, Daniel L., 2010. EYA1 mutations associated with the branchio-oto-renal syndrome result in defective otic development in Xenopus laevis. Biology of the Cell *102*, 277-292.

Liang, T.W., DeMarco, R.A., Mrsny, R.J., Gurney, A., Gray, A., Hooley, J., Aaron, H.L., Huang, A., Klassen, T., Tumas, D.B., Fong, S., 2000. Characterization of huJAM: evidence for involvement in cell-cell contact and tight junction regulation. American Journal of Physiology - Cell Physiology *279*, C1733-C1743.

Lindner, T.H., Njolstad, P.R., Horikawa, Y., Bostad, L., Bell, G.I., Sovik, O., 1999. A Novel Syndrome of Diabetes Mellitus, Renal Dysfunction and Genital Malformation Associated with a Partial Deletion of the Pseudo-POU Domain of Hepatocyte Nuclear Factor-1β. Human Molecular Genetics *8*, 2001-2008.

Lindström, M., Heikinheimo, A., Lahti, P., Korkeala, H., 2011. Novel insights into the epidemiology of Clostridium perfringens type A food poisoning. Food Microbiology *28*, 192-198.

Liu, Y., Nusrat, A., Schnell, F.J., Reaves, T.A., Walsh, S., Pochet, M., Parkos, C.A., 2000. Human junction adhesion molecule regulates tight junction resealing in epithelia. Journal of Cell Science *113*, 2363-2374.

Logan, M., Tabin, C., 1998. Targeted Gene Misexpression in Chick Limb Buds Using Avian Replication-Competent Retroviruses. Methods *14*, 407-420.

Lokmane, L., Heliot, C., Garcia-Villalba, P., Fabre, M., Cereghini, S., 2010. HNF1 functions in distinct regulatory circuits to control ureteric bud branching and early nephrogenesis. Development *137*, 347-357.

Martin, A.C., Goldstein, B., 2014. Apical constriction: themes and variations on a cellular mechanism driving morphogenesis. Development (Cambridge, England) *141*, 1987-1998.

Massa, F., Garbay, S., Bouvier, R., Sugitani, Y., Noda, T., Gubler, M.-C., Heidet, L., Pontoglio, M., Fischer, E., 2013. Hepatocyte nuclear factor 1β controls nephron tubular development. Development *140*, 886-896.

Meyer, T.N., Schwesinger, C., Bush, K.T., Stuart, R.O., Rose, D.W., Shah, M.M., Vaughn, D.A., Steer, D.L., Nigam, S.K., 2004. Spatiotemporal regulation of morphogenetic molecules during in vitro branching of the isolated ureteric bud: toward a model of branching through budding in the developing kidney. Developmental Biology *275*, 44-67.

Moriwaki, K., Tsukita, S., Furuse, M., 2007. Tight junctions containing claudin 4 and 6 are essential for blastocyst formation in preimplantation mouse embryos. Developmental Biology *312*, 509-522.

Mrsny, R.J., Brown, G.T., Gerner-Smidt, K., Buret, A.G., Meddings, J.B., Quan, C., Koval, M., Nusrat, A., 2008. A Key Claudin Extracellular Loop Domain is Critical for Epithelial Barrier Integrity. The American Journal of Pathology *172*, 905-915.

Muresan, Z., Paul, D.L., Goodenough, D.A., 2000. Occludin 1B, a Variant of the Tight Junction Protein Occludin. Molecular Biology of the Cell *11*, 627-634.

Muto, S., Hata, M., Taniguchi, J., Tsuruoka, S., Moriwaki, K., Saitou, M., Furuse, K., Sasaki, H., Fujimura, A., Imai, M., Kusano, E., Tsukita, S., Furuse, M., 2010. Claudin-2–deficient mice are defective in the leaky and cation-selective paracellular permeability properties of renal proximal tubules. Proceedings of the National Academy of Sciences of the United States of America *107*, 8011-8016.

Nagalakshmi, V.K., Yu, J., 2015. The ureteric bud epithelium: Morphogenesis and roles in metanephric kidney patterning. Molecular reproduction and development *82*, 151-166.

Nakayama, M., Nozu, K., Goto, Y., Kamei, K., Ito, S., Sato, H., Emi, M., Nakanishi, K., Tsuchiya, S., Iijima, K., 2010. HNF1B alterations associated with congenital anomalies of the kidney and urinary tract. Pediatric Nephrology *25*, 1073-1079.

Narasimha, M., Uv, A., Krejci, A., Brown, N.H., Bray, S.J., 2008. Grainy head promotes expression of septate junction proteins and influences epithelial morphogenesis. Journal of Cell Science *121*, 747-752.

Nicolaou, N., Pulit, S.L., Nijman, I.J., Monroe, G.R., Feitz, W.F.J., Schreuder, M.F., van Eerde, A.M., de Jong, T.P.V.M., Giltay, J.C., van der Zwaag, B., Havenith, M.R., Zwakenberg, S., van der Zanden, L.F.M., Poelmans, G., Cornelissen, E.A.M., Lilien, M.R., Franke, B., Roeleveld, N., van Rooij, I.A.L.M., Cuppen, E., Bongers, E.M.H.F., Giles, R.H., Knoers, N.V.A.M., Renkema, K.Y., 2016. Prioritization and burden analysis of rare variants in 208 candidate genes suggest they do not play a major role in CAKUT. Kidney International *89*, 476-486.

Nicolaou, N., Renkema, K.Y., Bongers, E.M.H.F., Giles, R.H., Knoers, N.V.A.M., 2015. Genetic, environmental, and epigenetic factors involved in CAKUT. Nat Rev Nephrol *11*, 720-731.

Nigam, S.K., Shah, M.M., 2009. How Does the Ureteric Bud Branch? Journal of the American Society of Nephrology *20*, 1465-1469.

Nunbhakdi-Craig, V., Machleidt, T., Ogris, E., Bellotto, D., White, C.L., Sontag, E., 2002. Protein phosphatase 2A associates with and regulates atypical PKC and the epithelial tight junction complex. The Journal of Cell Biology *158*, 967-978.

Obara-Ishihara, T., Kuhlman, J., Niswander, L., Herzlinger, D., 1999. The surface ectoderm is essential for nephric duct formation in intermediate mesoderm. Development *126*, 1103-1108.

Oberlander, T.F., Weinberg, J., Papsdorf, M., Grunau, R., Misri, S., Devlin, A.M., 2008. Prenatal exposure to maternal depression, neonatal methylation of human glucocorticoid receptor gene (NR3C1) and infant cortisol stress responses. Epigenetics *3*, 97-106.

Parikh, C.R., McCall, D., Engelman, C., Schrier, R.W., 2002. Congenital renal agenesis: Case-control analysis of birth characteristics. American Journal of Kidney Diseases *39*, 689-694.

Perner, B., Englert, C., Bollig, F., 2007. The Wilms tumor genes wt1a and wt1b control different steps during formation of the zebrafish pronephros. Developmental Biology *309*, 87-96.

Petrof, G., Nanda, A., Howden, J., Takeichi, T., McMillan, James R., Aristodemou, S., Ozoemena, L., Liu, L., South, Andrew P., Pourreyron, C., Dafou, D., Proudfoot, Laura E., Al-Ajmi, H., Akiyama, M., McLean, W.H.I., Simpson, Michael A., Parsons, M., McGrath, John A., 2014. Mutations in GRHL2 Result in an Autosomal-Recessive Ectodermal Dysplasia Syndrome. The American Journal of Human Genetics *95*, 308-314.

Pifer, P.M., Farris, J.C., Thomas, A.L., Stoilov, P., Denvir, J., Smith, D.M., Frisch, S.M., 2016. Grainyhead-like 2 inhibits the coactivator p300, suppressing tubulogenesis and the epithelial–mesenchymal transition. Molecular Biology of the Cell *27*, 2479-2492.

Piontek, J., Winkler, L., Wolburg, H., Müller, S.L., Zuleger, N., Piehl, C., Wiesner, B., Krause, G., Blasig, I.E., 2008. Formation of tight junction: determinants of homophilic interaction between classic claudins. The FASEB Journal *22*, 146-158.

Pyrgaki, C., Liu, A., Niswander, L., 2011. Grainyhead-like 2 regulates neural tube closure and adhesion molecule expression during neural fold fusion. Developmental biology *353*, 38-49.

Rajasekaran, A.K., Hojo, M., Huima, T., Rodriguez-Boulan, E., 1996. Catenins and zonula occludens-1 form a complex during early stages in the assembly of tight junctions. The Journal of Cell Biology *132*, 451-463.

Renfree, M.B., Fenelon, J., Wijiyanti, G., Wilson, J.D., Shaw, G., 2009. Wolffian duct differentiation by physiological concentrations of androgen delivered systemically. Developmental Biology *334*, 429-436.

Robertson, S.L., Smedley, J.G., McClane, B.A., 2010. Identification of a Claudin-4 Residue Important for Mediating the Host Cell Binding and Action of Clostridium perfringens Enterotoxin. Infection and Immunity *78*, 505-517.

Ruf, R.G., Xu, P.-X., Silvius, D., Otto, E.A., Beekmann, F., Muerb, U.T., Kumar, S., Neuhaus, T.J., Kemper, M.J., Raymond, R.M., Brophy, P.D., Berkman, J., Gattas, M., Hyland, V., Ruf, E.-M., Schwartz, C., Chang, E.H., Smith, R.J.H., Stratakis, C.A., Weil, D., Petit, C., Hildebrandt, F., 2004. SIX1 mutations cause branchio-oto-renal syndrome by disruption of EYA1–SIX1–DNA complexes. Proceedings of the National Academy of Sciences of the United States of America *101*, 8090-8095.

Saisawat, P., Tasic, V., Vega-Warner, V., Kehinde, E.O., Günther, B., Airik, R., Innis, J.W., Hoskins, B.E., Hoefele, J., Otto, E.A., Hildebrandt, F., 2012. Identification of two novel CAKUT-causing genes by massively parallel exon resequencing of candidate genes in patients with unilateral renal agenesis. Kidney International *81*, 196-200.

Saitou, M., Fujimoto, K., Doi, Y., Itoh, M., Fujimoto, T., Furuse, M., Takano, H., Noda, T., Tsukita, S., 1998. Occludin-deficient Embryonic Stem Cells Can Differentiate into Polarized Epithelial Cells Bearing Tight Junctions. The Journal of Cell Biology *141*, 397-408.

Saitou, M., Furuse, M., Sasaki, H., Schulzke, J.-D., Fromm, M., Takano, H., Noda, T., Tsukita, S., 2000. Complex Phenotype of Mice Lacking Occludin, a Component of Tight Junction Strands. Molecular Biology of the Cell *11*, 4131-4142.

Sanna-Cherchi, S., Caridi, G., Weng, P.L., Scolari, F., Perfumo, F., Gharavi, A.G., Ghiggeri, G.M., 2007. Genetic approaches to human renal agenesis/hypoplasia and dysplasia. Pediatric Nephrology *22*, 1675-1684.

Sanyanusin, P., Schimmenti, L.A., McNoe, L.A., Ward, T.A., Pierpont, M.E.M., Sullivan, M.J., Dobyns, W.B., Eccles, M.R., 1995. Mutation of the PAX2 gene in a family with optic nerve colobomas, renal anomalies and vesicoureteral reflux. Nature Genetics *9*, 358.

Sawyer, J.M., Harrell, J.R., Shemer, G., Sullivan-Brown, J., Roh-Johnson, M., Goldstein, B., 2010. Apical constriction: A cell shape change that can drive morphogenesis. Developmental Biology *341*, 5-19.

Schneeberger, E.E., Lynch, R.D., 1992. Structure, function, and regulation of cellular tight junctions. American Journal of Physiology - Lung Cellular and Molecular Physiology *262*, L647-L661.

Schuchardt, A., D'Agati, V., Pachnis, V., Costantini, F., 1996. Renal agenesis and hypodysplasia in ret-k- mutant mice result from defects in ureteric bud development. Development *122*, 1919-1929.

Shawlot, W., Behringer, R.R., 1995. Requirement for LIml in head-organizer function. Nature *374*, 425-430.

Simard, A. The role of Claudins during chick nephric duct formation. Thesis, 2014.

Simard, A., Di Pietro, E., Ryan, A.K., 2005. Gene expression pattern of Claudin-1 during chick embryogenesis. Gene Expression Patterns *5*, 553-560.

Simard, A., Pietro, E.D., Young, C.R., Plaza, S., Ryan, A.K., 2006. Alterations in heart looping induced by overexpression of the tight junction protein Claudin-1 are dependent on its C-terminal cytoplasmic tail. Mechanisms of Development *123*, 210-227.

Staehelin, L.A., 1973. Further Observations on the Fine Structure of Freeze-Cleaved Tight Junctions. Journal of Cell Science *13*, 763-786.

Stevenson, B.R., Siliciano, J.D., Mooseker, M.S., Goodenough, D.A., 1986. Identification of ZO-1: a high molecular weight polypeptide associated with the tight junction (zonula occludens) in a variety of epithelia. The Journal of Cell Biology *103*, 755-766.

Sun, J., Wang, X., Li, C., Mao, B., 2015. Xenopus Claudin-6 is required for embryonic pronephros morphogenesis and terminal differentiation. Biochemical and Biophysical Research Communications *462*, 178-183.

Takai, Y., Irie, K., Shimizu, K., Sakisaka, T., Ikeda, W., 2003. Nectins and nectin-like molecules: Roles in cell adhesion, migration, and polarization. Cancer Science *94*, 655-667.

Takasato, M., Little, M.H., 2015. The origin of the mammalian kidney: implications for recreating the kidney *in vitro*. Development *142*, 1937-1947.

Tanaka, M., Kamata, R., Sakai, R., 2005. EphA2 Phosphorylates the Cytoplasmic Tail of Claudin-4 and Mediates Paracellular Permeability. Journal of Biological Chemistry *280*, 42375-42382.

Tepass, U., Hartenstein, V., 1994. The Development of Cellular Junctions in the Drosophila Embryo. Developmental Biology *161*, 563-596.

Thomas, R., Sanna-Cherchi, S., Warady, B.A., Furth, S.L., Kaskel, F.J., Gharavi, A.G., 2011. HNF1B and PAX2 mutations are a Common Cause of Renal Hypodysplasia in the CKiD Cohort. Pediatric Nephrology (Berlin, Germany) *26*, 897-903.

Thorleifsson, G., Holm, H., Edvardsson, V., Walters, G.B., Styrkarsdottir, U., Gudbjartsson, D.F., Sulem, P., Halldorsson, B.V., de Vegt, F., d'Ancona, F.C.H., den Heijer, M., Franzson, L., Christiansen, C., Alexandersen, P., Rafnar, T., Kristjansson, K., Sigurdsson, G., Kiemeney, L.A., Bodvarsson, M., Indridason, O.S., Palsson, R., Kong, A., Thorsteinsdottir, U., Stefansson, K., 2009. Sequence variants in the CLDN14 gene associate with kidney stones and bone mineral density. Nat Genet *41*, 926.

Torres, M., Gomez-Pardo, E., Dressler, G.R., Gruss, P., 1995. Pax-2 controls multiple steps of urogenital development. Development *121*, 4057-4065.

Tsang, T.E., Shawlot, W., Kinder, S.J., Kobayashi, A., Kwan, K.M., Schughart, K., Kania, A., Jessell, T.M., Behringer, R.R., Tam, P.P.L., 2000. Lim1 Activity Is Required for Intermediate Mesoderm Differentiation in the Mouse Embryo. Developmental Biology *223*, 77-90.

Turner, J.R., Angle, J.M., Black, E.D., Joyal, J.L., Sacks, D.B., Madara, J.L., 1999. PKC-dependent regulation of transepithelial resistance: roles of MLC and MLC kinase. American Journal of Physiology - Cell Physiology *277*, C554-C562.

Uhlenhaut, N.H., Treier, M., 2008. Transcriptional regulators in kidney disease: gatekeepers of renal homeostasis. Trends in Genetics *24*, 361-371.

Ure, M., Heydari, E., Pan, W., Ramesh, A., Rehman, S., Morga, C., Pinsk, M., Erickson, R., Herrman, J., Dimke, H., Cordat, E., Lemaire, M., Walter, M., and Alexander, T. A variant in a *cis*-regulatory element enhances Claudin-14 expression and is associated with pediatric-onset hypercalciuria and kidney stones. Human Mutation *38* (2017): 649-657.

Utepbergenov, D.I., Fanning, A.S., Anderson, J.M., 2006. Dimerization of the Scaffolding Protein ZO-1 through the Second PDZ Domain. Journal of Biological Chemistry *281*, 24671-24677.

Van Itallie, C.M., Anderson, J.M., 1997. Occludin confers adhesiveness when expressed in fibroblasts. Journal of Cell Science *110*, 1113-1121.

Van Itallie, C.M., Anderson, J.M., 2006. Claudins and Epithelial Paracellular Transport. Annual Review of Physiology *68*, 403-429.

Van Itallie, C.M., Gambling, T.M., Carson, J.L., Anderson, J.M., 2005. Palmitoylation of claudins is required for efficient tight-junction localization. Journal of Cell Science *118*, 1427-1436.

Van Meer, G., Simons, K., 1986. The function of tight junctions in maintaining differences in lipid composition between the apical and the basolateral cell surface domains of MDCK cells. The EMBO Journal *5*, 1455-1464.

Vaser, R., Adusumalli, S., Leng, S.N., Sikic, M., Ng, P.C., 2015. SIFT missense predictions for genomes. Nature Protocols *11*, 1.

Weber, C.R., 2012. Dynamic properties of the tight junction barrier. Annals of the New York Academy of Sciences *1257*, 77-84.

Weber, S., Moriniere, V., Knüppel, T., Charbit, M., Dusek, J., Ghiggeri, G.M., Jankauskiené, A., Mir, S., Montini, G., Peco-Antic, A., Wühl, E., Zurowska, A.M., Mehls, O., Antignac, C., Schaefer, F., Salomon, R., 2006. Prevalence of Mutations in Renal Developmental Genes in Children with Renal Hypodysplasia: Results of the ESCAPE Study. Journal of the American Society of Nephrology *17*, 2864-2870.

Weber, S., Taylor, J.C., Winyard, P., Baker, K.F., Sullivan-Brown, J., Schild, R., Knüppel, T., Zurowska, A.M., Caldas-Alfonso, A., Litwin, M., Emre, S., Ghiggeri, G.M., Bakkaloglu, A., Mehls, O., Antignac, C., Network, E., Schaefer, F., Burdine, R.D., 2008. SIX2 and BMP4

Mutations Associate With Anomalous Kidney Development. Journal of the American Society of Nephrology: JASN *19*, 891-903.

Werth, M., Walentin, K., Aue, A., Schönheit, J., Wuebken, A., Pode-Shakked, N., Vilianovitch, L., Erdmann, B., Dekel, B., Bader, M., Barasch, J., Rosenbauer, F., Luft, F.C., Schmidt-Ott, K.M., 2010. The transcription factor grainyhead-like 2 regulates the molecular composition of the epithelial apical junctional complex. Development *137*, 3835-3845.

Wilcox, E.R., Burton, Q.L., Naz, S., Riazuddin, S., Smith, T.N., Ploplis, B., Belyantseva, I., Ben-Yosef, T., Liburd, N.A., Morell, R.J., Kachar, B., Wu, D.K., Griffith, A.J., Riazuddin, S., Friedman, T.B., 2001. Mutations in the Gene Encoding Tight Junction Claudin-14 Cause Autosomal Recessive Deafness DFNB29. Cell *104*, 165-172.

Winkler, L., Gehring, C., Wenzel, A., Müller, S.L., Piehl, C., Krause, G., Blasig, I.E., Piontek, J., 2009. Molecular Determinants of the Interaction between Clostridium perfringens Enterotoxin Fragments and Claudin-3. The Journal of Biological Chemistry *284*, 18863-18872.

Wong, V., Gumbiner, B.M., 1997. A Synthetic Peptide Corresponding to the Extracellular Domain of Occludin Perturbs the Tight Junction Permeability Barrier. The Journal of Cell Biology *136*, 399-409.

Woroniecki, R., Gaikwad, A.B., Susztak, K., 2011. Fetal environment, epigenetics, and pediatric renal disease. Pediatric Nephrology *26*, 705-711.

Xu, J., Wong, Elaine Y.M., Cheng, C., Li, J., Sharkar, Mohammad T.K., Xu, Chelsea Y., Chen, B., Sun, J., Jing, D., Xu, P.-X., 2014. Eya1 Interacts with Six2 and Myc to Regulate Expansion of the Nephron Progenitor Pool during Nephrogenesis. Developmental Cell *31*, 434-447.

Xu, P.-X., Adams, J., Peters, H., Brown, M.C., Heaney, S., Maas, R., 1999. Eya1-deficient mice lack ears and kidneys and show abnormal apoptosis of organ primordia. Nat Genet *23*, 113-117.

Yano, T., Kanoh, H., Tamura, A., Tsukita, S., 2017. Apical cytoskeletons and junctional complexes as a combined system in epithelial cell sheets. Annals of the New York Academy of Sciences *1405*, 32-43.

Yap, A.S., Niessen, C.M., Gumbiner, B.M., 1998. The Juxtamembrane Region of the Cadherin Cytoplasmic Tail Supports Lateral Clustering, Adhesive Strengthening, and Interaction with p120(ctn). The Journal of Cell Biology *141*, 779-789.

Yu, Z., Lin, K.K., Bhandari, A., Spencer, J.A., Xu, X., Wang, N., Lu, Z., Gill, G.N., Roop, D.R., Wertz, P., Andersen, B., 2006. The Grainyhead-like epithelial transactivator Get-1/Grhl3 regulates epidermal terminal differentiation and interacts functionally with LMO4. Developmental Biology *299*, 122-136.

Appendix

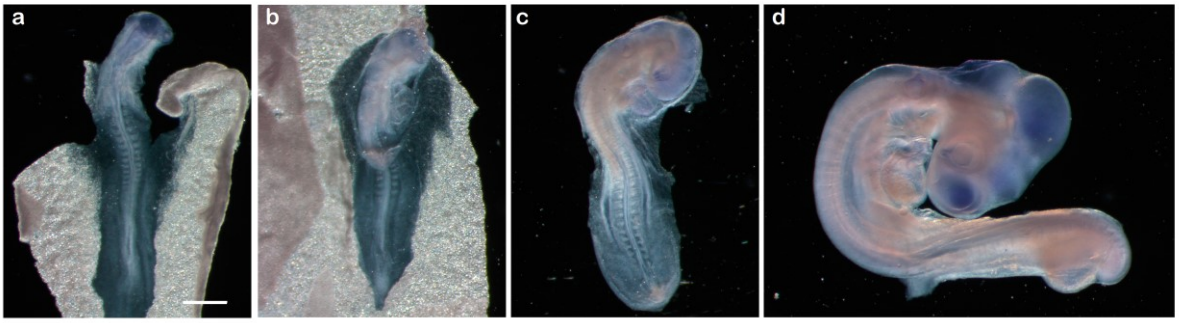

Figure A1. Whole Mount *In situ* Hybridization *Claudin-1* Sense Riboprobe in Chick

Whole mount *in situ* hybridization of chick embryos at HH11 (a), HH13 (b) HH15 (c) and HH19 (d) using a sense riboprobe for *Claudin-1*. Scale bar, 100 mm.

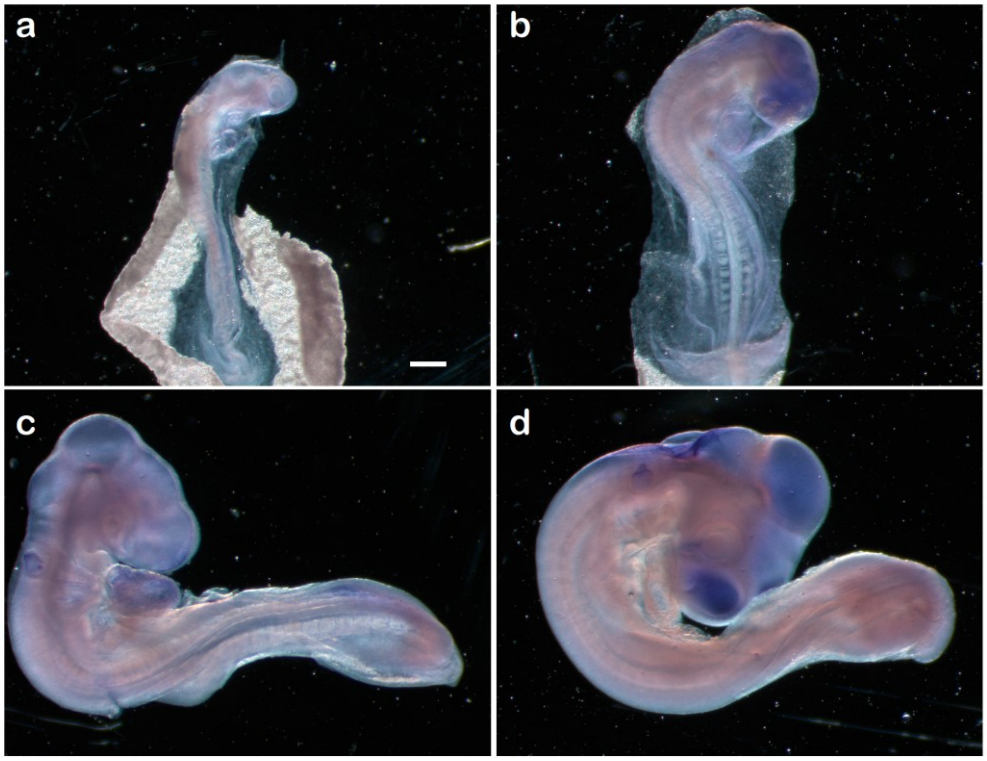

Figure A2. Whole Mount *In situ* Hybridization *Claudin-3* Sense Riboprobe in Chick

Whole mount *in situ* hybridization of chick embryos at HH13 (a), HH15 (b) HH17 (c) and HH19 (d) using a sense riboprobe for *Claudin-3*. Scale bar, 100 mm.

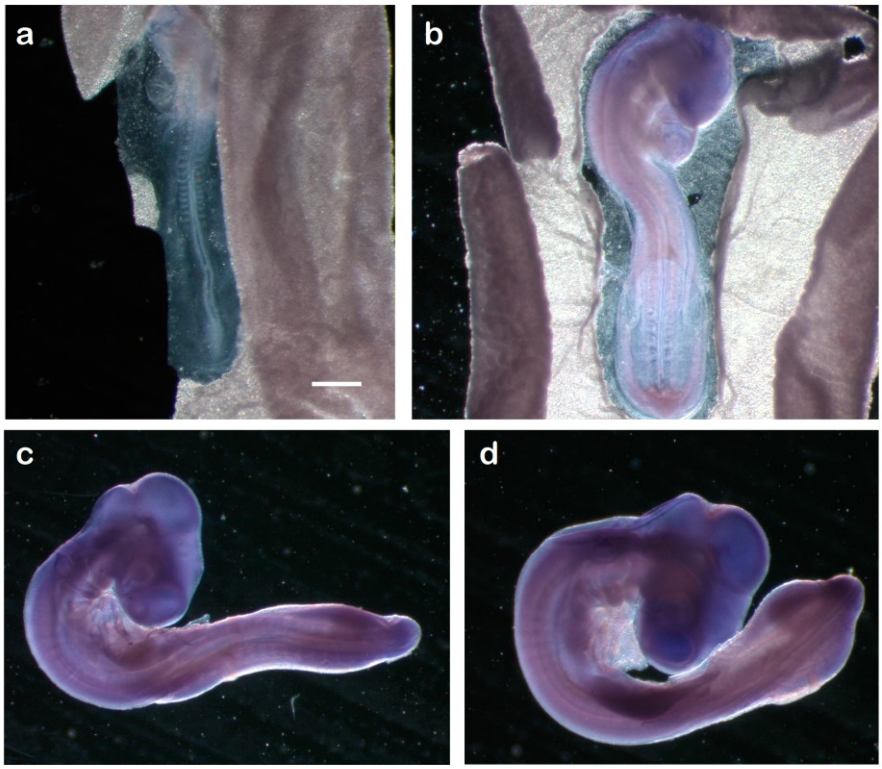

Figure A3. Whole Mount *In situ* Hybridization *Claudin-4* Sense Riboprobe in Chick

Whole mount *in situ* hybridization of chick embryos at HH12 (a), HH16 (b) HH17 (c) and HH18 (d) using a sense riboprobe for *Claudin-4*. Scale bar, 100 mm.

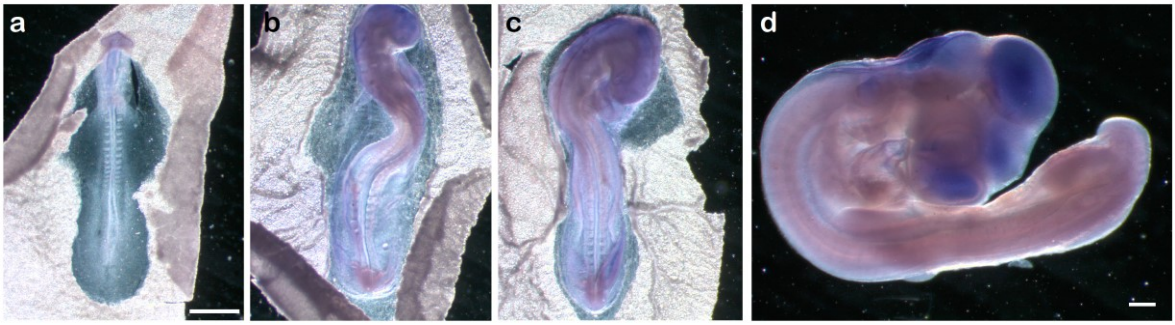

Figure A4. Whole Mount *In situ* Hybridization *Claudin-8* Sense Riboprobe in Chick

Whole mount *in situ* hybridization of chick embryos at HH11 (a), HH14 (b) HH16 (c) and HH19 (d) using a sense riboprobe for *Claudin-8*. Scale bar, 100 mm.

Figure A5. Whole Mount *In situ* Hybridization *Claudin-14* Sense Riboprobe in Chick

Whole mount *in situ* hybridization of chick embryos at HH10 (a), HH13 (b) HH16 (c) and HH17 (d) using a sense riboprobe for *Claudin-14*. Scale bar, 100 mm.